AN ABSTRACT OF THE THESIS OF

Gabriel Katul for the degree of Master of Science in

Civil Engineering presented on April 26, 1990 .

Title: Collection and Analysis of Evaporative Flux Data for Various Climates

Redacted for privacy

Abstract approved: _____

Richard H. Cuenca

Daily evaporative flux and meteorological data from three sites were collected and analyzed. Analysis included evaluation of several reference evapotranspiration estimating methods which were theoretically based on distinct physical laws. The estimating methods included pan evaporation, energy-based Priestly-Taylor, and combination methods with and without biological adjustments. The data set represented three sites with different climates. Analysis included comparisons of evapotranspiration estimating methods, statistical analysis, linear regression analysis, and a detailed study for possible seasonal trends. An attempt to quantify the effect of climate on the original Penman method and the original Priestly-Taylor method using three variables was performed. The variables included average air relative humidity, incoming shortwave radiation, and wind speed at 2 m height. Validation of the derived climatic coefficients for the three sites was performed using a subset of the three data sets and a fourth simulated data set.

Moving average analysis for the various evapotranspiration estimating methods was performed at each of the three sites. The objective was to estimate the optimum averaging interval for a particular estimating method at each site. Five days averaging interval was found

to be adequate to reduce substantially reduce the standard error of estimate and increase the coefficient of determination for all methods at each site.

Collection and Analysis of Evaporative Flux Data for Various Climates

By

Gabriel Katul

A THESIS

Submitted to

Oregon State University

in partial fulfillment of
the requirements for the
degree of

Master of Science

Completed April 26, 1990

Commencement June 1990

APPROVED:

Redacted for privacy

Assoc. Prof. of Civil Engineering in Charge of Major

Redacted for privacy

Head of Department of Civil Engineering

Redacted for privacy

Dean of Graduate School

Thesis presented by Gabriel Katul

Date thesis is presented April 26, 1990

ACKNOWLEDGEMENTS

Many talented people have contributed to the research that is embodied in this dissertation and deserve recognition. The most significant support came from Dr. Richard Cuenca (Associate Professor, Oregon State University). It was Dr. Cuenca who guided my education and stimulated my interest in technical and scientific research. His vision and education shall guide my career for many years to come.

I am also thankful for Dr. Jim Wright who have participated in making the data for this study available. Also to his agency, the United States Department of Agriculture for providing funding and scientific support.

My graduate committee member, Dr. David Bella, Dr. Jack Istok, and Dr. Warren Baker, all merit appreciation for their time and suggestions.

Special thanks goes to Dr. Antonio Martinez-Cob for his continued technical and moral support, his assistance in the analysis portion of this study, and the coffee we drank several overnights while working on the thesis. I am also thankful to the members of the Water Resources Engineering Team Samuel Ortega, Antonio Martinez-Cob, Jeff Nuss, and Will Nichols for the computer education and assistant offered to accomplish this work. Also, sincere thanks goes to the students of the agricultural engineering department who provided genuine nourishment of knowledge revealed in this study.

For giving me the opportunity, the preparation, and the encouragement for pursuing graduate school, I owe all that to Dr. George Ayoub (Chairman of Civil Engineering at the American University of Beirut) and Dr. Constantine Inglessias (Hydraulics professor at the American University of Beirut), and my fellow students Nadim Copty, Talal Balaa, and the class of 88 at the American University of Beirut.

My eternal thanks goes to my father, mother, brother, and sister whose contribution to my future cannot be expressed or described in words.

TABLE OF CONTENTS

LIST OF FIGURES

LIST OF TABLES

COLLECTION AND ANALYSIS OF EVAPORATIVE FLUX DATA FOR VARIOUS CLIMATES

1 INTRODUCTION

1.1 Background

This thesis is aimed at studying the effect of climate on estimating methods of the evaporative flux. The evaporative flux from the land surface constitutes an important part of the hydrologic cycle, second only to precipitation in total quantity (Linsley et al., 1982). It is estimated that in some regions, more than 70 percent of the evaporation is recycled as precipitation (Eagleson, 1986). The ability to quantify the evaporative flux from the land surface is essential to water resources planning and management at several scales ranging from farm to global. The following discussion emphasizes the application of the evaporative flux on several scales.

The present interest of many scientists is devoted to the global scale which allows the examination of global processes such as global warming. Several scientists speculate global warming should be unmistakable within a decade or two (Schneider, 1989). Concerns over potential change in climate have stimulated experimental and research studies to improve the understanding of land surface flux processes. Mathematical climate models, or general circulation models (GCMs), have been introduced to quantify the expected global warming. These models currently rely on a simplified soil moisture flux parameterization such as Budyko's bucket method (André et al., 1986), which increases the

uncertainty in the produced results. Interest in better evaporative flux estimating methods to be incorporated into GCMs is currently increasing (Laval et al., 1984; Dickinson, 1984). Large scale experiments have been conducted and more are planned for this purpose (Cuenca and Amegee, 1987; Cuenca and Noilhan, 1990).

At the watershed scale, basin management and characteristics are largely controlled by land surface processes. Components of the hydrologic cycle are being evaluated to assess availability of water resources (surface and groundwater) for future regulation, utilization, and planning. Aquifer contamination and flow of pollutants from sanitary landfills are major concerns that face civil and environmental engineers at the present. Precipitation induces deep percolation of contaminated water with several pollutants, and hence contamination of groundwater results when aquifer recharge occurs. Plant uptake of water has been considered by many engineers as a potential tool to reduce the amount of deep percolation. Predicting the maximum amount of evapotranspiration can be important in determining the amount of deep percolation responsible for groundwater contamination and recharge.

At the farm scale, estimating water use by crops is required for the design and operation of irrigation systems. Determination of irrigation system capacity to adequately size the distribution and application systems is based on the evaporative flux or plant requirements. Similar to structural engineering, where the applied load is essential to size an adequate and safe beam, in irrigation system design the evaporative flux is the load on the system. System operation, or irrigation scheduling, requires the estimation of crop water use on a daily, weekly, or monthly basis.

As a consequence, better quantification of the evaporative flux at farm scales is central to improve irrigation system design and operation. As a major water consumer, the civil and agriculture community will soon be forced to make optimum use of water in the presence of limited

supplies and increased demand due to population increase and contamination of major water resources. These resources include several major aquifers, lakes, streams, and seas around the world. Moreover, increases in power costs are encouraging many large farms in arid, semiarid, as well as humid regions to reevaluate water use efficiency. Improved crop water estimating methods can prove to be a useful tool for this purpose.

Another application at the field scale is the interest in recycling urban domestic wastewater on agricultural fields. Due to more stringent requirements on wastewater discharge in streams, environmental engineers are looking for land alternatives. During summer periods, stream flow is usually low, and hence concentration of the effluent treated sewage increases. The agriculture community might be facing shortage of water during that period. One solution may be recycling the wastewater on agriculture fields. In this case the objective is to discharge the maximum amount of wastewater that can be applied without impairing crop growth (Reed and Buzzel, 1973). Evaporative flux can assist in determining a lower limit on the application rate of wastewater on the agriculture field without impairing crop growth.

Modern interest in the quantification of crop water use from meteorological data started with the original Blaney-Criddle method (Blaney and Criddle, 1950). The method attempted to correlate temperature with evapotranspiration. The first successful attempt to quantify the evaporative flux as a land surface process initiated with the Penman combination equation (Penman, 1948). This method employs aerodynamic and energy balance approaches to estimate evaporation with measured meteorological parameters. Since Penman introduced his work, many improvements and advances have been made. Some advances are characterized by local calibration coefficients that result in accurate estimates only in the region where the local calibration coefficients were

derived. These methods can estimate the evaporative flux over a very short time period. However, spatial replication is prohibited by economic constraints.

Statistical methods are currently being evaluated which allow estimates of evapotranspiration from several measured points to be applied for an estimate at an unknown desired location. Several methods currently exist for this purpose. However, geostatistics has been successfully applied to evapotranspiration interpolation in Oregon for different climates (Cuenca and Amegee, 1987; Nuss, 1989; Martinez-Cob, 1990). The results enable efficient plotting of contour maps of reference evapotranspiration for the State of Oregon based on a square grid system.

Remotely sensed data have the potential to extend point measurements to a larger scale (Nichols, 1989). Optimum use of remotely sensed data for estimates of land surface processes such as the evaporative flux process at large scales is effectively accomplished in conjunction with ground based measurements of certain variables (Jackson, 1985). This combination of data collection schemes might be useful for GCM input. This study attempts to review several existing methods to evaluate the evaporative flux for various climates.

1.2 Objectives

The overall objective of this study is to examine the various methods of estimating the evaporative flux on a daily basis. The specific objectives of this research are:

1. Study the effect of climate on the performance of various evapotranspiration estimating methods. The methods chosen range from very simple pan evaporation to sophisticated energy balance and aerodynamic combination methods.

2. Quantify the effect of climate by simple climatic factors that can be obtained from general information about the climatic characteristics of the area (e.g. arid, semiarid, or humid). These climatic factors can serve as adjustment factors for the various methods evaluated.

3. Study the accuracy of radiation-based methods.

4. Test the derived climatic coefficients on a site not used in the calibration procedure.

The first objective of this study will require testing of several methods that have different physical phenomena. The process governing pan evaporation does not resemble the theoretical process of evapotranspiration (Sharma, 1985). Unlike pan evaporation, evapotranspiration is affected by meteorological, biological, and soil factors. Combination methods have sound theoretical basis, but require adjustments and calibration. The second objective provides the potential to use methods that have not been calibrated for a specific site to be applied to the desired site depending upon its climatic properties. The third objective is introduced after the successful attempt to measure net radiation from remote multispectral data (Jackson, et al., 1985).

Energy-based methods assume net radiation as the driving force of the evaporation process (Priestly and Taylor, 1972). If energy-based methods prove to be accurate compared to measured lysimeter data, then a convenient method to estimate the evaporative flux on a global scale might be introduced into a GCM. The final objective is an important step for any sound pilot study to insure the reliability and the accuracy of the derived climatic coefficients.

1.3 Data

The data collected for this study provide the opportunity to examine reference evapotranspiration methods and compare to measured lysimeter data at three sites with distinct climates. The location of the sites varies from the arid climate of Kimberly, Idaho, to the semiarid climate of Davis California, to the very humid climate of Versailles, France. The test site is located in the maritime climate of Corvallis, Oregon. This test site location serves as an intermediate site between the arid region of Kimberly, and the very humid climate of Versailles. The data base from Davis, Kimberly, and Versailles includes daily lysimeter data for several years. The lysimeter data available are considered to be very accurate, for the most precise weighing lysimeters were employed. Pan evaporation is also available at the Davis and Kimberly sites. Pan evaporation might prove to be another potential method for estimating reference evapotranspiration if properly calibrated. Standard meteorological data supporting the lysimeter data were also available for all sites to provide a complete data base for evaporative flux studies. Data bases covering such diverse climatic regimes have rarely been combined and used for the analysis and evaluation of reference evapotranspiration.

The Corvallis site is equipped with a Bowen ratio station that can estimate reference evapotranspiration every 20 minutes. The site supports an automatic meteorological station that collects several standard meteorological parameters every 15 minutes. Soil moisture measurements are also available for hydrologic balance studies using the neutron probe.

The promise of this diverse data set for the study of reference evapotranspiration is evident from the above discussion. The task of this study is to meet the outlined objectives with the available resources and data collected.

2 LITERATURE REVIEW

Significant research and effort has been devoted to evapotranspiration studies since the turn of the century. Part of this effort was basically related to water resources management and planning, more interest in better utilization of arid land, more awareness of water efficiency concepts, and finally, more attention to global warming hazards.

This section attempts to present the theoretical basis of several evapotranspiration methods that vary significantly in physical application. These methods include pan evaporation, energy-based methods, hydrologic based methods, and lysimetry. Before proceeding with this discussion, some general terms and basic definitions are given for the sake of clarity and consistency throughout this work.

2.1 Basic Definitions

Consistent definitions for evapotranspiration estimates are important in maintaining sound communication with the scientific community. For example, it is illogical and incorrect to mix up evapotranspiration calculations where some quantities are based on grass related crops and others based on alfalfa related crops. Another potential source of confusion is humidity related variables. There are many different expressions and a variety of instruments to quantify humidity terms. It is often desirable to convert from one form of humidity to another. The concepts often needed to convert from one form to another might not be straight forward, and an understanding of the basic definitions is essential. The definitions related to the terms of evapotranspiration were introduced in Burman et al., (1983). The humidity terms were adapted from Snyder et al., (1987).

Evaporation

Evaporation (E) is defined as the net rate of vapor transfer to the atmosphere from a given evaporating surface. In general, some vapor molecules will detach from a given water surface and some molecules will attach to the surface. The evaporation rate is the net difference between the two processes in a certain period of time. Units of evaporation commonly employed are inches or millimeters of liquid water.

Evapotranspiration

Evapotranspiration (ET) is defined as the process by which water vapor is transferred from the Earth's surface to the atmosphere. It includes evaporation of liquid water from soil and plant surfaces, and transpiration of liquid water from the roots through plant tissues expressed as the latent heat transfer per unit area or its equivalent depth of water per unit area.

Potential Evapotranspiration

Potential evapotranspiration (ET_{tp}) is defined as the maximum rate at which water, if fully available at a specific surface, would transpire from the plant or transfer from the soil expressed as the latent heat transfer per unit area or equivalent depth of water per unit area. In the derivations of different forms of the combination equations for estimating evapotranspiration, ET_{tp} is the evapotranspiration that occurs when the vapor pressure at the evaporating surface is at saturation.

This definition is not restricted to a prototype surface, but can be applied to any water transmitting surface. The use of potential evapotranspiration has been recently replaced in many areas by the term reference evapotranspiration to have a uniform surface for reference purposes.

Reference Evapotranspiration

Two definitions of reference evapotranspiration (ET_r) are used in the scientific and engineering literature. Doorenbos and Pruitt (1977) defined ET_r as the rate of water vapor transfer from an extensive green grass surface. The surface must be 8 to 15 cm in height, actively growing, completely covering and shading the ground, and evapotranspiration from this surface should not be restricted by water availability. The second definition of ET_r is based on alfalfa and was first proposed by Jensen et al., (1971). In the context of his study, ET_r represents the maximum water vapor that occurs under given climatic conditions with a field having a well watered agriculture crop with an aerodynamically rough surface. A surface crop such as alfalfa with 30 cm to 50 cm of top growth satisfies this requirement.

Vapor Pressure and Saturation Vapor Pressure

Snyder et al., (1987) defined vapor pressure (e_a) as the pressure (force per unit area) exerted by water vapor in moist air. The saturation vapor pressure (e_s) is the pressure (force per unit area) exerted by water vapor molecules in moist air if the air is saturated with respect to a flat surface of water. Saturation occurs when the number of water molecules detaching from and leaving the waters surface is equal to the number of water molecules attaching to the surface.

Relative Humidity and Dew-point Temperature

Relative humidity (RH) is the ratio of actual vapor pressure to saturation vapor pressure over water at a given temperature. Dew point temperature (T_d) is the temperature at which moist air becomes saturated with water vapor (RH=100%) if the air is cooled without changing barometric or atmospheric pressure.

2.2 Estimating Reference Evapotranspiration From Pan Evaporation

2.2.1 Introduction

The pan is the most widely used evaporation instrument today, and its application in hydrologic design and operation is of long standing (Linsely, 1982). Evaporation pans can be utilized for estimating reference or actual evapotranspiration over moderate periods of time if properly calibrated (Cuenca, 1989). Although criticism of the pan can be justified on theoretical grounds, many successful studies showed the potential accuracy of the pan to estimate hydrologic variables such as evaporation from lakes or reservoirs, and evapotranspiration from cropped surfaces (Pruitt et al., 1987). Pan evaporation was applied to estimate reference evapotranspiration for several climatic regimes varying from semiarid climate in California to the hot and arid climate in Saudi Arabia (Saeed, 1986).

The following sections explain the concepts and requirements of evaporation, the types of pans commonly used, and the procedure for computing reference evapotranspiration from pan evaporation.

2.2.2 Evaporation

This section discusses the factors controlling the evaporation process from an evaporating surface. Two physical conditions are necessary if the evaporation process from a given body is to persist. First, there must be a continual supply of energy in the form of heat to meet the latent heat requirement which is 590 cal gm^{-1} of water evaporated at 15 °C (Hillel, 1982). The heat can be supplied from the

body itself, thus causing it to cool, or it can be furnished from an outside source in the form of radiated or advected energy. Second, the vapor pressure in the atmosphere should be lower than the vapor pressure at the evaporating surface to establish a vapor gradient. The vapor molecules detached need to be transported away from the surface to reduce the amount of molecules that might reattach on the surface. This can be established by advection or diffusion or both. These two conditions are generally external to the evaporating surface, and are controlled by meteorological variables such as temperature, relative humidity, wind speed, solar radiation, and net radiation.

Determination of atmospheric evaporativity, the maximum flux at which the atmosphere can vaporize water from a surface, is performed by measuring these meteorological parameters external to the evaporating surface. However, as pointed out by Hillel (1982), atmospheric evaporativity is not entirely independent of the properties of the evaporating surface. For instance, the net radiation which is the driving supply of energy for evaporation is affected by reflectivity, emissivity, and thermal conductivity of the surface. This is another important reason to have a uniform reference surface to compare and evaluate evapotranspiration studies.

2.2.3 Pan Exposure

Pan exposure can affect the accuracy of pan measurements as well as pan calibration. It is imperative to define clearly the pan installation for a sound calibration. This section reviews the various pan exposures commonly employed throughout the world.

There are three types of exposures employed for pan installations. The first is the sunken type exposure. In this installation the pan is simply buried in the ground. Burying pans in the ground has the advantage of reducing boundary effects, such as radiation on the side walls, and heat exchange between the atmosphere and the pan. However, operational problems usually arise when pans are buried in the ground. Added to that, sunken pans generally accumulate trash, are more difficult to install, clean, repair, and detecting leaks might be difficult.

Another critical point to consider when pans are placed in the ground is height of vegetation adjacent to the pan rim. Although sunken pans are less affected by boundary effects when compared to other installations, heat exchange with the soil can play a significant role in the pan evaporation. Heat exchange can change annual evaporation from a two meter deep pan by ten percent and a five meter deep pan by seven percent (Linsely, 1982).

The second type of exposure commonly encountered is the floating type. This exposure is commonly used to estimate evaporation from large reservoirs, dams, or lakes. The evaporation from a pan floating in a water surface more nearly approximates evaporation from the lake. However, observational difficulties might be a potential inconvenience in this case. Furthermore, splashing frequently renders measured data unreliable.

The third type of exposure is the surface type. Pans exposed above the ground experience greater evaporation than sunken pans due to boundary effects. Boundary effects include excessive interception of radiative energy causing higher evaporation from the pan than actually occurs. These unrealistic effects can be reduced or eliminated by insulating the pan. The principal advantages of having a surface type of exposure compared to other alternatives are economy, ease of installation, operation, and maintenance.

2.2.4 Types of Pans

There are several sunken pans used throughout the world. However, only two have gained prominence in the United States. These are the Colorado pan and the Bureau of Plant Industry Pan (BPI).

The Colorado pan is square in shape, 91.5 cm on a side, and 46 cm deep. The BPI pan is circular, 183 cm in diameter, and 61 cm deep. This pan provides the best estimate for lake evaporation because of its large size (Linsely, 1982).

The standard National Weather Service Class A pan is the most widely used evaporation pan installed on the surface in the United States. It is manufactured from unpainted galvanized iron, 122 cm in diameter, and 25.4 cm in depth.

Various pans are in common use throughout the world and the need for standardization of pans is being recognized and urged by the scientific community. The two most widely used pans in the world are the Class A pan and the GGI-3000, the standard pan of the U.S.S.R. The GGI-3000 has a circular shape, 3000 cm^2 in surface area and 61.8 cm in diameter. The depth is 60 cm at the wall and somewhat deeper at the center. It is fabricated from galvanized sheet iron. A precipitation gage of similar dimensions and the pan are both sunk in the ground close to each other.

2.2.5 Pan Coefficients

The relation between pan evaporation and reference evapotranspiration is given by equation [1]:

$$ETr = K_p E_{pan} \qquad [1]$$

ET_r= reference evapotranspiration, mm d^{-1}

E_{pan}= pan evaporation, mm d^{-1}

K_p= pan coefficient

The pan coefficient is a function of relative humidity, pan siting, wind run, fetch distance, and pan type. In pan installation, fetch pertains to the distance upwind for prevailing day time wind condition (Cuenca, 1989). The wind run is measured at 2 m height or converted to the equivalent 2 m wind run using the equation [2]:

$$U_{2m} = U_z\left[\left(\frac{2.0}{z}\right)^{0.2}\right] \qquad [2]$$

U_{2m}= equivalent wind speed at 2 m, m s^{-1}

U_z= wind speed measured at height z, m s^{-1}

z= height of measurement, m

Tabulated values for the pan coefficient for the class A pan as a function of pan environment are presented in Jensen, (1974), Doorenbos and Pruitt, (1977), and Cuenca (1989). Cuenca and Jensen (1988) developed a simplified regression equation, suitable for computerized applications, to approximate the table results. Equation [3] presents the regression equation developed :

$$Kp = 0.475 - 0.24x10^{-3}U_{2m} + 0.00516(RH) + 0.00118(d) - 0.16x10^{-4}(RH)^2 - 0.101x10^{-5}(d)^2 - 0.8x10^{-8}RH^2(U_{2m}) - 1.0x10^{-8}(RH)^2(d) \qquad [3]$$

U_{2m}= equivalent wind speed at 2 m, km d^{-1}

RH= mean air relative humidity, percent

d= fetch distance of green crop, m

The equation assumes the fetch distance d is limited to 1000 m or less. This equation may not produce a good fit of the table at some published values.

2.3 Estimating Reference Evapotranspiration From Energy-Based Methods

2.3.1 Introduction

The energy balance at the Earth's surface is made up of four major fluxes. Energy available at the Earth's surface is derived from absorbed solar radiation and terrestrial radiation, the combination of which is termed net radiation.

Energy transfer to or from the soil surface is termed soil heat flux, and is assumed positive by convention when the soil is warming. Energy transfer associated with heating or cooling the air mass above the surface is termed sensible heat flux. By convention, the sensible heat flux is taken positive when the air mass is warming.

Energy associated with water vapor movement is termed latent heat flux. The latent heat flux is assumed positive when vapor is transported from the surface to the atmosphere. The relation between the above mentioned fluxes is known as the energy balance. This method is viewed by many researchers as a basic building cell for many other reference evapotranspiration estimating methods. It provides a sound theoretical formulation for the derivation of other expressions that attempt to estimate the evaporative flux component as a land surface process. The Bowen ratio method, the combination methods, and the Priestly-Taylor method are based on the energy conservation principal.

2.3.2 The Bowen Ratio Method

Reduced costs and complexity are encouraging applied researchers

to consider the Bowen ratio method for measuring evapotranspiration (De Pescara et al., 1988). The popularity of this method is due to the fact that surface properties, wind speeds, and height above the canopy are not essential to the method (Kanemasu, 1979).

As mentioned earlier, the method is based on the energy conservation principal. This principle is described by equation [4]:

$$Rn = Le + H + G \qquad [4]$$

Rn= net radiation, W m^{-2}
Le= latent heat flux, W m^{-2}
H = sensible heat flux, W m^{-2}
G = soil heat flux, W m^{-2}

Net radiation is the energy available at the Earths surface derived from absorbed solar radiation and terrestrial radiation. In mathematical terms:

$$R_n = R_s - R_r + L_i - L_r \qquad [5]$$

Rn= net radiation, W m^{-2}
R_S= incident shortwave radiation, W m^{-2}
R_r= reflected shortwave radiation, W m^{-2}
L_i= incident longwave radiation, W m^{-2}
L_r= reflected longwave radiation, W m^{-2}

The Bowen ratio β was derived by Bowen in 1926. Bowen defined the sensible to latent heat flux as the Bowen ratio. Stated mathematically:

$$\beta = \frac{H}{Le} \qquad [6]$$

Flux gradient relationships are used to describe the one dimensional vertical transport of a scalar within the free air above the surface. For fluxes of sensible heat (H) and water vapor (Le) these expressions are:

$$H = \rho C_p K_H \frac{\partial T}{\partial z} \quad [7]$$

$$Le = K_V \frac{\partial q}{\partial z} \quad [8]$$

ρ= air density

C_p= specific heat at constant pressure

K_H= eddy diffusivity of heat

T= time averaged air temperature

K_V= eddy diffusivity of vapor

q= vapor density

z= height above the surface

In general, the eddy diffusivities of heat and water are not known; however, under many conditions, they are assumed to be equal (Bowen, 1920). The Bowen ratio can now be formulated by dividing the previous two equations (equation [7] and equation [8]):

$$\beta = \frac{\rho C_p K_H \frac{\partial T}{\partial z}}{K_V \frac{\partial q}{\partial z}} \quad [9]$$

Simplifying the above ratio, and approximating the partial derivatives by discrete differences, equation [10] can be obtained:

$$\beta = \gamma \left[\frac{T_1 - T_2}{e_{a1} - e_{a2}} \right] \quad [10]$$

γ= psychrometeric constant, mb $^{\circ}C^{-1}$

T_1, T_2= air temperature at two levels, $^{\circ}C$

e_{a1}, e_{a2}= vapor pressure at two levels, mb

The vapor pressure and the temperature must be measured at the same two levels.

Rewriting the energy equation:

$$Le + H = R_n - G \quad [11]$$

Using the definition of the Bowen ratio and combining with equation [11], equations [12] and [13] are obtained for the two unknowns H and Le:

$$H = \frac{\beta(R_n - G)}{1 + \beta} \qquad [12]$$

$$Le = \frac{(R_n - G)}{1 + \beta} \qquad [13]$$

Thus estimates of Le and H may be obtained by measuring air temperature and vapor pressure at two heights, net radiation, and soil heat flux. Errors in measurements affect β directly. However, errors in β do not affect the flux estimates linearly. Note, the above equations are not defined when β approaches -1.

The Bowen ratio approach requires similarity of the vertical profiles of temperature and vapor pressure (Tanner, 1988). Another assumption that has entered the above derivation is one-dimensional flow of water vapor and heat. Any component of wind that may result in an upward movement of heat and vapor might offset this assumption. This assumption should be kept in mind when site for a Bowen ratio station are under investigation.

The energy balance given in equation [4] assumes the energy required to heat the crop canopy and the energy required for photosynthesis are negligible. These two terms are small compared to the other components of the energy balance equation, and neglecting them is justifiable without loss of accuracy (Kanemasu, 1979).

Despite the restrictive assumptions, the Bowen ratio method has the ability to provide site specific Le estimates with a spatial resolution of 200 m, and temporal resolution of less than one hour (Tanner, 1988). Furthermore, this method requires no local calibration, and has performed well in large scale experiments (André et al., 1988).

2.3.3 The Combination Methods

2.3.3.1 Introduction

Scientists showed limited interest in evapotranspiration as a land surface formulation before Penman published the first scientifically sound equation to estimate grass evapotranspiration. The Penman equation was introduced 42 years ago. However, it may be one of the vital equations today, probably more vital today than when it was first published. The improvements in electronic technology have made it possible to automatically measure several of the meteorological components mentioned in the original Penman work.

At the time Penman published his equation, two theoretical approaches to evaporation from saturated surfaces were commonly employed. The first was based on an aerodynamic formulation in which evaporation is regarded as due to turbulent transport of vapor by a process of eddy diffusion. The second was an energy approach in which evaporation is regarded as one of the ways of degrading incoming radiation. A combination was suggested by Penman which was an important break-through in quantifying evaporation (Penman, 1948). This combination eliminated the need to measure surface temperature and offered the opportunity to estimate reference evapotranspiration strictly from meteorological variables as will be shown in the following sections.

In his original method, Penman applied this combination technique to compute evaporation from a free water surface, from bare soil, and then from grass. Penman started his formulation by computing evaporation from a free water surface, and then attempted to generalize his equation for evaporation from grass and from bare soil by introducing a loss function that reduces water evaporation from a free surface.

Evaporation from bare soil involves complex factors as well as atmospheric conditions. Transpiration adds to these physical conditions biological features that are difficult to quantify. The following sections discuss some of the derivations, assumptions, and features that Penman based his formulation on for grass.

2.3.3.2 Theoretical Derivation

As mentioned previously, two requirements must be met to permit continued evaporation. There must be a supply of energy to provide the latent heat of vaporization, and there must be some mechanism for removing vapor, i.e. there must be a sink for vapor.

The aerodynamic approach was formulated by Penman (1948) to quantify the terms of a semi-empirical formulation derived by Dalton (1801). Dalton recognized the driving aerodynamic force of evaporation, and decided that evaporation must be proportional to the atmospheric demand and a vapor removing mechanism. Dalton stated these basic ideas by the following formulation:

$$ETr = (e_{os} - e_a) f(u) \qquad [14]$$

e_{os}= saturation vapor pressure at the evaporating surface

e_a= actual vapor pressure

f(u)= wind function representing vapor removal by horizontal wind

The energy approach assumes evaporation is directly proportional to the amount of energy available. Shortwave exchanges between the sun and the sky, and longwave exchanges between the Earth and the sky constitute the available energy for evaporation. It should be noted this available energy is a function of the evaporating surface because reflected shortwave and longwave radiation are involved. This available

energy is transformed to kinetic energy in the water molecules, and more molecules will possess the threshold velocity for escaping from the evaporating surface. The available energy can be computed from the energy balance equation.

Penman (1948) combined the aerodynamic and the energy balance equations into a single formulation. He applied the analogy of Reynolds (1847) which states that the transport mechanism for heat and momentum in turbulent flow are the same. The sensible heat flux term of the energy balance equation can be written as follows:

$$H = \gamma f(u)(T_o - T) \quad [15]$$

H= sensible heat flux, mm

T_o= air temperature at evaporating surface, °C

T= air temperature at some height above the surface, °C

f(u)= wind function representing vapor removal transport, mm mb^{-1}

γ= psychrometeric constant, mb $°C^{-1}$

Cuenca (1985) reported that a Taylor series expansion can be used to expand the term (e_{os} - e_a) of equation [14] as:

$$e_{os} = e_s + \frac{d(e_s)}{d(T)}(T_o - T) + err \quad [16]$$

e_{os}= saturation vapor pressure at the evaporating surface, mb

T_o= air temperature at evaporating surface, °C

T= air temperature at some height above surface, °C

e_s= saturation vapor pressure at T, mb

err= error term for higher order derivatives, mb

The first derivative can be replaced by Δ, the slope of the saturation vapor pressure versus temperature curve. The error term can be neglected since it contains higher order derivative terms of e_s. With this simplification, the equation for e_{os} can be written as:

$$e_{os} = e_s + \Delta(T_o - T) \quad [17]$$

Substituting this result into equation [14], equation [18] can be obtained:

$$ETr = \{e_s + \Delta(T_o - T) - e_a\} f(u) \quad [18]$$

Rearranging equation [18] to solve for the difference between surface and air temperature, we get :

$$T_o - T = \frac{\frac{ETr}{f(u)} - (e_s - e_a)}{\Delta} \quad [19]$$

Replacing equation [19] into equation [15] we get:

$$H = \gamma f(u)\left\{\frac{ETr}{\Delta f(u)} - \frac{(e_s - e_a)}{\Delta}\right\} \quad [20]$$

Substituting equation [20] in the energy balance equation, and rearranging terms to solve for reference evapotranspiration, equation [21] is obtained:

$$ETr = \frac{\Delta}{\Delta + \gamma}(R_n - G) + \frac{\gamma}{\Delta + \gamma} f(u)(e_s - e_a) \quad [21]$$

Δ= slope of saturation vapor pressure-temperature curve, mb

γ= K^{-1}

R_n= psychrometeric constant, mb K^{-1}

G= net radiation, mm d^{-1}

f(u)= soil heat flux, mm d^{-1}

$e_s - e_a$= aerodynamic wind function, mm d^{-1} mb^{-1}
vapor pressure deficit, mb

In the original publication of Penman (1948), the wind function was defined as follows (Allen, 1986):

$$f(u) = 0.263(a_w + b_w u) \quad [22]$$

a_w= empirical constant

b_w= empirical coefficient

u= wind speed at 2 m height, m s^{-1}

Penman used for a_w and b_w the values of 1 and 0.537, respectively, for short grass cover. The original equation of Penman neglected the soil heat flux term G for daily estimates of grass evapotranspiration and computed net radiation as:

$$R_n = (1-\alpha_s)R_s - \sigma T^4\left(0.56 - 0.092(e_a)^{\frac{1}{2}}\right)\left(0.1 + 0.90\frac{n}{N}\right) \quad [23]$$

α_s= surface albedo, dimensionless

R_s= incoming shortwave radiation, mm d^{-1}

σ= Stefan-Boltzman constant (2 x 10^{-9} mm d^{-1} K^{-4})

T= mean air temperature, K

n= actual sunshine hours for the day

N= maximum possible sunshine hours

The net radiation equation is made up of two terms. The first term represents the net shortwave radiation at the surface (incident shortwave less reflected shortwave from the surface), and the second term represents the net longwave radiation at the surface (incident longwave less reflected longwave at the surface).

Surface albedo α_s is defined as the ratio of reflected shortwave radiation to incident shortwave radiation for a certain reflecting surface. Surface albedo is affected by the nature of the evaporating surface. Equation [21] requires the vapor pressure deficit as an input for computing reference evapotranspiration. The computation of vapor pressure deficit requires the saturation vapor pressure as an input.

It should be mentioned at this point the method of computing saturation vapor pressure is critical to the accuracy of equation [21]. Uncertainties and errors have arisen in the application of this equation because of misconceptions regarding calculation of vapor pressure deficit (Cuenca and Nicholson, 1982). The original Penman method assumes saturation vapor pressure is computed on the basis of air temperature above the evaporating surface or in this case the crop

canopy. Saturation vapor pressure, for a constant atmospheric pressure, is related to temperature using the relation derived by Murray (1967):

$$e_s = 6.1078 \exp\left(\left\{\frac{17.27T}{T+237.30}\right\}\right) \quad [24]$$

e_s= saturation vapor pressure, mb

T= air temperature, °C

The actual vapor pressure can be computed from average air relative humidity using equation [25]:

$$e_a = e_s\left(\frac{RH}{100}\right) \quad [25]$$

ea= actual vapor pressure, mb

RH= air relative humidity, %

The psychrometeric constant γ of equation [21] can be computed using equation [26]:

$$\gamma = \frac{C_p P}{L\epsilon} \quad [26]$$

C_p= specific heat of dry air, (1.0042 J °C gm^{-1})

P= atmospheric pressure, mb

L= latent heat of vaporization, J gm^{-1}

ϵ= the mass ratio of water vapor to dry air (0.62198), dimensionless

The atmospheric pressure is defined as the pressure (force per unit area) exerted by all gases in moist air. Another frequent term for atmospheric pressure is barometric pressure.

Atmospheric pressure varies to some extent with the passage of frontal systems. However these variations can be ignored in normal estimations of reference evapotranspiration (Burman et al., 1983). Atmospheric pressure varies with elevation above sea level. The U.S.

standard atmosphere assumes temperature decreases at the rate α_l = 6.5 °C km^{-1} with the standard sea level temperature being equal to 288 K. The ideal gas law may be integrated to yield the average air pressures for any given location by the expression (Roberson and Crowe, 1980)

$$P = P_o\left[\frac{(T_o - \alpha_l EL)}{T_o}\right]^{\frac{g}{\alpha_l R}} \quad [27]$$

P= atmospheric pressure at any elevation, mb
P_o= atmospheric pressure at mean sea level, mb
T_o= standard sea level temperature, K
α_l= lapse ratio, K km^{-1}
g= gravitational acceleration, (9.806 m s^{-2})
R= gas constant of air, (287 J kg^{-1} K^{-1})
EL= elevation above the mean sea level, km

A simple linear regression curve was developed to simplify the equation [27], in which atmospheric pressure was related to elevation (Cuenca, 1989):

$$P = 1013 - 0.1093(EL) \quad [28]$$

P= atmospheric pressure at the desired elevation, mb
EL= elevation above mean sea level, m

The latent heat of vaporization L of equation [26] can be related to wet bulb temperature using the expression:

$$L = 2500.8 - 2.3668T_{wet} \quad [29]$$

L= latent heat of vaporization, J gm^{-1}
T_{wet}= wet bulb temperature, °C

The wet bulb temperature is defined as the air temperature obtained when liquid water is evaporated into air until saturation occurs with no change in barometric pressure or total heat content of moist air

(Snyder et al., 1987). It is common to replace the wet bulb temperature in the above equation by air temperature with little loss in accuracy (Burman et al., 1983).

The slope of the saturation vapor pressure-temperature curve can be determined using an empirical approximation sufficiently accurate for applications with the Penman equation (Cuenca, 1989). This equation is dependent on mean air temperature as shown in equation [30]:

$$\Delta = 2.0(0.00738T + 0.8072)^7 - 0.00116 \qquad [30]$$

Δ= slope of saturation pressure, mb $^{\circ}C^{-1}$

T= mean air temperature, $^{\circ}C$

The original Penman method does not take into account the biological aspect of the plant. A modification of this equation is discussed in the subsequent section.

2.3.3.3 Penman-Monteith Method

The original Penman method computes reference evapotranspiration for grass without any regards to stomatal resistance terms. Monteith (1965) showed the latent heat flux from unsaturated surfaces is dependent on the latent heat of vaporization (L), the net radiation (R_n), the density and specific heat of air, and two diffusive resistance terms, r_a and r_s. Monteith derived from basic principles the relation between the above mentioned variables mathematically (Monteith, 1965; Thom and Oliver 1976):

$$Le = \frac{\Delta R_n + \rho C_p \frac{(e_s - e_a)}{r_a}}{L\left(\Delta + \gamma\left(1 + \frac{r_s}{r_a}\right)\right)} \qquad [31]$$

Le= latent heat flux, kg m^{-2} s^{-1}

R_n= net radiation, W m^{-2}

C_p= specific heat of dry air, J kg^{-1} K^{-1}

ρ= density of air, kg m^{-3}

e_s= saturated vapor pressure, mb

e_a= actual vapor pressure, mb

L= latent heat of vaporization, J kg^{-1}

r_{av}= aerodynamic resistance term, s m^{-1}

r_c= bulk stomatal resistance of the canopy, s m^{-1}

γ= psychrometeric constant, mb K^{-1}

Δ= slope of saturation vapor pressure-temperature curve, mb K^{-1}

From this relation, Monteith (1965) discussed the concepts and theoretical relationships of aerodynamic and canopy resistance in the evaporative process and incorporated his results into a Penman combination type equation (Allen, 1986) of the form:

$$ET_r = \frac{\Delta}{\Delta + \gamma^*}(R_n - G) + \frac{\gamma}{\Delta + \gamma^*}E_a \qquad [32]$$

Δ= slope of the saturation vapor pressure-temperature curve, mb K^{-1}

γ= psychrometeric constant, mb K^{-1}

γ^*= modified psychrometeric constant, mb K^{-1}

R_n= net radiation, mm d^{-1}

G= soil heat flux, mm d^{-1}

E_a= aerodynamic vapor transport term, mm d^{-1}

The modified psychrometeric constant incorporates the resistance terms r_{av} and r_c and is related to the psychrometeric constant as shown in equation [33]:

$$\gamma^* = \gamma\left(1 + \frac{r_c}{r_{av}}\right) \qquad [33]$$

The r_{av} term is a function of the wind speed at height z, surface roughness length for transport of momentum and vapor, and the zero plane displacement height within the vegetative surface. In mathematical terms, the relation between the above mentioned variables is given by equation [34]:

$$r_{av} = \frac{\left\{\ln\left(\frac{z-d}{z_{om}}\right)\right\}\left\{\ln\left(\frac{z-d}{z_{ov}}\right)\right\}}{k^2 u_z} \quad [34]$$

r_{av}= aerodynamic resistance to water, s m^{-1}

z= wind, air temperature, and vapor measurement height, mm

d= zero plane displacement height within vegetation, mm

z_{om}= surface roughness length for momentum transport, mm

z_{ov}= surface roughness length for vapor transport, mm

k= von Kármán constant of proportionality, 0.41

u_z= average daily wind speed at height z, m s^{-1}

The canopy resistance is estimated from the leaf area index as shown in equation [35]:

$$r_c = \frac{100}{0.5LAI} \quad [35]$$

r_c= canopy bulk stomatal resistance, s m^{-1}

LAI= leaf area index, dimensionless

If d, z_{om}, and z_{ov} are not measured, some empirical relations can be used to obtain an estimated value (Tanner and Pelton, 1960; Brutsaert, 1982; Allen, 1986):

$$d = 0.67h_c \quad [36]$$

$$z_{om} = 0.123h_c \quad [37]$$

$$z_{ov} = 0.1z_{om} \quad [38]$$

The mean canopy height (h_c) can be easily estimated or measured.

The aerodynamic term E_a has the form (Allen, 1986):

$$E_a = (8.64x10^7)\frac{\rho C_p(e_s - e_a)}{L\gamma r_{av}} \quad [39]$$

E_a= aerodynamic vapor transport term, mm d^{-1}

C_p= specific heat of dry air, J kg^{-1} K^{-1}

ρ= density of air, kg m^{-3}

e_s= saturated vapor pressure, mb

e_a= actual vapor pressure, mb

L= latent heat of vaporization, J kg^{-1}

r_{av}= aerodynamic resistance term, s m^{-1}

γ= psychrometeric constant, mb K^{-1}

The air density ρ can be computed using equation [40]:

$$\rho = \frac{0.0003484(P + \epsilon(e_d))}{T_a\left(1 + \frac{e_d}{P}\right)} \quad [40]$$

ρ= density of air, g cm^{-3}

P= atmospheric pressure, mb

ϵ= mass ratio of vapor to dry air, 0.62198

T_a= mean air temperature, K

e_d= vapor pressure at mean dewpoint temperature, mb

Allen (1986) recommends the use of the 1972 Kimberly-Penman equation developed by Wright and Jensen (1972) and modified by Wright (1982) to compute the psychrometeric constant, the net radiation, and the soil heat flux. Wright and Jensen (1972) compute net radiation using equation [41]:

$$R_n = (1 - \alpha_s)R_s - 0.5\sigma(T^4_{max} + T^4_{min})\left(\alpha\frac{R_s}{R_{so}} + b\right) \quad [41]$$

α_s= surface albedo, dimensionless

R_s= incoming shortwave radiation, mm d^{-1}

R_{so}= clear sky incoming shortwave solar radiation, mm d^{-1}

σ= Stefan-Boltzman constant (2 x 10^{-9} mm d^{-1} K^{-4})

T= mean air temperature, K

a, b= empirical coefficients obtained from tables (Jensen, 1974; Doorenbos and Pruitt, 1977; Wright, 1982; Cuenca, 1989)

The saturation vapor pressure at mean air temperature is computed from equation [42]:

$$e_s = \frac{e_{smax} + e_{smin}}{2} \quad [42]$$

e_s= saturation vapor pressure, mb

e_{smax}= saturation vapor pressure at maximum air temperature, mb

e_{smin}= saturation vapor pressure at minimum air temperature, mb

T= air temperature, °C

The saturation vapor pressure at maximum and minimum temperature are computed using equation [24] and replacing the average daily air temperature by the maximum and minimum air temperatures. The saturation vapor pressure at dewpoint temperature to be used in equation [40] is computed using equation [24] if dewpoint temperature is available, otherwise e_{smin} can be used instead of e_d if RH_{max} approaches 100%.

The soil heat flux can be computed from equation [43]:

$$G = C_s(T - T_{3pd}) \quad [43]$$

G= soil heat flux, mm

C_s= specific heat of soil, mm °C^{-1}

T= air temperature, °C

T_{3pd}= mean air temperature for the prior three days, °C

The albedo (α_s) is a function of the ratio of the incoming shortwave radiation and the clear sky incoming shortwave radiation, the month, and the day of the month. These variables were combined into the following empirical equation by Wright (1982; 1987). If the ratio of the incoming shortwave radiation to the clear sky radiation exceeds 0.7:

$$\alpha_s = 0.29 + 0.06\sin\{30(M + 0.0333N + 2.25)\} \quad [44]$$

α_s= surface albedo, dimensionless

M= month

N= day of month

sin= sine function, degrees

If the ratio of the incoming shortwave radiation to clear sky shortwave radiation does not exceed 0.7, then the surface albedo (α_s) is assumed constant at 0.3.

All the input parameters to compute reference evapotranspiration using the Penman-Monteith method can be estimated. It should be noted the Penman-Monteith method predicts crop evapotranspiration. However, when the resistance terms of alfalfa or grass are used, the evapotranspiration computed is considered reference evapotranspiration.

2.3.4 Priestly-Taylor Method

The Priestly-Taylor approach was introduced to emphasize that large scale parameterization of the surface fluxes are related to energetic considerations over land while formulas of the bulk aerodynamic type are more suitable over the sea. For drying surfaces, it was assumed that the evaporation rate was given by the same formula for evaporation over saturated sites multiplied by a factor (Priestly and Taylor, 1972). The spatial resolution considered by the Priestly-Taylor approach was derived from the Global Atmospheric Research Program (GARP) and is of the order of several hundreds of kilometers.

Mathematically stated, the Priestly-Taylor approach can be considered as a truncated Penman equation as shown by the following expression (Priestly and Taylor, 1972; Burman et al., 1983):

$$ETr = \alpha \frac{\Delta}{\Delta + \gamma}(R_n - G) \quad [45]$$

Δ= slope of saturation vapor pressure-temperature curve, mb $^{\circ}K^{-1}$

γ= psychrometeric constant, mb $^{\circ}K^{-1}$

Rn= net radiation, mm d^{-1}

G= soil heat flux, mm d^{-1}

α= proportionality constant

The approach adopted by Priestly-Taylor defines α using equation [46]:

$$\frac{Le}{Le + H} = \alpha\left(\frac{\Delta}{\Delta + \gamma}\right) \quad [46]$$

Δ= slope of the saturation vapor pressure, mb $^{\circ}K^{-1}$

γ= psychrometeric constant, mb $^{\circ}K^{-1}$

Le= latent heat flux, mm d^{-1}

H= sensible heat flux, mm d^{-1}

α= proportionality constant

Priestly and Taylor derived the limits of α by noting:

$$R_n - G = H + Le \quad [47]$$

From equation [47] they concluded that Le < (Rn - G) if H is positive (e.g. no advection). Therefore, combining this fact with equation [45] α is less than $\frac{\Delta+\gamma}{\Delta}$. From equation [21], Le > $\frac{\Delta}{\Delta+\gamma}(Rn - G)$ if the vapor pressure deficit is positive . Combining this fact with equation [41] α is greater than unity. In conclusion, α will vary between unity, and $\frac{\Delta+\gamma}{\Delta}$.

Priestly and Taylor estimated α to be 1.26 for saturated surfaces free from advection (Priestly and Taylor, 1972).

2.4 Estimating Evapotranspiration from Hydrologic balance Methods

2.4.1 Introduction

Hydrologic balance models rely on the mass conservation principle of water in a fixed control volume. In general, the control volume extends in area to the field plot were the data are collected. The depth of the control volume equals the root zone of the crop.

Soil moisture is commonly required to be able to estimate how much water is stored or lost from the control volume. The neutron probe has proven to be a convenient and effective means of measuring soil moisture content at various depths in the soil profile (Cuenca, 1988; Burman et al., 1983). Water applied to the control volume is usually measured by a rain gage. The source of this water may be irrigation or precipitation. Precipitation intensity is commonly assumed constant over the control volume. This may not be true in the case of extremely large areas (i.e. > 1,000 km^2).

2.4.2 Theory

The hydrologic balance is a detailed statement of the law of conservation of matter which states that matter can neither be created nor destroyed but can only be changed from one state or location to another (Hillel, 1982). The change in root zone moisture content is governed by:

$$dW = \int_0^{z_r} \int_{t_1}^{t_2} \frac{d\theta}{dt} dt dz \qquad [48]$$

dW= change in storage of water, mm

z_r= root zone depth, mm

t_1= initial time period, days

t_2= final time period, days

θ= soil water content, volumetric basis, mm

This equation can be integrated to yield equation [49] for a control volume of thickness z_r, and for a period starting at t_1 and ending at t_2. Equation [49] simply states that for a period of time, the incoming less the outgoing water from a control volume equals the change in the amount of water.

$$P_r + I + R_o = E + T_r + D + \Delta W \qquad [49]$$

P_r= Precipitation, mm

I= Irrigation, mm

R_o= Surface runoff, mm

E= Evaporation, mm

T_r= Transpiration, mm

D= Deep percolation, mm

ΔW= Change in amount of water, mm

Equation [49] can be simplified by neglecting the effect of surface runoff and computing the effect of evaporation and transpiration as one term, evapotranspiration (ET). Note this term (ET) can be computed if precipitation, irrigation, deep percolation, and the change in water volume are known. The discussion in the following section displays methods of estimating or measuring these quantities. The subsequent figure explains schematically the defined terms.

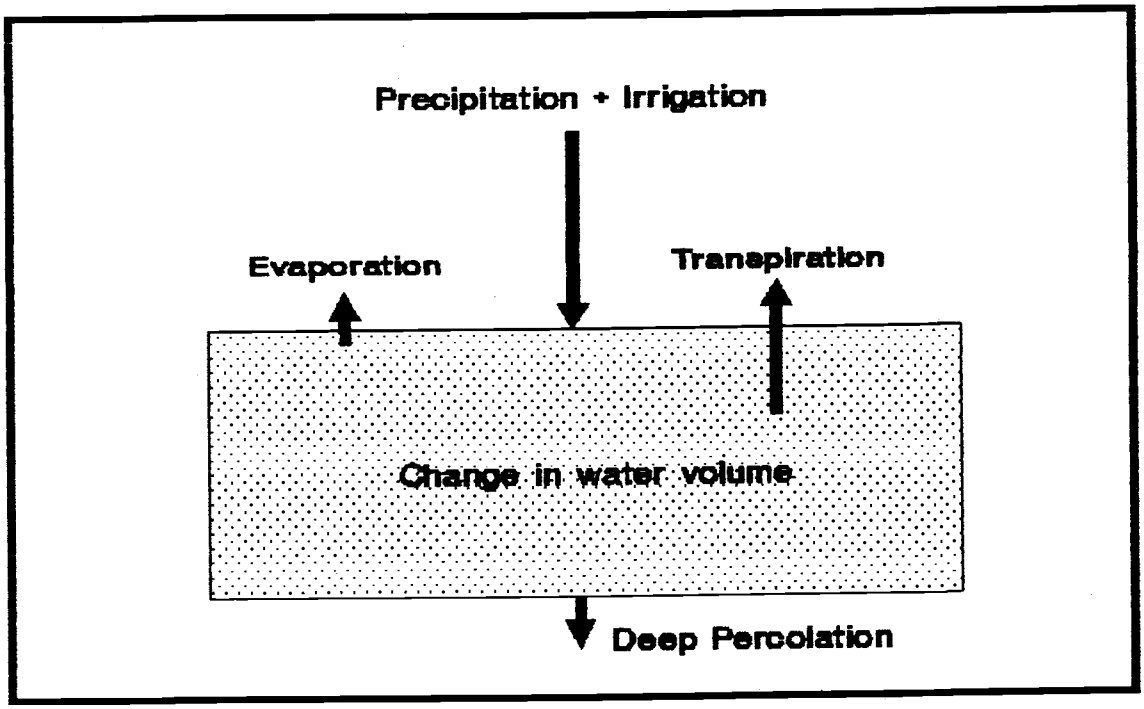

Figure 1. Hydrologic balance components.

The change in amount of water in the control volume is computed by measuring the soil moisture change over a specific time period between two consecutive soil moisture measurements. Mathematically stated:

$$\Delta W = \Sigma[\Delta\theta_i h_i] \qquad [50]$$

ΔW= change in water volume over a certain period, mm

$\Delta\theta_i$= change in volumetric water content

h_i= depth of layer, mm

Note that Σh_i = depth of the control volume, usually equals the root zone of the planted crop.

In the above discussion, it was assumed no water flow occurs laterally across the control volume and the fluctuations of the water

table occur at a depth much deeper than the root zone depth from the surface. Also, it is assumed that no water enters the control volume through capillary rise from the water table.

The deep percolation component is computed by equation [51]:

$$D = (P_r + I) - FC - W_i \quad [51]$$

D= deep percolation, mm

FC= field capacity, mm

(P_r+I)= applied water, mm

W_i= initial moisture content in the soil profile, mm

Field capacity is defined as the volumetric water content at which the rate of internal drainage is appreciably diminished. In the past, field capacity was assumed to be a physical property of the soil. In recent years, with the development of theory and more precise instrumental techniques in the study of unsaturated flow processes, the field capacity concept is recognized as arbitrary and not a soil intrinsic property (Hillel, 1982).

Several arbitrary laboratory or field measurements have been proposed to compute field capacity. Examples include:

1. The amount of water held after the rate of drainage of gravitational water is appreciably diminished. This usually takes place within 1-3 days.

2. The soil moisture content when the matric potential in the soil is 0.1 - 0.3 bars.

These examples are still being used in the field of water resources, and no better criteria have been established to measure field capacity. For the purpose of this study, we will assume field capacity occurs after 2 to 3 days after an intense storm or irrigation event.

Deep percolation is assumed to be the excess amount of applied water with respect to field capacity. By measuring the soil moisture content and amount of applied water over a certain period of time, the deep percolation can be computed for this period.

The hydrologic balance equation can be written for a reference crop (grass) as described by equation [52] to compute reference evapotranspiration ET_r. In this equation, all terms are measured or estimated, and therefore ET_r can be computed.

$$ETr = P_r + I - \Delta W - D \qquad [52]$$

2.5 Estimating Evapotranspiration from Lysimeters

2.5.1 Definition of Lysimetry

The term "lysimeter" was derived from the Greek words "lysis" and "metron" meaning dissolving and measuring, respectively. This term is thus applicable to any device used for examining the rate and amount of water percolating through a porous medium (Aboukhaled et al., 1982).

The Aboukhaled (1982) defined lysimeters as large containers filled with soil situated in the field to reflect the field environment, with bare or vegetated surfaces (crops or grass) for estimating the evapotranspiration of a growing crop or reference cover, or for determining the evaporation rate from bare soils. Lysimeters are distributed worldwide and over the years different types have been developed allowing for various technical solutions to be applied to the measurement of evapotranspiration.

2.5.2 Theory

The principal equation governing lysimetry is the same as the hydrologic balance equation. For purpose of convenience, it will be repeated here:

$$P_r + I + R_o = E + T_r + D + \Delta W \quad [49]$$

P_r= precipitation, mm
I= irrigation, mm
R_o= surface runoff, mm
E= evaporation, mm
T_r= transpiration, mm
D= deep percolation, mm
ΔW= change in amount of water, mm

The surface runoff into or out of the lysimeter is generally zero because the protruding rims of the lysimeter will prevent surface water movement laterally. Precipitation and irrigation are measured using a standard rain gage or calibrated cans. Drainage water is usually collected and measured in a drainage chamber at the bottom of the lysimeter. The distinction between hydrologic approaches and lysimetry is in the measurement of the stored water volume ΔW as well as the actual measurement of deep percolation. The measurements also vary from one type of lysimeter to another. The next section describes briefly the various types of lysimeters.

2.5.3 Types of Lysimeters

The method by which the change in water storage is measured determines the type of lysimeter. Lysimeters can be broadly classified

as non-weighing or weighing types. Basically non-weighing types enable the determination of evapotranspiration for a given period of time by deducting the drainage water collected from the total water input. In the weighing type, evapotranspiration and the drainage components can be determined simultaneously and independently.

There are several types of non-weighing lysimeters, namely:

1. Drainage lysimeters without a water table
2. Compensation lysimeters with a constant groundwater table
3. Compensation lysimeters with a surface water table

Drainage lysimeters without a water table are considered to be the simplest of all non-weighing types. In general, provisions are made at the bottom of the lysimeter container to collect and measure volumetrically the deep percolation of excess water. Precipitation and irrigation are measured by means of a standard rain gage or calibrated cans. The soil in the lysimeter is either maintained close to field capacity or is saturated periodically. Reference evapotranspiration (ETr) for a given period is considered as the difference between applied water and that drained. Mathematically stated:

$$ETr = (P_r + I) - D \qquad [53]$$

Compensation lysimeters with a constant groundwater table operate by maintaining a constant water table in the lower portion of the lysimeter. During evapotranspiration, water from the water table moves into the root zone by capillary rise. The drop in the water level is compensated for automatically by a floating device and the amount necessary to maintain the constant level volumetrically determines evapotranspiration.

Compensation lysimeters with constant surface water level operate by maintaining a constant water level above the soil surface of the lysimeter. This can be achieved by periodic addition of water or by

means of a floating regulating device. This type of lysimeter is suited for infiltration studies. However, its application in evapotranspiration studies is very limited.

There are several types of weighing lysimeters:

1. Mechanical weighing lysimeters
2. Electronic weighing lysimeters
3. Hydraulic lysimeters
4. Floating lysimeters

Different types of mechanical balances are used to measure changes in the weight of the container and soil mass due to evapotranspiration, precipitation, or irrigation. Provisions of an outer container or retaining wall allows free movement of the inner container enclosing the soil mass and crop. The inner container is either weighed periodically by lifting it from its support or is placed directly on a specially designed mechanical balance which constantly records changes in the container weight (Aboukhaled et al., 1982).

The principle of the electronic weighing lysimeter is very similar to that of the mechanical lysimeter. Changes in weight of the inner container and the soil mass are measured electronically using strain gauges or electric load cells. The inner container is often placed on a balancing frame which, through counter weights, reduces the actual weight on the strain gauge.

Weighing lysimeters with hydraulic load cells measure the weight changes of the lysimeter differently than mechanical types. The total weight of the lysimeter is distributed over hydraulic load cells (e.g. flexible bags, pressure bags, etc..) and the pressure of the fluid in the load cells is read by a manometer. Changes in weight of the lysimeter due to evapotranspiration, irrigation, or precipitation cause a change in the height of the fluid in the manometer. The manometer readings require calibration, which can be obtained from static or dynamic loading. The static calibration involves loading or unloading the

hydraulic cells by known weights and reading the corresponding manometer height changes. The dynamic loading involves a more complicated procedure. A container with a volume of water is placed on the hydraulic cells. The water is emptied from the container at a constant discharge and readings of the manometer are recorded at certain time intervals. At equal time intervals, the weight changes versus the manometer readings are plotted yielding a calibration curve.

Floating lysimeters can achieve a high level of accuracy and are much more cost effective than mechanical lysimeters. The operation of floating lysimeters is based on Archimedes hydrostatic flotation principle. The soil container floats on a suitable liquid (e.g. H_2O, or more common $ZnCl_2$) held in an outer container. Changes in weight of the lysimeter due to evapotranspiration or irrigation are measured by changes in the flotation of liquid level.

3 MATERIALS AND METHODS

The instrumentation used to collect and analyze the data in this study are described in this chapter. The theory and formulation behind each collection and analysis method was described in Chapter 2. Data were collected at the Davis in California, Kimberly in Idaho, Versailles in France, and Corvallis in Oregon. Validation studies are cited were appropriate.

3.1 Site Characteristics and Climate

This section describes each site and the climatic characteristics at each site. Meteorological variables such as temperature, wind speed, incoming shortwave radiation, and others, were recorded at all sites. Lysimeter data measuring evapotranspiration were available at Davis, Kimberly, and Versailles. The Corvallis site employed a Bowen ratio system to estimate the evaporative flux from reference grass.

3.1.1 Davis Experimental Site

The Davis site is located at a latitude of 38 ° N and an elevation of 16 m. The climate at Davis is a low-elevation, semiarid climate. Seven years of daily lysimeter data for grass were available from 1965-1971. Pan evaporation corresponding to these seven years support the Davis data set. Daily values for incoming shortwave radiation, ratio of actual to maximum possible sunshine hours, maximum air temperature, minimum air temperature, maximum air relative humidity, minimum air relative humidity, wind run at pan height, and wind run at 2 m height were available.

3.1.2 Kimberly Experimental Site

The Kimberly site is located at a latitude of 42 ° N and an elevation of 1195 m. The climate at Kimberly is a high elevation, arid climate. Three years of daily lysimeter data for alfalfa were available from 1969-1971. Pan evaporation corresponding to these three years support the Kimberly data set. Daily values for incoming shortwave radiation, ratio of actual to maximum possible sunshine hours, maximum air temperature, minimum air temperature, dew point temperature, wind run at pan height, and wind run at 2 m height were available.

3.1.3 Versailles Experimental Site

The Versailles site is located at a latitude of 49 °N and an elevation of 52 m. The climate at Versailles is a low elevation, humid climate. Daily lysimeter data from 1968 to 1976 were available for reference grass. Pan evaporation was not available. However, net radiation, shortwave radiation, and the standard meteorological variables were available. The Versailles site is at the other end of the climatic spectrum from the Kimberly site.

3.1.4 Corvallis Experimental Site

The Corvallis site is located at a latitude of 42 ° N and an elevation of 68 m. The climate at Corvallis is maritime. A few months (September, 1989 - December, 1989) of hourly Bowen ratio data for grass were available. Hourly values for incoming shortwave radiation, reflected

shortwave radiation, soil heat flux, net radiation, latent heat flux, sensible heat flux, maximum air temperature, minimum air temperature, maximum air relative humidity, minimum air relative humidity, wind run at 3 m height, and soil moisture were available.

The following table summarizes the site characteristics described above.

Table 1. Site characteristics.

Site	Corvallis	Davis	Kimberly	Versailles
Latitude, deg	42 N	40 N	42 N	48.97 N
Longitude, deg	123.31	121.74	114.37	2.45 E
Elevation, m	68	18	1195	52
Climate	maritime	semiarid	arid	humid
Years of record	3 months	6 years	3 years	9 years

3.2 Reference Evapotranspiration Data

This section is devoted to reference evapotranspiration measurement techniques for various the experimental sites. Weighing lysimeters were used to measure reference evapotranspiration at Davis, Kimberly, and Versailles. These lysimeters vary in accuracy, dimensions, and properties. The following section discusses the design and installation of the various lysimeters used in this study. The Corvallis Bowen ratio system will also be considered in this section.

3.2.1 The Davis Lysimeter

The lysimeter at Davis was installed in 1958-1959 at the University of California at Davis. The lysimeter is circular, 6 m in diameter, 29 m^2 in area, and 1 m deep. The circular design results in a smaller value for the ratio of the perimeter to the area of the lysimeter which will reduce wall effects. This design minimized the necessary lysimeter volume and the retaining wall thickness necessary to contain the soil mass. The balance system used for determining the weight of the lysimeter is of the mechanical type with a capacity of 50 tons. The weight of the lysimeter was recorded with an automatic printing setup every 2 minutes. The lysimeter is supported on 4 main reinforced concrete square footings of 1.25 m on the side. Drainage water is collected in a circular pit, 1.85 m in diameter, and discharged to a 0.3 m diameter perforated pipe. For temperature control, a 6 mm thick fiberglass tank resting at the bottom of the lysimeter is provided.

It is important to provide temperature control at the bottom of the lysimeter since the thermal isolation between the bottom of the lysimeter and the soil may influence the rate of evaporation due to thermal gradients. Thermal effects of air arising or descending between the containing and retaining walls is minimized by sealing the cap at the ground and minimizing the wall gap area. The wall gap area of the Davis lysimeter is 3 percent. The lysimeter proved to be reliable in determining evapotranspiration to 0.03 mm of water depth (Pruitt and Angus, 1960). This lysimeter is considered to be one of the most accurate lysimeters in the world. A schematic cross section of the lysimeter is shown in Figure 2.

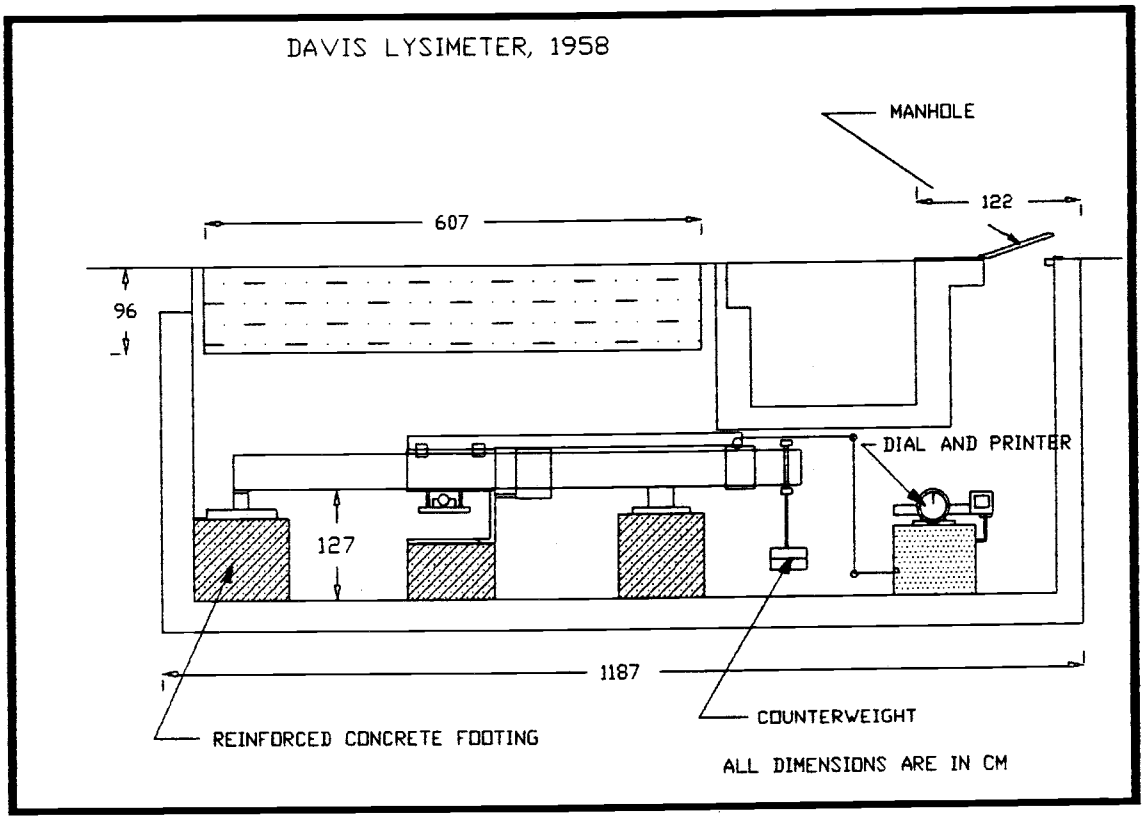

Figure 2. The Davis lysimeter (Aboukhaled et al., 1982).

The soil in and around the lysimeter is a disturbed Yolo loam with no change in structure and without horizons within the first meter. The lysimeter cover is Alta fescue grass with irrigation at 50 % depletion of soil-moisture content (Pruitt and Angus, 1960). This irrigation scheduling is ample to maintain reference grass conditions.

3.2.2 The Kimberly Lysimeter

The lysimeter at Kimberly was installed in 1968 in a 2.8 ha plot (Wright and Jensen, 1972; Wright, 1982). The lysimeter is a square tank

1.83 m on the side and 1.22 m deep. The original design of the lysimeter was introduced by Ritchie and Burnett (1967) in Arizona. The lysimeter was supported on a sensitive mechanical platform scale equipped with a counter balance mechanism. Net weight of the tank was transferred to an electronic load cell. Weight changes resulting from evapotranspiration, precipitation, or irrigation were recorded throughout the growing season.

The water content of the soil within the lysimeter and the surrounding field was monitored with tensiometers. Irrigations were generally scheduled so that water availability within the crop root zone would not limit transpiration. To insure that water would not be limiting, the field was irrigated when the tensiometers at 5 cm read higher than 0.6 atm. The precision of the lysimeter is $\pm$ 0.05 mm (Wright and Jensen, 1972). The lysimeter cover was alfalfa maintained at reference state as described in Section 2.1. Figure 3 is a schematic of the components of the Kimberly lysimeter.

For the purpose of this study, it was necessary to have uniform reference crop. Since the Davis, Versailles, and the Corvallis sites employed grass, the measured alfalfa reference evapotranspiration from the Kimberly lysimeter were converted to a grass reference grass using the relation:

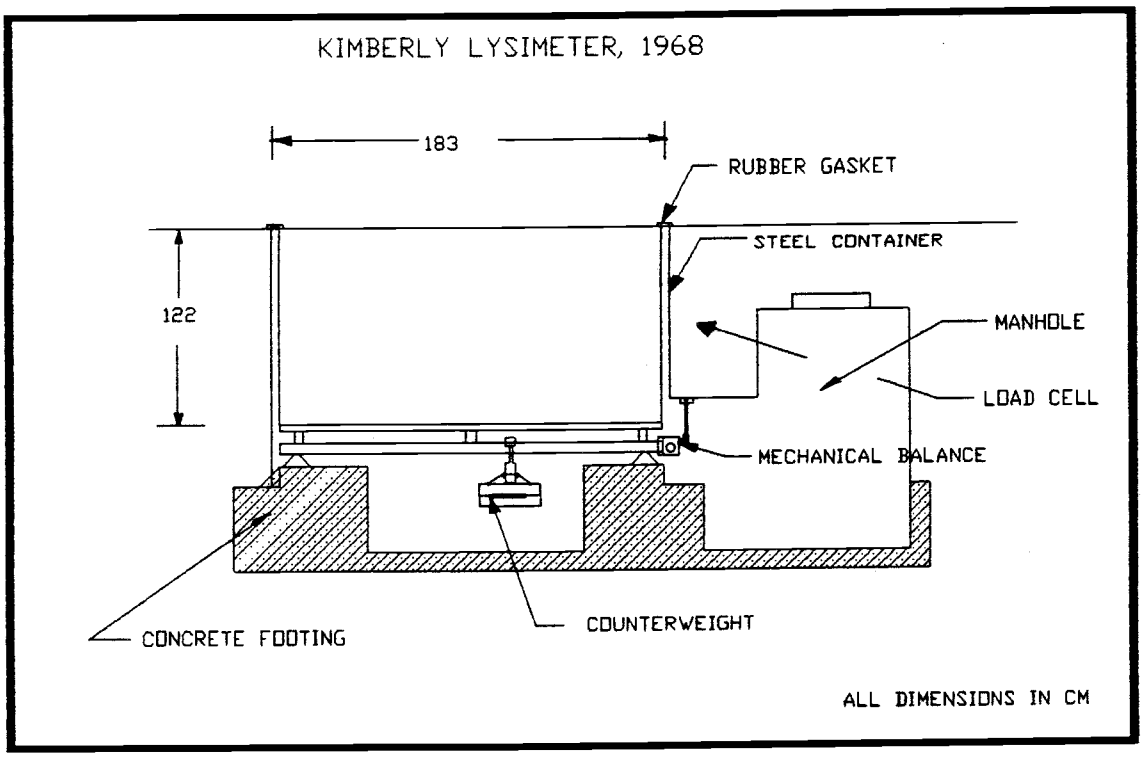

Figure 3. The Kimberly lysimeter (Aboukhaled et al., 1982).

$$ETr_{(alfalfa)} = K_c ETr_{(grass)} \quad [54]$$

$ETr_{(grass)}$= reference grass evapotranspiration, mm

$ETr_{(alfalfa)}$= reference alfalfa evapotranspiration, mm

K_c= crop coefficient

The crop coefficient K_c is a function of relative humidity, wind speed, and the harvesting interval. Doorenbos and Pruitt (1977) presented values of K_c for different average air relative humidity, wind speed, and harvest periods relating reference grass and alfalfa. For humid sites with relative humidity exceeding 70 %, and light to moderate wind speed not exceeding 5 m s^{-1}, the value of K_c is 1.05. For dry climates with relative humidity not exceeding 20 % and light to moderate wind speeds, the value of K_c is 1.15. For strong wind speed (e.g. > 5 m s^{-1}) the value of K_c is 1.25. Linear interpolation was used to obtain the

K_c value for intermediate conditions. The Kc values presented above are for peak conditions. The peak values were chosen since maximum evapotranspiration corresponding to reference state was desired.

3.2.3 The Versailles Lysimeter

The strain gauge lysimeter was installed and tested in 1964-1965 at Versailles, France. The lysimeter was circular in shape with a surface area of 5 m^2, and a diameter of 2.5 m. The depth of the lysimeter was 0.6 m, and the volume 2.84 m^3. The lysimeter was supported by three strain gauges placed on a steel frame at 120 °. The change in lysimeter weight caused strain compression and signals that were recorded on an 115 volts electronic potentiometer to an accuracy of 0.15 mm. At the bottom of the lysimeter, a drainage chamber made with a drilled portion of a sphere was covered with 0.15 m gravel and 0.1 m fine sand. The soil was placed above the sand. A vertical conduit was placed in the drainage chamber for pumping out excess water. The advantages of this method of measurement are that load cells can accept for a short period overload by as much as 50 % of the design value. Moreover, changes in temperature have no effect on the measurement system (Grebet, 1982). The system is described more fully by Archer et al., (1970) and Grebet (1965).

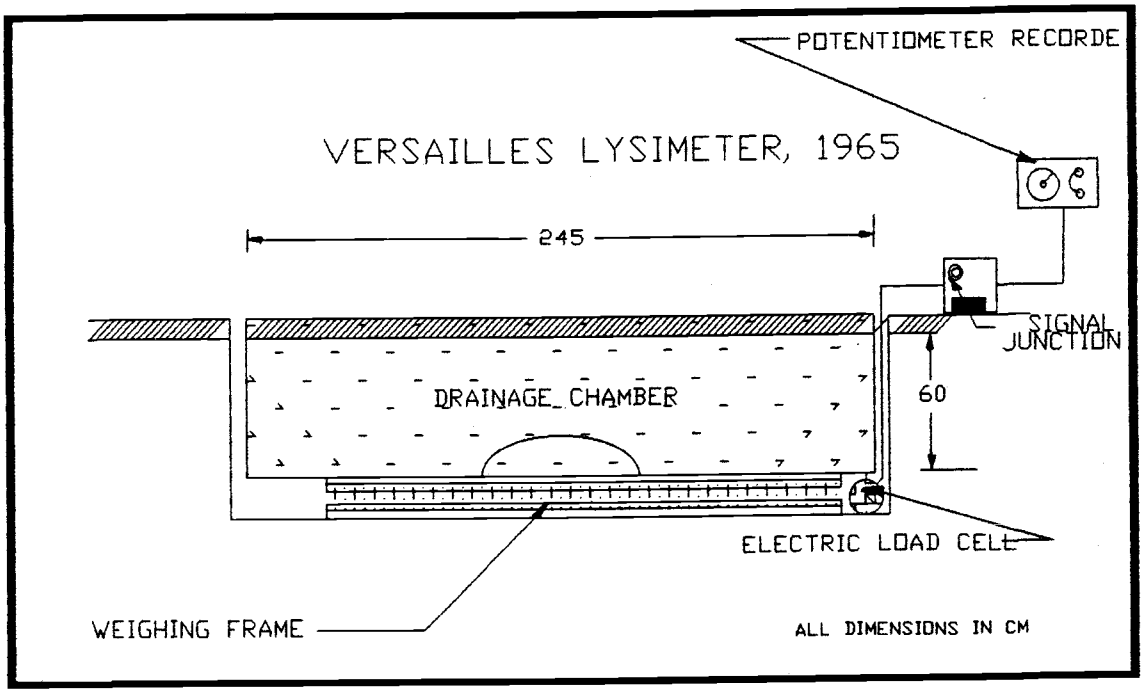

Figure 4. The Versailles lysimeter (Aboukhaled et al., 1982).

The following table summarizes the lysimeter characteristics for each site.

Table 2. Summary of lysimeter characteristics.

Site	Davis	Kimberly	Versailles
Crop	Grass	Alfalfa	Grass
Shape	Circular	Square	Circular
Surface area (m^2)	29	3.35	5
Depth (m)	0.96	1.22	0.6
Volume (m^3)	27.84	4.1	3.0
Capacity (tons)	50	6.1	5.3
Mechanism	Mechanical weighing	Electronic weighing	Strain gauges
Accuracy (mm)	0.03	0.05	0.15
Years of data used	1965-1971	1969-1971	1968-1976
Year installed	1958	1968	1964

3.2.4 The Corvallis Bowen Ratio Station

The Bowen ratio system was installed at the Schmidt Farm (1.85 ha) in Corvallis near Oregon State University. The system was set up in July, 1989 and was fully operational at the end of September, 1989. In this system, unshielded, unaspirated 76 μm chromel-constantan thermocouples (Type E) are used to measure temperature at 2 levels. The lower level arm is 30 cm above the ground surface, and the upper arm is 1.30 m above the ground surface.

A fetch condition of 30:1 is achieved by this set up. This set up was not free from problems. Radiative heating of the thermocouple junctions is a major source of error (Tanner, 1987). However, air velocities of 0.5 m s^{-1} eliminate the majority of the resulting error because of the small junction size. Higher wind speeds were observed throughout the day in the limited data set collected. Similar heating of both the upper and the lower junctions is also relied upon to minimize temperature gradient errors.

Dewpoint is estimated by alternately drawing air from each level through a single cooled mirror hygrometer. A 4 minute cycle is used, measuring for 1.25 minutes, then switching to the other level and equilibrating for 0.75 minutes before measuring again at the corresponding level. Mixing chambers placed upstream from the hygrometer are needed to average the air volume from each level because of sampling time differences between the two levels. For the available size of the mixing chambers, the air flow rate is 5 cm^3 s^{-1}. Dewpoint temperature is converted to actual vapor pressure by the micrologger using the equation derived by Murray, (1976).

$$e_a = 6.1078 \exp\left\{\frac{17.27 T_d}{T_d + 237.30}\right\} \qquad [55]$$

e_a= vapor pressure, mb

T_d= dew point temperature, °C

The net radiation is measured by a 4 ohm Fritchen type net radiometer. The net radiation recorded by this sensor was noted to be higher than that recorded by several sensors, including the Swissteco and CSI Shenk, by 10 % during an extensive study on various net radiometers performed during the summer of 1989 (Allen, 1989). Results of this study included a recommended calibration equation, described below, to reduce the net radiation measured by the Fritchen net radiometer.

$$R_{nadj} = 0.9297 R_{nmeas} - 17.4 \quad [56]$$

Rnadj= adjusted net radiation, W m-2

Rnmeas= measured net radiation by the Fritchen net radiometer, W m^{-2}

To measure soil heat flux, two heat flux plates are buried in the soil at a depth of 8 cm. The average temperature of the soil layer above the plates is measured using 2 parallel thermocouples. The heat flux at the surface is then calculated by adding the average heat flux measured by the two plates to the energy stored in the soil layer as shown in equation [57].

$$G = G_{plate} + G_{stored} \quad [57]$$

G= average soil heat flux at the surface, W m^{-2}

Gplate= average measured soil heat flux at 8 cm, W m^{-2}

Gstored= soil heat stored between the plate and the surface, W m^{-2}

Figure 5 indicates the placement of the soil thermocouples and the soil heat flux plate.

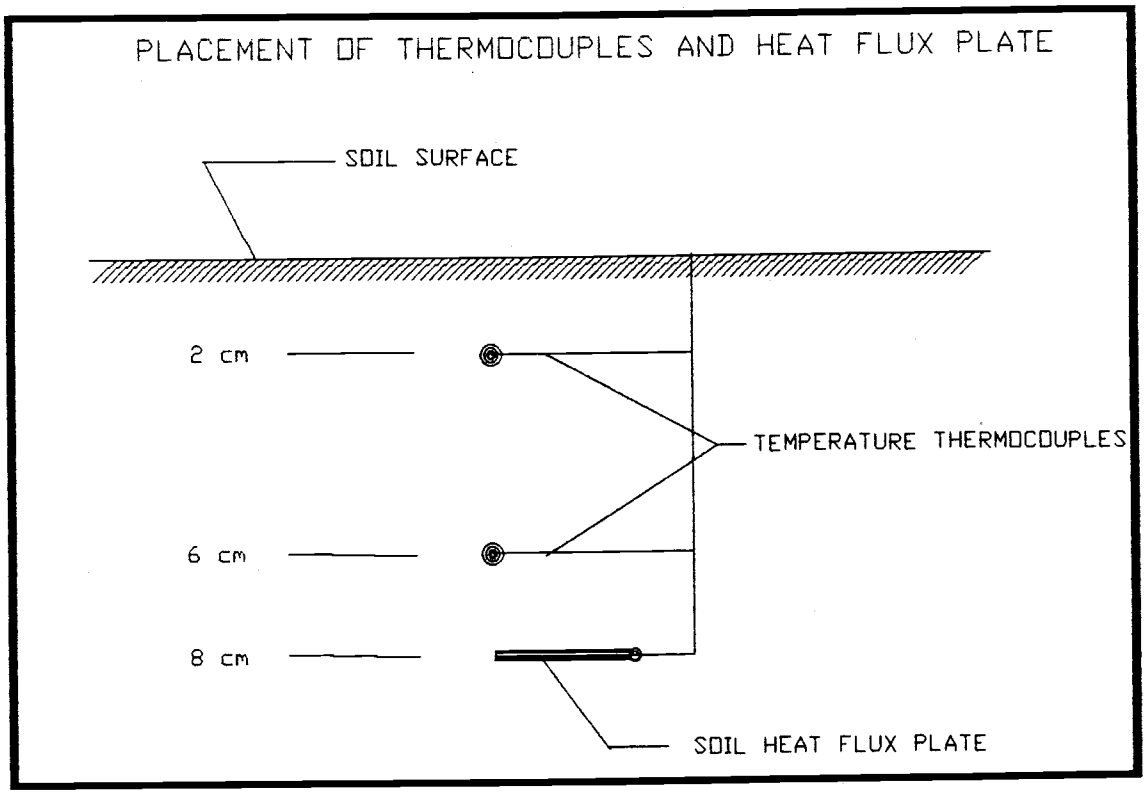

Figure 5. Placement of soil heat flux plate and thermocouples.

The soil heat stored between the plate and the surface is calculated by multiplying the change in average soil temperature over the averaging period by the soil heat capacity. The specific heat of the soil is computed by adding the specific heat of the dry soil to that of the soil water as shown in equation [58].

$$SPH = BD(C_s + \theta_m CW) \quad [58]$$

SPH= soil specific heat, J m^{-3} $^{\circ}C^{-1}$

BD= bulk density of the soil, kg m^{-3}

θ_m= water content on a mass basis, dimensionless

C_S= specific heat of dry soil, J kg^{-1} $^{\circ}C^{-1}$

CW= specific heat of liquid water, J kg^{-1} $^{\circ}C^{-1}$

Measurement and control are done with a small portable micrologger, model CR21X, furnished by Campbell Scientific Inc. Variables measured are averaged and recorded every 20 minutes. The latent heat flux, the soil heat flux, and the sensible heat flux were computed using the SPLITWIZ software. This program uses the formulation developed and discussed in Section 2.3.2. The components of the Bowen ratio station are shown in Figure 6.

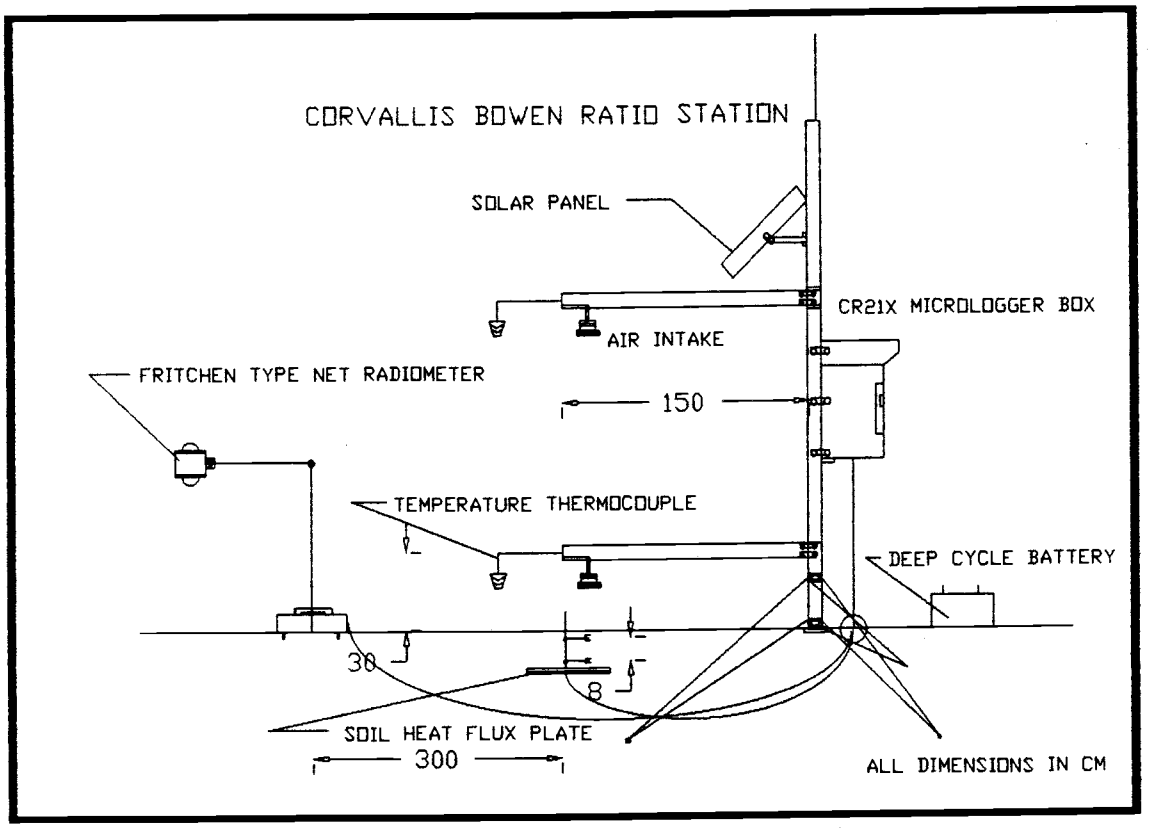

Figure 6. The Corvallis Bowen ratio station.

The following table summarizes the variables measured by the Bowen ratio station at the Corvallis site for the grass reference.

Table 3. Summary of Bowen ratio variables.

Variable	Sensor Type	Accuracy
Air temperature	Chromel-constantan thermocouples	± 0.005 °C
Vapor pressure	Cooled mirror dewpoint hygrometer	± 0.01 kPa
Soil temperature	Soil thermocouple	± 0.01 °C
Soil heat flux at 8 cm	Soil flux plate	varies with soil conditions
Net radiation	Fritchen type net radiometer	± 10 W m^{-2}

3.3 Pan Evaporation Data

Pan evaporation data were available at the Davis and Kimberly sites. These data were correlated with measured evapotranspiration from the lysimeters. The effect of climate on the accuracy of estimating reference evapotranspiration from pan evapotranspiration was considered.

The standard National Weather Service Class A pan was used in this study. It is manufactured from unpainted galvanized iron, 122 cm in diameter, and 25.4 cm in depth. It is exposed on a wood frame to promote air circulation beneath the pan. The water level initially is set at 20 cm, and instructions recommend that the pan be filled when the water level drops to 18 cm. Water surface level is measured by a hook gage in a stilling well and evaporation is computed as the difference between observed levels. Adjustments for precipitation, measured by a standard rain gage close to the pan, are required. Figure 7 demonstrates the class A pan evaporimeter.

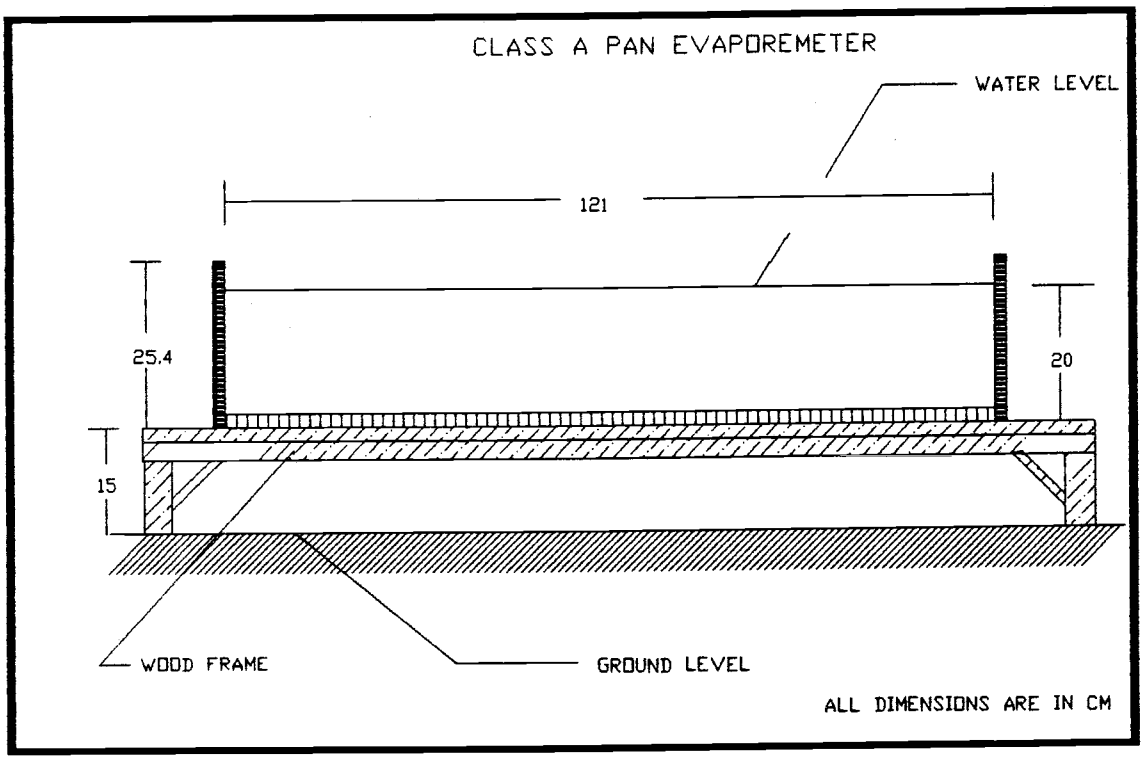

Figure 7. The Weather Service class A pan.

The pans at Davis and Kimberly were surrounded by a cropped irrigated grass surface. Since the grass was kept at reference state (8 cm to 15 cm), no adjustments were necessary for tall crops surrounding the pan or for dry conditions within the pan environment.

3.4 Meteorological Data

Daily meteorological observations were available for the full year for Davis from 1965 to 1971. Daily observations for Kimberly were available only for the growing season corresponding to the period from April to

October for 1969 to 1971. Daily observations for Versailles for 1968 to 1976 were also available. The meteorological variables of interest and the original units of measurements are summarized in Table 4.

Table 4. Daily meteorological observations and units.

Variables	Davis	Kimberly	Versailles
Maximum temperature	°C	°F	°C
Minimum temperature	°C	°F	°C
Dew point	-	°F	°C
Maximum relative humidity	%	-	%
Minimum relative humidity	%	-	%
Wind run	km	miles	km
Pan evaporation	mm	in.	-
Evapotranspiration	mm	in.	mm
Solar radiation	ly d^{-1}	ly d^{-1}	ly d^{-1}

Because relative humidity measurements were not available for Kimberly, an estimation was performed. Since the dewpoint temperature was measured early in the morning (0700 hrs), maximum and minimum relative humidity can be estimated (Burman et al., 1983; Salgado, 1985; Cuenca, 1989) by:

$$RH = \left(\frac{(112 - 0.1T + T_d)}{(112 + 0.9T)}\right)^8 \qquad [59]$$

RH= air relative humidity, %

Td= dew point temperature, °C

T= air temperature, °C

The maximum relative humidity for the day was computed using the minimum and the dewpoint temperatures. The minimum relative humidity was computed using the maximum and the dewpoint temperatures for the day. The average relative humidity was computed using the average air and dewpoint temperatures.

For the Corvallis site, the meteorological data were collected using a Campbell Scientific CR 21 Micrologger and automated weather station. A data average was recorded for 15 minutes intervals. Incoming and reflected shortwave radiation, wind velocity and direction were measured at 3 m above the soil surface. All other parameters were measured at 2 m except the soil temperature. The meteorological parameters measured at Corvallis are:

a. Day and time of recording.
b. Maximum, minimum, and mean wind speed (km h^{-1}) at 3 m height.
c. Maximum, minimum, and mean air temperature, (°C).
d. Maximum, minimum, and mean relative humidity, (%).
e. Maximum, and average total incoming shortwave radiation, (W m^{-2}).
f. Maximum, and average total reflected shortwave radiation, (W m^{-2}).
g. Maximum, minimum, and average soil temperature at 10 cm, (°C).
h. Cumulative precipitation, (mm).
i. Time of maximum and minimum for items b,c,d,e, and g above.

These variables were averaged from 15 minutes to hourly data and combined with the Bowen ratio data to give a complete meteorological and radiation data set for the Corvallis site.

3.5 Reference Evapotranspiration Computations

To fulfill the objectives listed in Chapter 1, four estimating methods were considered. These methods include pan evaporation, the Priestly-Taylor method, the original Penman method, and the Penman-Monteith method. Data availability limited the application of the pan evaporation and the Penman-Monteith to Davis and Kimberly. The original Penman, and the Priestly-Taylor were applied to all sites.

Unfortunately, not all the lysimeter data available could be utilized and some days were removed because of possible faulty meteorological data, missing data, or alfalfa harvesting at Kimberly. When the alfalfa was harvested, at least a fourteen days period was removed from the data set for the alfalfa to recover. The alfalfa was cut on May 28 and July 24 for 1969, June 24 and August 25 for 1970, and June 18 and August 8 for 1971. Several missing days were noted in the Versailles data set.

The following Section describes the method of estimating reference evapotranspiration, and the methodology followed to evaluate the performance of each method as well as comparisons between estimating methods for each site.

3.5.1 Pan Evaporation Method

Theoretically speaking, the process of water evaporation from a free water surface is distinct from that of evapotranspiration from a soil-plant system. Yet previous work demonstrated strong correlation between pan evaporation and reference evapotranspiration (Salgado, 1985; Doorenbos and Pruitt, 1977; Saeed, 1986).

To utilize the pan evaporation method for estimating reference evapotranspiration, the pan coefficient must be known. Theoretically, the pan coefficient is obtained by calibrating the pan with measured lysimeter data. This deficiency precluded the use of pan evaporation data for estimating reference evapotranspiration because the pan coefficient is difficult to determine.

The sites employed in evaluating the pan evaporation method were Davis and Kimberly. Two methods were employed to estimate the pan coefficient. The first method assumes the pan coefficient constant throughout the year for Davis and throughout the growing season for

Kimberly. The second method varies the pan coefficient on a daily basis employing relative humidity and wind speed. However, a constant fetch distance was assumed in both methods.

The procedure employed in each site for the data analysis can be summarized in the following steps:

1. Estimate the average wind speed for the period of interest.
2. Estimate the average air relative humidity for the period of interest.
3. Estimate the fetch distance for the period of interest.
4. Use equation [3] in Section 2.2.5 to estimate the pan coefficient for the period of interest.
5. Use equation [1] to estimate daily reference evapotranspiration for the period of interest.

3.5.2 Priestly-Taylor Method

The Priestly-Taylor method was considered to evaluate energy-based methods. Two alternative approaches were suggested for evaluating the Priestly-Taylor methods. The first alternative was to assume a constant α. The second alternative was to vary α according to some meteorological variables. The constant value of α used in the first alternative was 1.26 as suggested by Priestly and Taylor (1972). The method of constant α was termed, for the purpose of this study, the original Priestly-Taylor method, and the method of variable α was termed the modified Priestly-Taylor method.

The attempt to improve on the accuracy of the Priestly-Taylor method was suggested since α should take into account factors affecting evaporation in addition to net radiation. Since the method does not consider the effect of temperature, vapor pressure and relative

humidity, an attempt to incorporate the integrated effects of these variables can be included in an estimate of α based on meteorological variables.

In Section 2.3.4, it was shown that α varies between unity and $\frac{\Delta+\gamma}{\Delta}$. A method to interpolate the value of α between the unity and $\frac{\Delta+\gamma}{\Delta}$ was investigated. The value of α is close to unity when the vapor pressure deficit is zero and the only mechanism for evapotranspiration is the energy mechanism. On the other hand, if the vapor pressure deficit is maximum, then α should approach the upper bound of $\frac{\Delta+\gamma}{\Delta}$.

The vapor pressure deficit was used to linearly interpolate between the lower and upper limits of α. The maximum possible vapor pressure deficit was computed by estimating the average saturation vapor pressure and the minimum vapor pressure as computed from the minimum relative humidity. The difference between these two quantities is considered as the maximum possible vapor pressure deficit for the day. α can be computed using the equation [60]:

$$\alpha = 1 + \left(\frac{(\gamma + \Delta)}{\Delta} - 1\right)\frac{\Delta e}{\Delta e_{max}} \qquad [60]$$

Δ= slope of the saturation vapor pressure, mb $^{\circ}K^{-1}$

γ= psychrometeric constant, mb $^{\circ}K^{-1}$

Δe= average vapor pressure deficit, mb

Δe_{max}= maximum possible vapor pressure deficit for the day, mb

Daily reference evapotranspiration values were computed using the procedure outlined in Section 3.5.2 for the original and modified Priestly-Taylor methods.

Since minimum daily air relative humidity was not available in Versailles, long term minimum monthly values for relative humidity were used to estimate the maximum possible vapor pressure deficit used in

estimating α. This procedure introduces an additional variation from the methodology applied in Davis and Kimberly for computing α and an additional in consistency.

The method to compute ET_r using the original Priestly-Taylor and the modified Priestly-Taylor methods is given in the following steps:

1. Compute the saturation vapor pressure from equation [24] using the average daily temperature.
2. Compute the actual vapor pressure from equation [25] using the saturation vapor pressure obtained from step 1 and the average daily relative humidity.
3. Compute the net radiation from equation [23] using the actual vapor pressure, measured incoming shortwave radiation, measured air temperature, and measured ratio of actual to maximum possible sunshine hours.
4. Compute the atmospheric pressure using equation [28] and site elevation.
5. Compute the latent heat of vaporization using equation [29] and average air temperature.
6. Compute the psychrometeric constant from equation [26] using the atmospheric pressure computed in step 4, the specific heat of dry air, the latent heat of vaporization from step 5, and the ratio of water vapor to dry air.
7. Compute the slope of the saturation vapor pressure-temperature curve using equation [30] and air temperature.
8. Assuming the average soil heat flux to be zero for the day, daily reference evapotranspiration can be computed using equation [45] and net radiation from step 3, the psychrometeric constant from step 6, and the slope of the saturation vapor pressure-temperature curve from step 7.
9. Compute the average estimated reference evapotranspiration and the variance for the period of interest.

3.5.3 Original Penman Method

The original Penman method was considered to evaluate combination methods. The method was not calibrated for any of the three sites. Therefore, there is not any artificial bias for any particular site. The Penman method takes into account the aerodynamic effects contributing to evapotranspiration unlike the Priestly-Taylor. The method to compute evapotranspiration for the three sites is given in the following steps:

1. Compute the saturation vapor pressure from equation [24] using the average daily temperature.
2. Compute the actual vapor pressure from equation [25] using the saturation vapor pressure obtained from step 1 and the average daily relative humidity.
3. Compute the net radiation from equation [23] using the actual vapor pressure, measured incoming shortwave radiation, measured air temperature, and measured ratio of actual to maximum possible sunshine hours.
4. Compute the atmospheric pressure using equation [28] and site elevation.
5. Compute the latent heat of vaporization using equation [29] and average air temperature.
6. Compute the psychrometeric constant from equation [26] using the atmospheric pressure computed in step 4, the specific heat of dry air, the latent heat of vaporization from step 5, and the ratio of water vapor to dry air.
7. Compute the slope of the saturation vapor pressure-temperature curve using equation [30] and air temperature.
8. Compute the wind function f(u) using equation [22] and the average daily wind speed at the equivalent 2 m height.
9. Compute the vapor pressure deficit by subtracting the actual vapor pressure obtained in step 2 from the saturation vapor

pressure computed in step 1.

10. Compute the average daily reference evapotranspiration using equation [21].

In general, the Penman equation can be formulated as a linear combination of the energy component and the aerodynamic component.

$$ETr = P1 + P2 \quad [61]$$

P1= energy component, mm

P2= aerodynamic component, mm

Referring to the original Penman equation, P1 and P2 can be formulated as:

$$P1 = \frac{\Delta}{\Delta + \gamma}(R_n - G) \quad [62]$$

$$P2 = \frac{\gamma}{\Delta + \gamma} f(u)(e_s - e_a) \quad [63]$$

3.5.4 Penman-Monteith Method

The Penman-Monteith method is a method that is gaining wide acceptance and application. It accounts for many processes responsible for evapotranspiration including energy, aerodynamic, and biological factors. The method requires several input parameters that are difficult to quantify or measure; nevertheless, the method is considered to be very accurate.

Allen (1986) presented values for the resistance terms at Davis and Kimberly. These values were employed in computing reference evapotranspiration using the Penman-Monteith and are reproduced in Table 5.

Table 5. Crop information for Davis and Kimberly (Allen, 1986).

Variables	Davis	Kimberly
Estimated Mean Crop Height (mm)	120	570
Estimated Zero Plane Displacement (mm)	80	380
Estimated z_{om} (mm)	15	70
Estimated z_{ov} (mm)	1.5	7
Estimated LAI	2.8	5.0
Estimated Canopy Resistance r_c (s m^{-1}) during peak periods	70	40

The procedure employed to compute daily evapotranspiration using the Penman-Monteith is outlined in the following steps. It should be noted the values computed by the Penman-Monteith for Kimberly were based on alfalfa and were converted to equivalent grass using a crop coefficient as discussed in Section 3.2.2.

1. Compute the saturation vapor pressure from equation [42] using maximum and minimum air temperature and equation [24].
2. Compute the actual vapor pressure from equation [25] using the saturation vapor pressure obtained from step 1 and the average daily relative humidity.
3. Compute the surface reflectance depending upon whether equation [44] applies or not. If equation [44] applies, the month and day of month are required as input. If equation [44] is not applicable the surface reflectance is 0.3.
4. Compute the net radiation from equation [41] using measured incoming shortwave radiation, measured maximum and minimum air temperature, and ratio of incoming shortwave radiation to maximum possible clear sky shortwave radiation.
5. Compute the atmospheric pressure using equation [28] and site elevation.
6. Compute the latent heat of vaporization using equation [29] and average air temperature.
7. Compute the psychrometeric constant from equation [26] using

the atmospheric pressure computed in step 4, the specific heat of dry air, the latent heat of vaporization from step 5, and the ratio of water vapor to dry air.

8. Compute the slope of the saturation vapor pressure-temperature curve using equation [30] and air temperature.

9. Compute the modified psychrometeric constant from equation [33] and information provided in Table 5 for resistance terms at each site.

10. Compute the density of air using equation [40] from measured air temperature, atmospheric pressure computed in step 5, the latent heat of vaporization computed in step 6, and the vapor pressure at mean dewpoint temperature.

12. Compute the aerodynamic vapor transport term from equation [39] using specific heat of dry air, the saturated vapor pressure computed in step 1, the actual vapor pressure computed in step 2, information provided the aerodynamic resistance in table 5, and the density of air computed in step 11.

13. Compute the soil heat flux from equation [43] using the soil specific heat, the average daily air temperature, and the mean air temperature for the prior three days.

14. Compute the mean daily reference evapotranspiration from equation [32].

3.6 Statistical Analysis

This section presents the statistical formulation and methods developed and employed for each estimating method at each site. The analysis was divided in two parts. The first part compared estimated reference evapotranspiration with lysimeter evapotranspiration for each method at each site on a year by year basis. The second type of analysis evaluated each method at each site by comparing the estimated values with the lysimeter data for all available years combined together into one data set without regard to time.

The purpose of the first part of the data analysis was to check whether there were consistent seasonal trends, consistent correlation, or consistent overestimation or underestimation by the method under consideration. Several tools ranging from graphical to statistical were employed for this purpose.

To check whether there was a seasonal trend, the error of estimation was computed and analyzed. The error of estimation was computed using equation [64]:

$$Error = ETr_{(lys)} - ETr_{(computed)} \qquad [64]$$

$ETr_{(lys)}$= measured evapotranspiration, mm d^{-1}

$ETr_{(computed)}$= computed evapotranspiration, mm d^{-1}

Analysis of the error was performed graphically by:

1. Plotting the computed error versus time.
2. Plotting the frequency of occurrence of an error within an error interval versus the error interval.
3. Plotting the cumulative computed reference evapotranspiration and cumulative measured evapotranspiration versus Julian day.

The first plot can indicate the season or month when the method tends to overestimate or under estimate ET_r by observing whether the points fall below or above the zero axis. The second plot can indicate

whether the errors were normally distributed throughout the year. The third plot can indicate the time period of the year were the method deviated from the measured lysimeter data by comparing the slopes of the cumulative plots. The cumulative plots can aid in making decisions about the correlation of the method with the lysimeter since the summation dampens extreme values that may have resulted from short-term measurement errors.

The statistical tools and checks included the following:

1. Check whether the over all error of estimate was significantly different from zero. This check was important to confirm whether the average error of estimate was different from zero for the year under study .

2. Perform regression analysis for each method for each year at each site. Linear regression analysis was used to test agreement and variation between estimated values and measured values. In addition, the slope of the regression line was computed to check whether it was different from unity. If the slope is not significantly different from unity, then a unit change in the estimated value corresponds to a unit change in the measured data. Included in the regression analysis is the coefficient of determination (r^2) which can quantify the correlation between estimated and measured reference evapotranspiration. It was important to check whether the correlation was steady from year to year for each method at each site.

3. Compute the raw standard error of estimate (SEE) using the raw data, and the standard error of estimate of the regression line (SEER) for each year, and check if both vary significantly from year to year.

The second part of the analysis combined all available years in one data set for each site. Regression analysis, SEE, SEER, and r^2 were

computed to compare estimation methods and to identify which methods performed best under given climatic conditions. Two regression models were applied in this study. The models were of the form:

$$ETr_{(est)} = a + bETr(computed) \quad [65]$$

$$ETr_{(est)} = bETr(computed) \quad [66]$$

$ETr_{(est)}$= estimated evapotranspiration using the regression coefficients, mm d^{-1}

$ETr_{(computed)}$= computed reference evapotranspiration, mm d^{-1}

a= constant of regression

b= slope of regression

The first model was applied to check correlation and SEER. The second model could indicate whether there is a relative conversion ratios between the daily lysimeter ET_r and the estimating method employed. Forcing the regression through the origin has the advantage of integrating all errors into the slope of the regression line. In addition, the slope of the regression can be interpreted as the ratio of measured to estimated evapotranspiration.

Moving average ET_r were computed for several averaging days to establish the optimum averaging time period for each method at each site. The coefficient of determination between the moving average lysimeter data and the moving average computed reference evapotranspiration was computed for each averaging period to quantify the increase in correlation with the number of days used in the averaging. Combining the SEE and r^2 at each site for each estimating method for various averaging days, the optimum averaging period can be obtained. This was accomplished graphically by computing SEE and r^2 for each averaging period for each method at each site and plotting SEE versus r^2.

In Kimberly, provisions were made not to average values from year to year since in Kimberly the data starts with April and ends in October. Additional errors might be introduced by averaging ET_r

values from April with values from the previous year October while performing the moving average computations for all three years. Therefore, the last day in each year at Kimberly was assumed constant, and was not averaged with the value of April of the next year. Similar provisions where made in Versailles were several months were missing from the data set.

The variables used in evaluation of the estimating methods include:

1. The Z statistics
2. The coefficient of variation (CV)
3. The raw standard error of estimate (SEE) and the standard error of estimate of the regression fit (SEER).

They are described in the next section.

3.6.1 Z statistical Test

This section describes how the Z test was employed in the data analysis and method evaluation. The Z test was applied in two types of analysis. The first type of analysis involved checking whether the error of estimate was statistically different from zero for each year at each site and for each method. The second application of the Z test was in the regression analysis. In this case, the Z test indicated whether the slope of the regression line b was significantly different from unity.

The Z test in lieu of the t test was used since the data contained more than 120 observations in each type of analysis. With a sample size larger than 120 observations, the Z test is more appropriate than a t test with an infinite sample size (Devore and Peck, 1986). For the error analysis, the null hypothesis for the Z test claims the population characteristic is equal to the hypothesized value. The population characteristic is the difference between the average computed reference evapotranspiration using a certain method for the period of available

data and the lysimeter average for the same period. The hypothesized value is zero. The alternative hypothesis can have one of the following forms:

(i) The population characteristic is greater than the hypothesized value.

(ii) The population characteristic is less than the hypothesized value.

(iii) The population characteristic is not equal to the hypothesized value.

The alternative hypothesis for the purpose of this study has form (iii). The Z statistics can be computed using equation [67]:

$$Z = \frac{| ETr_{(lys)} - ETr_{(Computed)} | - 0}{\left(\frac{s_1^2 + s_2^2}{n}\right)^{\left(\frac{1}{2}\right)}} \qquad [67]$$

Z= Z statistics, dimensionless

s_1= standard deviation of lysimeter data, mm d^{-1}

s_2= standard deviation of computed ET_r, mm d^{-1}

n= number of days used

The computed Z is compared to a critical Z. The critical Z is obtained from a statistical table for the Z test. The significance level employed in this study was 0.05 to achieve a 95% confidence level. The Z critical from statistical tables (Devore and Peck, 1986) was 1.96.

If the Z computed does not exceed the critical value, there is not enough statistical evidence to reject the null hypothesis and accept the alternative hypothesis. In this case, the average computed reference evapotranspiration is not statistically different from the measured average value and the method does not overpredict or underpredict for the period of available data.

For the slope of the regression analysis, a similar procedure was used. The population characteristic is the slope of the regression line and the hypothesized value is unity.

3.6.2 Coefficient of Variation (CV)

This coefficient indicates the degree of variation of the data set. It is computed by simply dividing the mean of the data by the standard deviation. It is commonly represented in percentile.

$$CV = (meanETr)\left(\frac{100}{s}\right) \quad [68]$$

CV= coefficient of variation, percent

$meanET_r$= average computed or measured ET_r, mm d^{-1}

s= standard deviation of computed or measured ET_r, mm d^{-1}

3.6.3 Standard Error of Estimation, SEE and SEER

In the context of this study, the standard error of estimation (SEE) refers to the standard error of the estimation of raw computed reference evapotranspiration data using methods such as the pan or the combination equations. This value is not related to regression analysis, and is different from the standard error of estimate obtained for the regression fit which in this study is termed SEER.

The equation used to computed the SEE or the SEER is the same and is given below:

$$SEE = \left(\frac{\sum (ETr_{(lys)} - ETr_{(computed)})^2}{n-2} \right)^{\left(\frac{1}{2}\right)} \quad [69]$$

Note that [n-2] was used instead of n since we assumed the variables were independent and therefore the degree of freedom was n-2. The SEER was also computed using equation [69]. $ET_{r(computed)}$ in this case was calculated using the regression coefficients a and b.

4 ANALYSIS AND RESULTS

This section describes the analysis performed and the results obtained for the various estimating methods at each site. The methods discussed in this chapter include the pan evaporation method with constant annual and variable pan coefficients, Priestly-Taylor method with constant and variable coefficient α, and two combination methods, the original Penman method and the Penman-Monteith method. As described in Section 3.6, two types of analysis were performed. The first type was confined to studying the errors on a daily basis from year to year. This was essential to check whether the method was biased in each year during a particular season or month. It was necessary to study the results year by year to verify whether the bias was invariable. To check whether the correlation between the estimating method and the lysimeter was uniform from year to year, regression analysis was performed on a year by year basis. The second type of analysis included an evaluation of the performance of the each method at each site. All the available data points were used at each site without regard to time. Regression analysis employing two models were utilized to evaluate and recommend the optimum method at each site. Climatic calibration coefficients were derived from the second type of analysis to improve the performance of the estimating method. Validation studies to test the calibration coefficients were performed. Moving averages for specified number of days were applied to reduce the scatter and estimate the optimum averaging interval. The coefficient of determination and the standard error of estimates were computed. A relation between the standard error of estimate, the coefficient of determination, and the number of days in the averaging period was obtained for each site and method. Before results are presented, it is necessary to establish some basic statistics for each lysimeter to perform the Z test for the errors of estimates.

4.1 Statistical Analysis For Available Lysimeter Data

This section presents some basic statistical results computed for each lysimeter at each site for each year to perform the Z statistical test. The null hypothesis was stated in Section 3.6.1 and assumed the error of estimate was zero. The critical Z statistic was 1.96. The subsequent sections utilize the results presented in Table 6 for error analysis. Table 6 displays the number of days used in each year at each site.

Table 6. Summary of lysimeter data statistics.

Site Location	Year	Days Used	Mean Measured ETr (mm d^{-1})	Standard Deviation (mm d^{-1})	Coefficient Of Variation (%)
Davis	1965	332	3.81	2.31	60.78
	1966	330	4.01	2.24	55.80
	1967	343	3.59	2.08	58.07
	1968	343	3.78	2.39	63.11
	1969	339	3.86	2.26	58.55
	1970	342	3.77	2.35	62.45
	1971	351	3.76	2.28	60.70
Kimberly	1969	169	4.92	2.30	46.72
	1970	147	4.88	2.10	43.00
	1971	142	4.45	2.56	57.56
Versailles	1968	219	2.30	1.53	66.40
	1969	272	2.17	1.68	77.54
	1971	168	2.91	1.48	50.82
	1972	194	2.36	2.54	50.13
	1973	187	2.70	1.71	63.42
	1974	153	3.05	1.48	48.51
	1975	246	2.45	1.77	72.10
	1976	266	3.17	2.20	69.41

4.2 Pan Evaporation Method

As discussed in Sections 1.3, 3.1.1, 3.1.2, and 3.3, pan evaporation data were available at Davis and Kimberly. The potential to estimate reference evapotranspiration from these data was examined. A suggested procedure for estimating the class A pan coefficient utilizing meteorological data and fetch distance was discussed in Section 3.5.1. Two approaches were used to compute pan coefficients. The first approach employs a constant pan coefficient and the second approach varies the pan coefficient on a daily basis. Section 4.2.1 presents the results obtained by utilizing this procedure to obtain the pan coefficient.

4.2.1 Estimating Pan Coefficients

One of the important variables affecting the pan coefficient is the fetch distance (d). The average fetch distance for the period of interest was computed using an estimated pan coefficient and meteorological data. The period of interest for Davis was the full year (January 1 to December 31). The period of interest for Kimberly was the growing season (April 1 to October 31).

Average wind speed and mean air relative humidity were computed for a period of seven years for Davis (1965-1971). The pan coefficient was obtained by performing a linear regression between daily pan evaporation data and daily reference evapotranspiration for the combined seven years. The slope of the regression was called the estimated pan coefficient.

The regression was forced through the origin to integrate all errors into the regression slope. Using the average wind speed, average air relative humidity for the seven years of data combined, and the estimated pan coefficient, the fetch distance was solved for iteratively

for Davis using equation [3]. The midpoint iteration technique with a convergence criteria of 0.001 m was employed. The computed fetch distance was 40 m rounded to the nearest meter. This fetch distance was assumed constant throughout the analysis for Davis.

Similar analysis was performed for Kimberly. The period used to compute the average air relative humidity and wind speed was the growing season for three years (1969-1971). The computed fetch distance was 17 m and was rounded to 20 m. The computed fetch distance coincided with the expected fetch conditions for the Kimberly site.

The class A pan at Kimberly was situated at the center of a 45 m by a 36 m grass plot. The grass was irrigated from April to October. During the periods from January to April and from October to December, the grass was considered in a dormant stage and was not irrigated. This average fetch distance was assumed constant for each individual year in the analysis. Table 7 summarizes the fetch distances used at Davis and Kimberly.

Table 7. Summary of fetch distances for Davis and Kimberly.

Site	Wind Speed ($m\ s^{-1}$)	Mean Relative Humidity (%)	Fetch Distance (m)
Davis	2.32	66.67	40
Kimberly	2.70	58.18	20

Using the fetch distances indicated in Table 7 with mean annual wind speed and relative humidity, the annual pan coefficients were calculated from equation [3] for Davis and Kimberly.

The results of equation [3] and the pan coefficients obtained by regressing the pan evaporation with lysimeter reference evapotranspiration for the corresponding year are summarized in Table 8 for Davis and Table 9 for Kimberly. The annual pan coefficients obtained by regressing pan evaporation with reference evapotranspiration for each year is termed measured pan coefficient since the measured lysimeter reference evapotranspiration was employed. The regression performed to obtain the measured pan coefficient was forced through the origin to integrate all errors into the computed regression slope.

Table 8. Summary of annual pan coefficients for Davis.

Year	Wind Speed ($m\ s^{-1}$)	Mean Relative Humidity (%)	Estimated Pan Coefficient	Measured Pan Coefficient
1965	2.07	73.05	0.76	0.79
1966	2.32	65.20	0.73	0.76
1967	2.17	66.81	0.74	0.76
1968	2.33	67.82	0.74	0.72
1969	2.36	66.80	0.74	0.74
1970	2.53	63.20	0.72	0.69
1971	2.46	63.68	0.72	0.73
Avg	2.32	66.67	0.74	0.74

Table 9. Summary of annual pan coefficients for Kimberly.

Year	Wind Speed ($m\ s^{-1}$)	Mean Relative Humidity (%)	Estimated Pan Coefficient	Measured Pan Coefficient
1969	2.75	56.56	0.68	0.67
1970	2.69	59.28	0.68	0.68
1971	2.60	58.66	0.69	0.65
Avg	2.68	58.17	0.68	0.67

The agreement between the estimated and measured pan coefficient for Davis was good. The errors in the pan coefficient ranged from 0 to 4.5 percent for Davis. The maximum percent error occurred in 1970 with an estimated pan coefficient of 0.72 and a measured pan coefficient of 0.69. Similar conclusions can be inferred from Table 9 for Kimberly. The maximum deviation in Kimberly occurred in 1971. The estimated pan coefficient for 1971 was 0.69 and the measured pan coefficient obtained from regression was 0.65.

The previous discussion assumed the pan coefficient constant throughout the year. An attempt to vary the pan coefficient on a daily basis was considered at both sites. In this approach, the fetch distance computed for each site was assumed constant for each day and each year. The pan coefficient was computed on a daily basis using average daily air relative humidity and average daily wind speed at 2 m height. The subsequent section presents the results of the two pan methods with constant and variable pan coefficient. The term modified pan method was used for the variable pan coefficient method.

4.2.2 Pan Evaporation Method With Constant Pan Coefficient

This section presents the results of the analysis performed for the constant annual pan coefficient method for Davis and Kimberly. The analysis includes two parts. The first part presents the error analysis, and the second presents the regression analysis.

4.2.2.1 Error Analysis

Error analysis was performed in accordance with the procedure discussed in Section 3.6 for the three sites. The error was calculated by subtracting computed reference evapotranspiration from measured lysimeter data. The Z test was employed to check whether the average error computed using the pan evaporation with constant pan coefficient was significantly different from zero. The results are summarized in Table 10 for Davis and Table 11 for Kimberly. Included in Tables 10 and 11 are the standard error of estimation, SEE. The standard error of estimation was computed using equation [69].

Table 10. Summary of Z statistics for pan evaporation method, Davis.

Year	Mean Estimated ETr (mm d^{-1})	Standard Deviation (mm d^{-1})	Coefficient Of Variation (%)	SEE (mm d^{-1})	Z Statistic (T/F)
1965	3.62	2.22	61.30	0.67	1.07 (T)
1966	3.78	2.20	57.98	0.74	1.26 (T)
1967	3.42	2.07	60.34	0.71	1.03 (T)
1968	3.78	2.55	67.52	0.66	0.02 (T)
1969	3.82	2.27	59.42	0.69	0.25 (T)
1970	3.78	2.50	66.21	1.00	0.07 (T)
1971	3.67	2.17	59.03	0.77	0.51 (T)

Table 11. Summary of Z statistics for pan evaporation method, Kimberly.

Year	Mean Estimated ETr (mm d^{-1})	Standard Deviation (mm d^{-1})	Coefficient Of Variation (%)	SEE (mm d^{-1})	Z Statistic (T/F)
1969	4.66	1.75	37.62	1.03	1.20 (T)
1970	4.60	1.46	31.87	1.36	1.36 (T)
1971	4.50	1.75	38.78	1.46	0.20 (T)

The null hypothesis was true for each year in Davis and Kimberly and the average annual error was not different from zero. This

indicates that the pan evaporation method can be used for estimating average reference evapotranspiration for annual periods in Davis and Kimberly.

Normal probability distribution analysis of the error was performed at both sites to check whether the scatter was random in the growing season. Figures 8, 9, 10, and 11 are sample plots presented to display the normal distribution checks performed for each year in Davis and Kimberly.

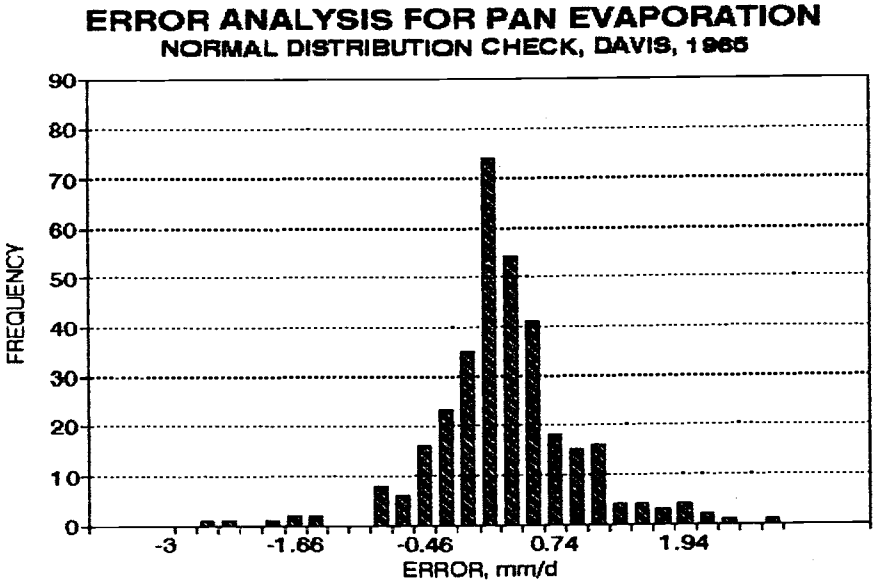

Figure 8. Plot of the error distribution versus frequency of occurrence for pan evaporation, Davis, 1965.

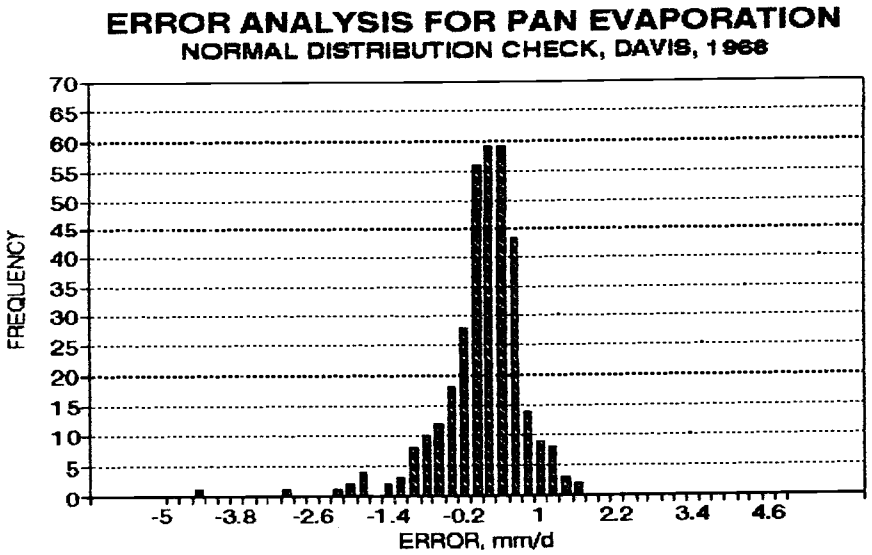

Figure 9. Plot of the error distribution versus frequency of occurrence for pan evaporation, Davis, 1968.

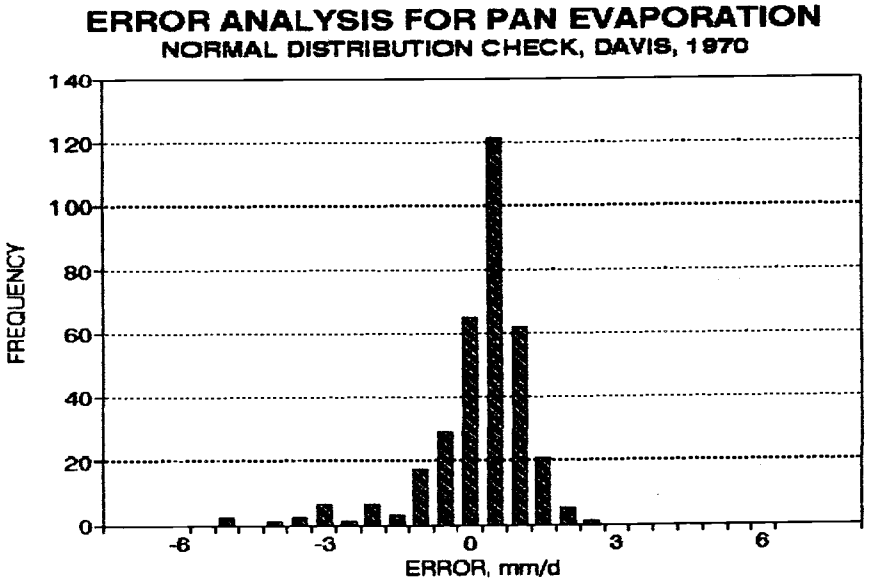

Figure 10. Plot of the error distribution versus frequency of occurrence for pan evaporation, Davis, 1970.

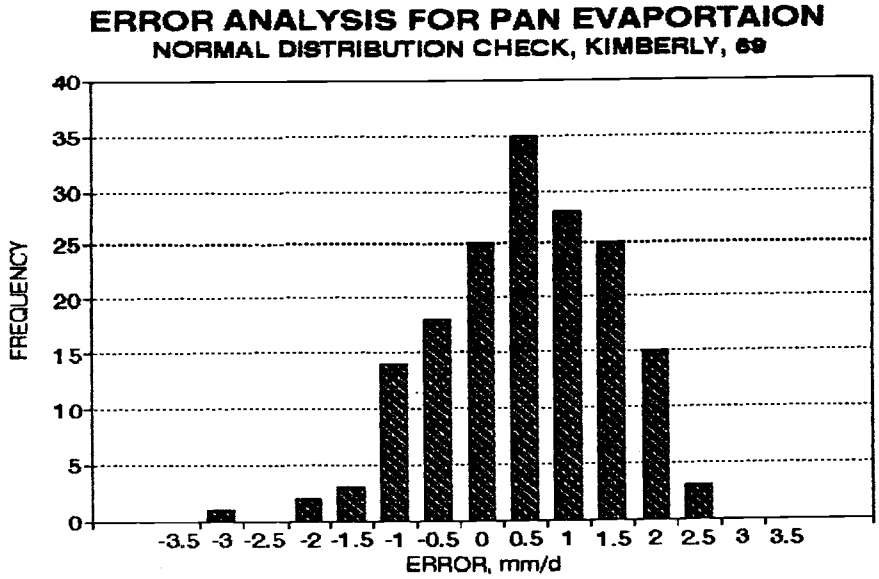

Figure 11. Plot of the error distribution versus frequency of occurrence for pan evaporation, Kimberly, 1969.

The highest frequencies at both sites correspond to the error intervals close to zero. This confirms the Z test results and the method was not biased for the growing season. In addition, the shape of the error distribution graphs appears normal.

These were typical normal distribution graphs obtained for the pan evaporation method. These plots indicate the errors tend to cancel each other during the growing season at Davis and Kimberly. However, no indication can be inferred whether for some particular month or season the error was normal. In order to inspect whether this was the case, the error of estimation was plotted versus Julian day for both sites. Sample graphs for 1965, 1968, 1970 at Davis and 1969 at Kimberly are presented in Figures 12, 13, 14, and 15 respectively.

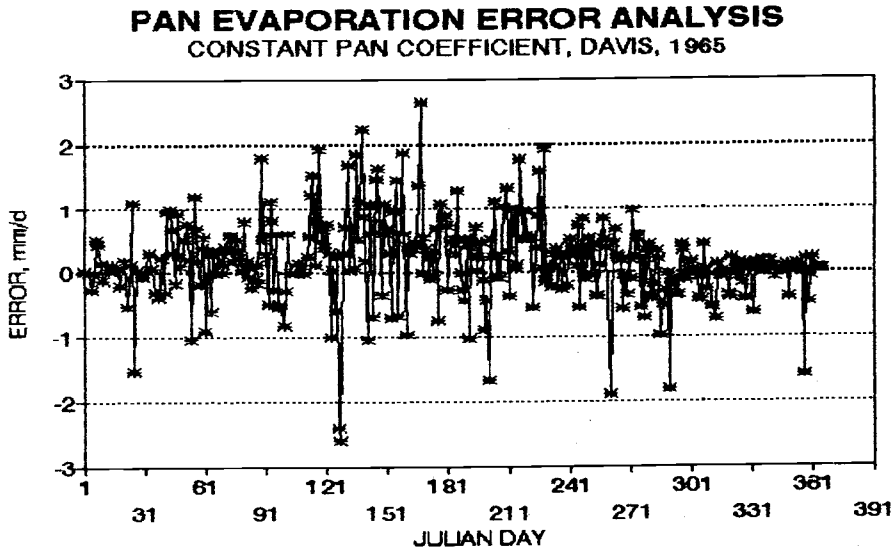

Figure 12. Plot of error versus Julian day for pan evaporation, Davis, 1965.

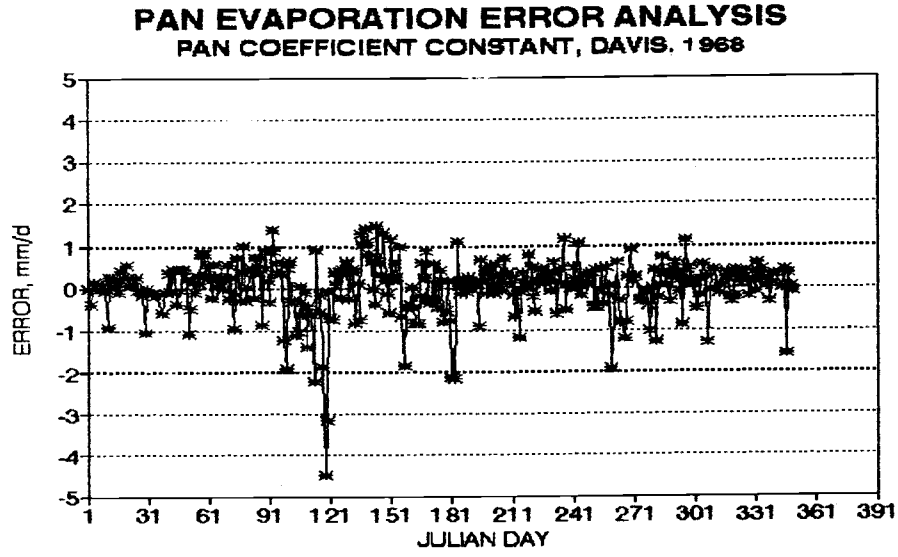

Figure 13. Plot of error versus Julian day for pan evaporation, Davis, 1968.

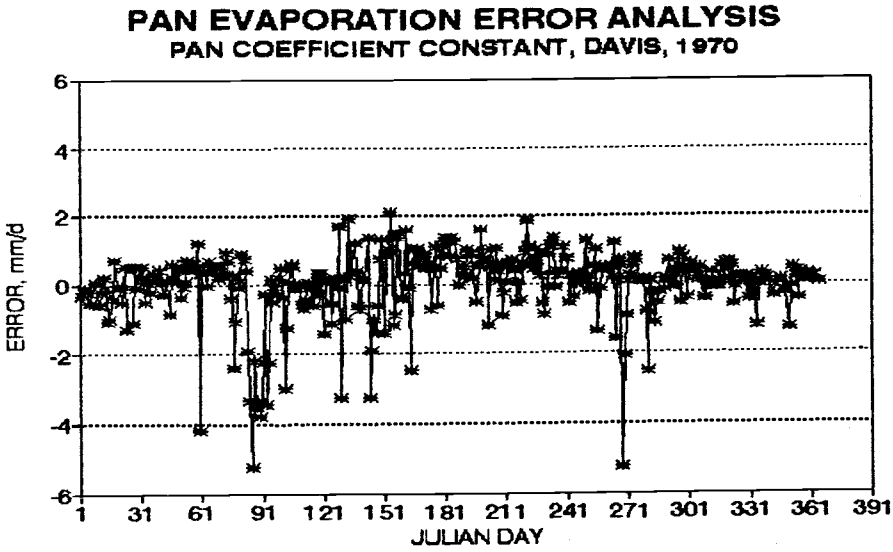

Figure 14. Plot of error versus Julian day for pan evaporation, Davis, 1970.

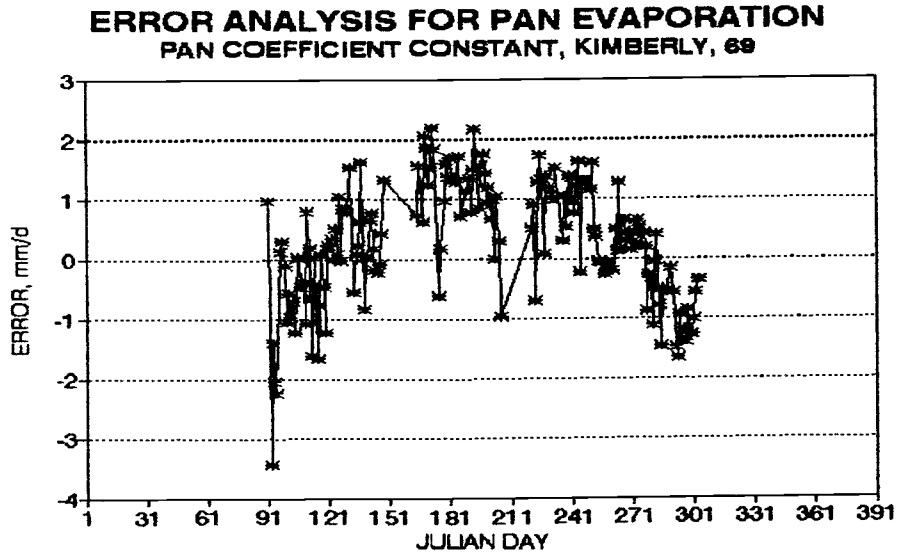

Figure 15. Plot of error versus Julian day for pan evaporation, Kimberly, 1969.

For 1965 the pan evaporation underestimated reference evapotranspiration from Julian day 184 to Julian day 243 at Davis. This indicated the pan evaporation method for 1965 tended to underestimate reference evapotranspiration from July to September. Therefore, for the summer of 1965 the errors were not randomly distributed.

For 1970, the pan evaporation method underpredicted reference evapotranspiration from day 181 to day 241. This corresponds to the same period observed in 1965. For 1968, which was the typical plot for Davis, no such seasonal trends were noted.

It was noted for 1969 at Kimberly, the pan underestimated reference evapotranspiration during the period ranging from Julian day 181 to Julian day 271. This period corresponds to the months of June, July, and August. The same seasonal trend was noted in 1970.

To further validate the seasonal observations, the cumulative ETr versus Julian day was plotted for each year at each site. The slope of the cumulative curve can indicate the Julian day in which the drift from the lysimeter occurred. Sample cumulative plots for Davis are presented in Figures 16, 17, and 18 for 1965, 1968, and 1970, respectively. A sample cumulative plot for Kimberly is presented in Figure 19 for 1969.

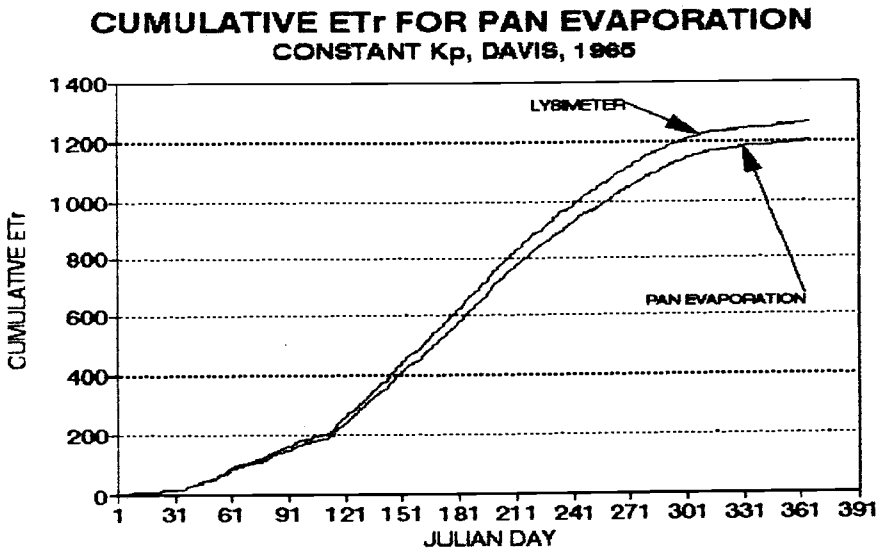

Figure 16. Cumulative ETr (mm) versus Julian day for pan evaporation, Davis, 1965.

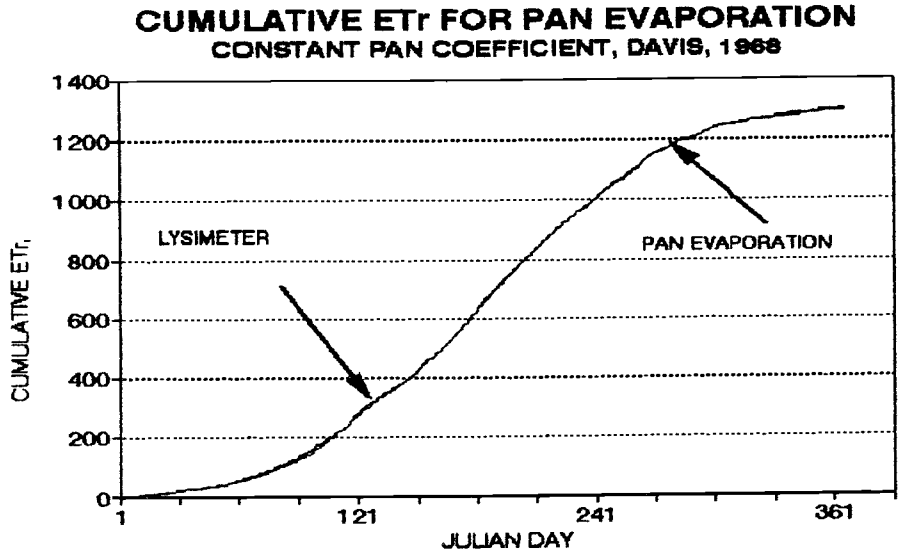

Figure 17. Cumulative ETr (mm) versus Julian day for pan evaporation, Davis, 1968.

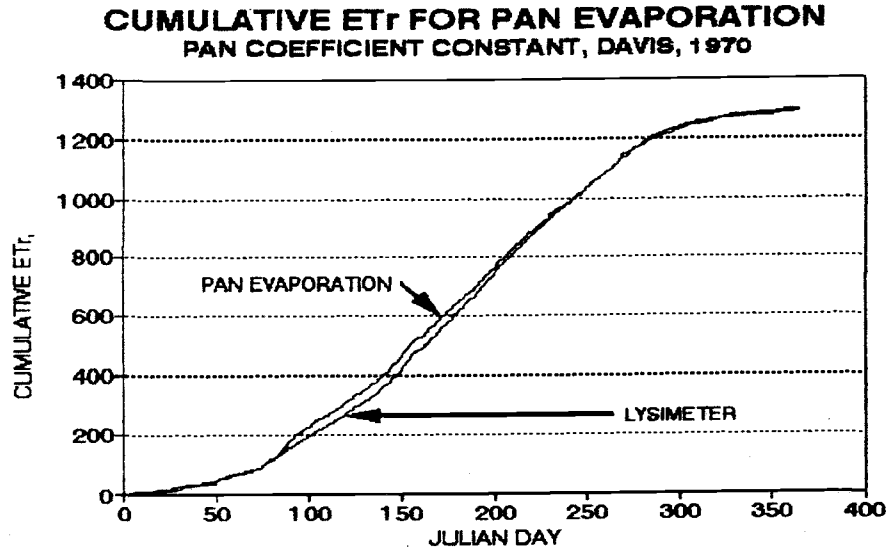

Figure 18. Cumulative ETr (mm) versus Julian day for pan evaporation, Davis, 1970.

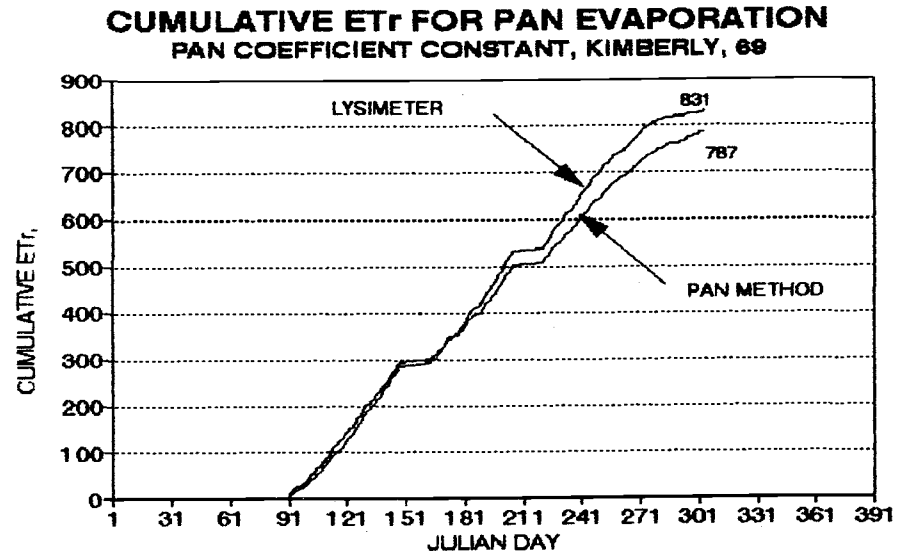

Figure 19. Cumulative ETr (mm) versus Julian day for pan evaporation, Kimberly, 1969.

For Davis, 1965, the slope of the cumulative estimated reference evapotranspiration drifted in value from the lysimeter. This drift confirmed the speculations of the error analysis graph presented. Figure 16 shows the drift of slopes from the lysimeter was appreciable from day 181 to 241. The slopes then are equal for the fall months. In 1968, the two cumulative graphs traced each other closely indicating strong correlation between the estimated and measured evapotranspiration. The 1968 plot was considered the representative plot for the remaining years.

In Kimberly, it was noted the slopes vary from each other during the period ranging from day 181 to day 271. After Julian day 271 it was noted the slopes of the cumulative plots are equal. Therefore, the pan tends to underestimate reference evapotranspiration for the period ranging from Julian day 181 to Julian day 271. The same trend was noted for 1970 and 1971. In addition, the pan cumulative plot flattens out at the end of fall at the same rate as the lysimeter.

4.2.2.2 Regression Analysis

Linear regression analysis between estimated reference evapotranspiration and measured reference evapotranspiration was performed at Davis and Kimberly. Results of the regression are outlined in the Tables 12 and 13 for Davis and Kimberly, respectively. The Z statistic test was utilized to check whether the slope of the regression was significantly different from unity. The null hypothesis in this case states the slope of the regression line is not statistically different from 1.0. Note that the Z critical is 1.96 since the sample size exceeds 120 observations for Davis and Kimberly for each year.

Included in the regression analysis are the coefficient of determination and the standard error of estimate for the fit (SEER) for each year at Davis.

Table 12. Summary of regression analysis for pan evaporation method, Davis.

Year	Coefficient of Determination (r^2)	SEER mm d^{-1}	Slope of Regression	Constant of Regression	Z Statistic (95 %) (T/F)
1965	0.92	0.65	1.01	0.18	0.14 (T)
1966	0.90	0.69	0.97	0.34	1.78 (T)
1967	0.89	0.68	0.95	0.33	2.61 (F)
1968	0.94	0.61	0.905	0.36	7.36 (F)
1969	0.91	0.68	0.95	0.23	3.03 (F)
1970	0.84	0.94	0.86	0.53	7.35 (F)
1971	0.89	0.76	0.99	0.12	0.42 (T)

Table 13. Summary of regression analysis for pan evaporation method, Kimberly.

Year	Coefficient of Determination (r^2)	SEER (mm d^{-1})	Slope of Regression	Constant of Regression	Z Statistic (95 %) (T/F)
1969	0.84	0.92	1.20	-0.68	5.02 (F)
1970	0.65	1.25	1.16	-0.45	2.27 (F)
1971	0.71	1.40	1.23	-1.10	3.45 (F)

Table 12 indicates four out of seven years at Davis the slope was significantly different from unity. However, strong correlation was noted. The coefficient of determination equalled or exceeded 0.89 for six out of seven years. This indicated consistent correlation between the pan evaporation method and the lysimeter. The weakest correlation was noted in year 1970 were the pan tended to underestimate reference evapotranspiration during the summer as noted in Section 4.2.2.1.

It was noted in Kimberly that the coefficient of determination was low for 1970. The slopes of the regression curves were statistically significant from unity indicating a unit change in lysimeter reference evapotranspiration did not correspond to a unit change in the pan estimated reference evapotranspiration. In addition, the SEER were consistently higher than Davis except for one year.

4.2.3 Pan Evaporation Method With Variable Pan Coefficient

The daily pan coefficient at Davis and Kimberly was computed using equation [3], average air relative humidity and wind speed, and a constant fetch distance estimated for each site. This method was called the modified pan evaporation method.

4.2.3.1 Error Analysis

Error analysis was performed in accordance with the procedure discussed in Section 3.6 for the three sites. The error was calculated by subtracting computed reference evapotranspiration from measured lysimeter data. The Z test was used to check whether the average growing season error computed using the pan evaporation with variable pan coefficient was significantly different from zero. The results are summarized in Table 14 for Davis and Table 15 for Kimberly.

Table 14. Summary of Z Statistics for modified pan evaporation method, Davis.

Year	Mean Estimated ETr (mm d^{-1})	Standard Deviation (mm d^{-1})	Coefficient Of Variation (%)	SEE (mm d^{-1})	Z Statistics (T/F)
1965	3.58	2.25	63.03	0.66	0.38 (T)
1966	3.85	2.10	54.44	0.64	0.80 (T)
1967	3.52	2.05	58.13	0.57	0.41 (T)
1968	3.82	2.42	63.32	0.52	0.16 (T)
1969	3.88	2.19	56.65	0.58	0.10 (T)
1970	3.79	2.30	60.69	0.75	0.14 (T)
1971	3.76	2.14	56.89	0.67	0.04 (T)

Table 15. Summary of Z statistics for modified pan evaporation method, Kimberly.

Year	Mean Estimated ETr (mm d^{-1})	Standard Deviation (mm d^{-1})	Coefficient Of Variation (%)	SEE (mm d^{-1})	Z Statistics (T/F)
1969	4.57	1.65	36.16	1.06	1.61 (T)
1970	4.64	1.45	31.82	1.47	1.14 (T)
1971	4.43	1.72	38.80	1.68	0.08 (T)

The null hypothesis was true for each year in Davis and Kimberly and the average annual error was not different from zero at both sites. This indicates that the pan evaporation method can be used for estimating average reference evapotranspiration for the growing season without significant loss of accuracy.

For Kimberly, the SEE were not substantially lower than the constant pan coefficient method. For 1969, an increase in SEE was even noted. For 1970, the SEE was reduced by 0.07 mm d^{-1}. For 1971, the SEE was reduced by 0.06 mm d^{-1}.

4.2.3.2 Regression Analysis

Tables 15 and 16 present the regression performed between estimated and measured ET_r for both sites. The coefficients of determination obtained using the variable pan evaporation coefficient for Davis were equal or higher than the coefficients of determination obtained using the constant coefficient. Therefore, it can be concluded a higher correlation between measured and computed ET_r results when the pan coefficient was varied. The SEER for the variable pan coefficient were reduced when compared to the constant pan coefficient method at Davis.

In addition, the slope of the regression was statistically equal to unity six out of seven years unlike the pan evaporation method with constant pan coefficient. A unit change in estimated ET_r corresponded to a unit change in measured ET_r consistently at Davis. The regression analysis at Kimberly indicates that the coefficient of determination did increase and the SEER did drop. The standard error of estimate increased in Kimberly by varying the pan coefficient on a daily basis, and the method was not pursued for both sites.

Table 16. Summary of regression analysis for modified pan evaporation method, Davis.

Year	Coefficient of Determination (r^2)	SEER (mm d^{-1})	Slope of Regression	Constant of Regression	Z Statistic (95 %) (T/F)
1965	0.92	0.65	1.00	0.06	0.17 (T)
1966	0.92	0.62	1.03	0.03	1.70 (T)
1967	0.93	0.55	0.98	0.13	1.30 (T)
1968	0.96	0.51	0.97	0.01	2.90 (F)
1969	0.94	0.59	1.00	0.01	0.00 (T)
1970	0.91	0.74	0.98	0.10	1.88 (T)
1971	0.92	0.66	1.02	-0.08	1.21 (T)

Table 17. Summary of regression analysis for modified pan evaporation method, Kimberly.

Year	Coefficient of Determination (r^2)	SEER mm d^{-1}	Slope of Regression	Constant of Regression	Z Statistic (95 %) (T/F)
1969	0.85	0.90	1.28	-0.91	6.55 (F)
1970	0.69	1.17	1.20	-0.66	3.25 (F)
1971	0.76	1.31	1.31	-1.33	4.96 (F)

4.3 Original Priestly-Taylor Method

This section presents the error analysis and regression analysis for the original Priestly-Taylor method for Davis, Kimberly, and Versailles. The original Priestly-Taylor method assume the net radiation as the driving components of reference evapotranspiration. The method assumes a constant α equal to 1.26 as recommended by Priestly and Taylor over saturated surfaces. The lysimeters were irrigated for maintaining reference conditions, and the surface can be assumed close to field capacity.

The Versailles site serves as the low advection, humid site in this study. The climatic conditions of Versailles adhere to the assumptions presented by Priestly and Taylor (1972). Allen (1986) demonstrated the Priestly-Taylor equation provided good estimates at Coshocton, Ohio where humidities are high and advection is minimal. Coshocton and Versailles have very similar climates. The subsequent section presents the results for the original Priestly-Taylor analysis.

4.3.1 Error Analysis

The error analysis was performed in accordance with the procedure discussed in Section 3.6. The results are summarized in the Table 18, 19, and 20 for Davis, Kimberly, and Versailles respectively.

Table 18. Summary of Z statistic for original Priestly-Taylor method, Davis.

Year	Mean Estimated ETr (mm d^{-1})	Standard Deviation (mm d^{-1})	Coefficient Of Variation (%)	SEE (mm d^{-1})	Z Statistic (T/F)
1965	3.19	2.22	69.22	1.37	3.47 (F)
1966	3.66	2.31	63.21	1.22	1.95 (T)
1967	3.44	2.34	68.20	1.20	0.88 (T)
1968	3.59	2.42	67.47	1.11	1.04 (T)
1969	3.55	2.47	69.74	1.13	1.73 (T)
1970	3.55	2.34	65.87	1.06	1.21 (T)
1971	3.44	2.28	66.28	1.12	1.83 (T)

Table 19. Summary of Z statistic for original Priestly-Taylor, Kimberly.

Year	Mean Estimated ETr (mm d^{-1})	Standard Deviation (mm d^{-1})	Coefficient Of Variation	SEE (mm d^{-1})	Z Statistic (T/F)
1969	3.66	1.39	38.11	1.82	6.13 (F)
1970	3.67	1.31	35.70	1.78	5.90 (F)
1971	3.98	1.13	28.47	1.79	2.04 (F)

For Davis, the null hypothesis was true for six years out of seven, and the method can be used for estimating average annual ET_r without significant loss in accuracy. The errors over the year were normally distributed throughout. Sample plots in Figures 20, 21, and 22 for 1965, 1968, and 1970 display the normal distribution checks for Davis. For Kimberly, the null hypothesis was false for each year and the method cannot be used for estimating average annual ET_r without significant loss in accuracy. The errors do not appear to be normally distributed throughout the year. Figure 23 displays a typical distribution check

Table 20. Summary of Z statistic for original Priestly-Taylor method, Versailles.

Year	Mean Estimated ETr (mm d^{-1})	Standard Deviation (mm d^{-1})	Coefficient Of Variation	SEE (mm d^{-1})	Z Statistic (T/F)
1968	2.53	1.33	52.74	0.66	1.89 (T)
1969	2.27	1.56	68.85	0.57	0.70 (T)
1971	2.74	1.37	49.90	0.73	0.35 (T)
1972	2.53	1.25	49.20	0.64	1.40 (T)
1973	2.76	1.59	57.44	0.73	0.39 (T)
1974	2.70	1.68	61.98	0.66	0.45 (T)
1975	2.46	1.60	64.87	0.67	0.08 (T)
1976	2.74	1.57	57.26	1.08	2.57 (F)

for Kimberly. For Versailles, the null hypothesis was false only one year, and the method can be used for estimating average annual ETr without significant loss in accuracy. The deviation from lysimeter values were normally distributed throughout the year. A sample plot displayed in Figure 24 shows the normal distribution check performed at Versailles.

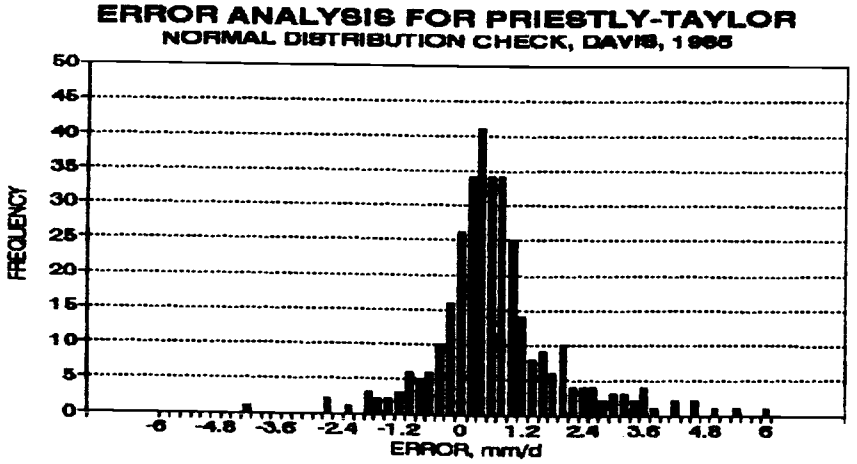

Figure 20. Plot of the error distribution versus frequency of occurrence for original Priestly-Taylor, Davis, 1965.

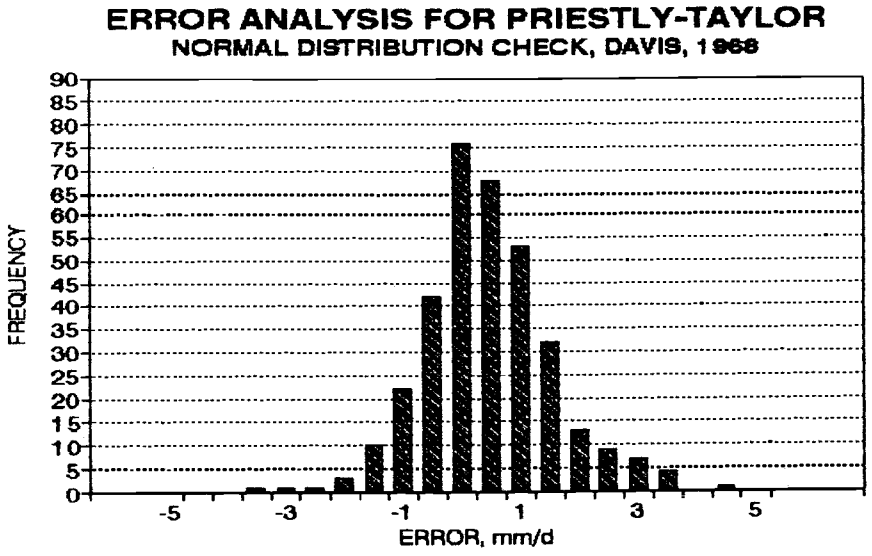

Figure 21. Plot of the error distribution versus frequency of occurrence for original Priestly-Taylor, Davis 1968.

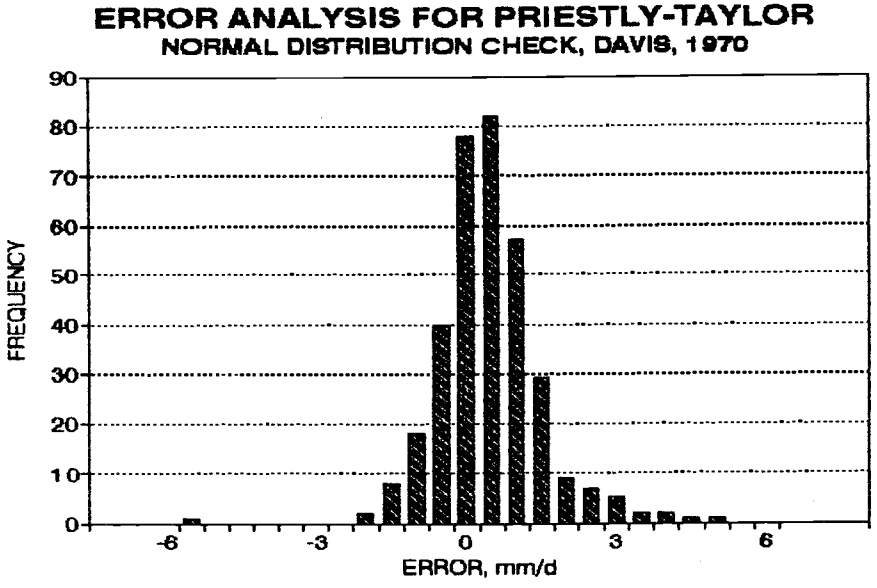

Figure 22. Plot of the error distribution versus frequency of occurrence for original Priestly-Taylor, Davis 1970.

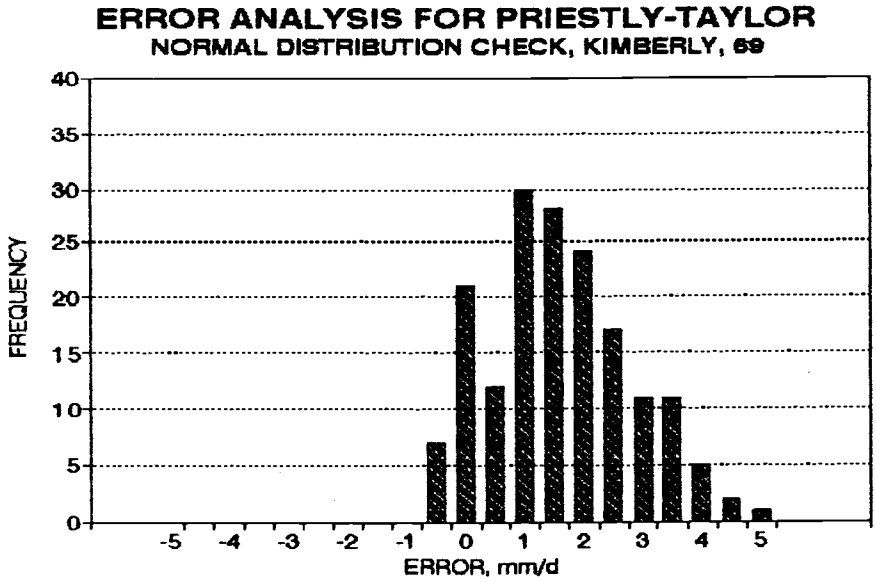

Figure 23. Plot of the error distribution versus frequency of occurrence for original Priestly-Taylor, Kimberly, 1969.

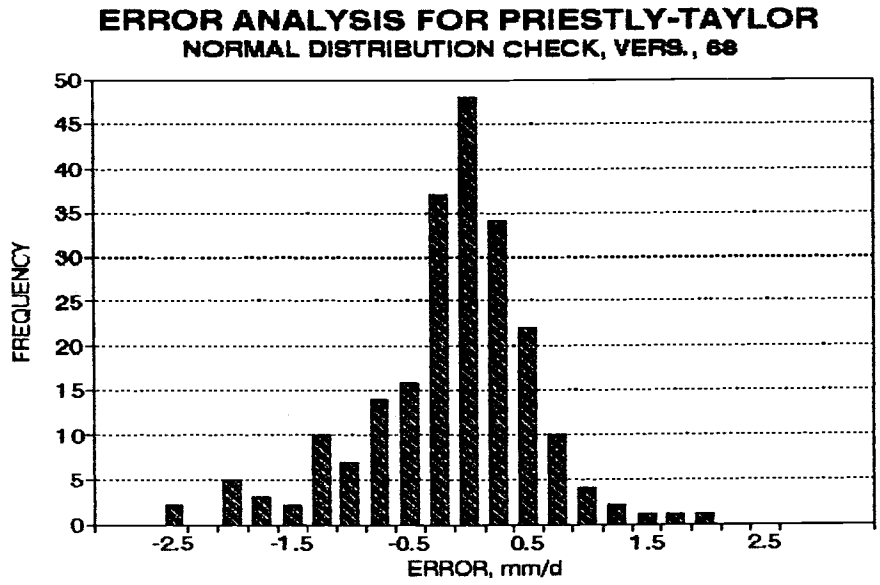

Figure 24. Plot of the error distribution versus frequency of occurrence for original Priestly-Taylor, Versailles, 1968.

For Davis, the highest frequencies correspond to the error intervals close to zero except for 1965 at Davis. Note in 1965, the Z test indi-

cated the average annual computed reference evapotranspiration was statistically different from the average annual lysimeter evapotranspiration. Therefore the maximum frequency did not occur at zero. However, in all cases the error was characterized by a bell-shaped normal curve.

The error of estimation was plotted versus Julian day for each year at Davis, Kimberly, and Versailles to check whether the method tends to overpredict or underpredict during a specific season or month. Sample graphs for 1965, 1968, and 1970 for Davis are shown in Figures 25, 26 and 27. Sample graphs for Kimberly and Versailles are presented in Figures 28 and 29 respectively.

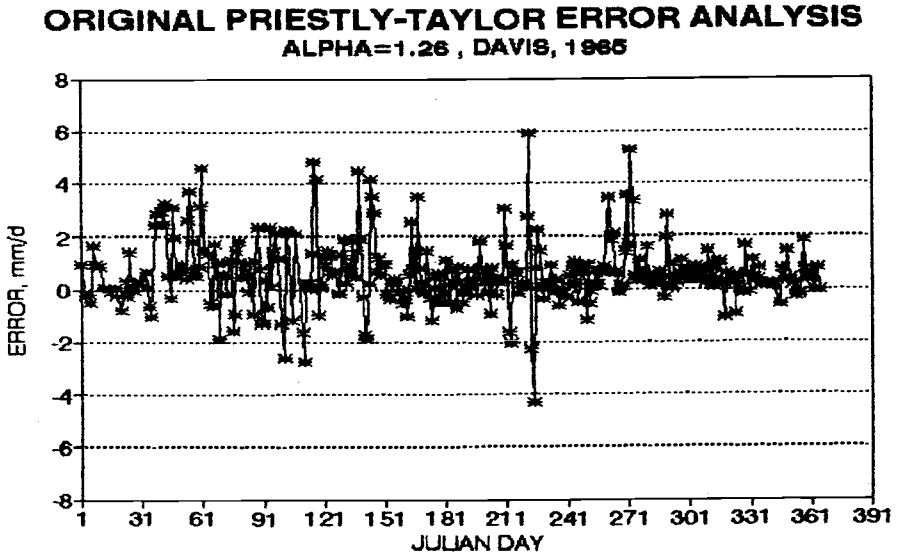

Figure 25. Plot of error versus Julian day for original Priestly-Taylor method, Davis, 1965.

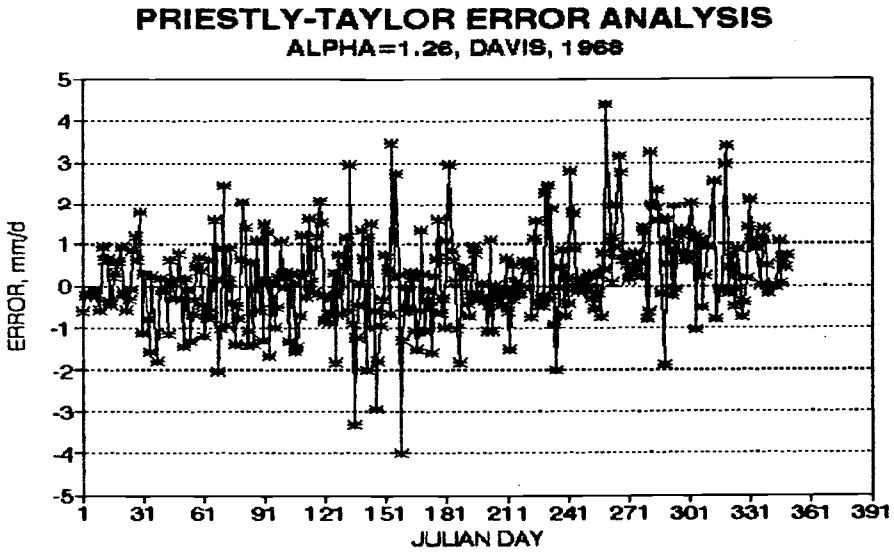

Figure 26. Plot of error versus Julian day for original Priestly-Taylor method, Davis, 1968.

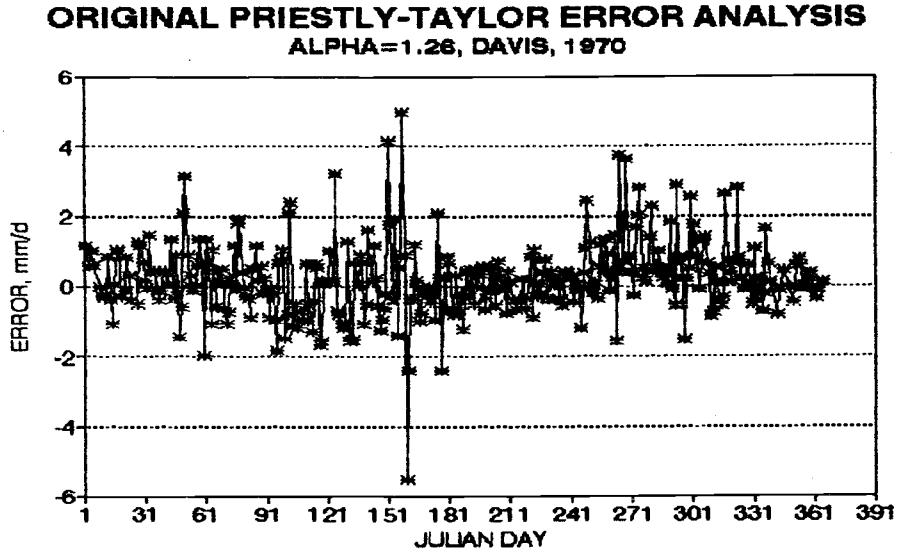

Figure 27. Plot of error versus Julian day for original Priestly-Taylor method, Davis, 1970.

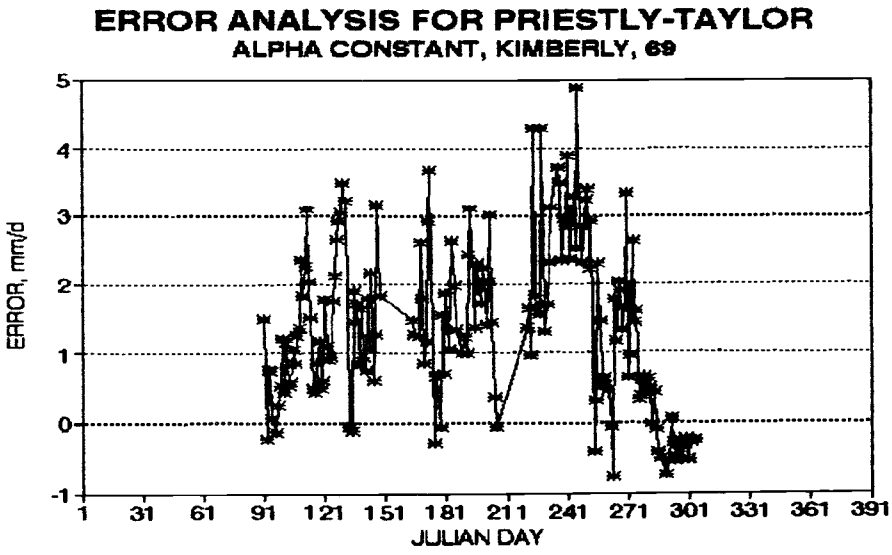

Figure 28. Plot of error versus Julian day for original Priestly-Taylor, Kimberly, 1969.

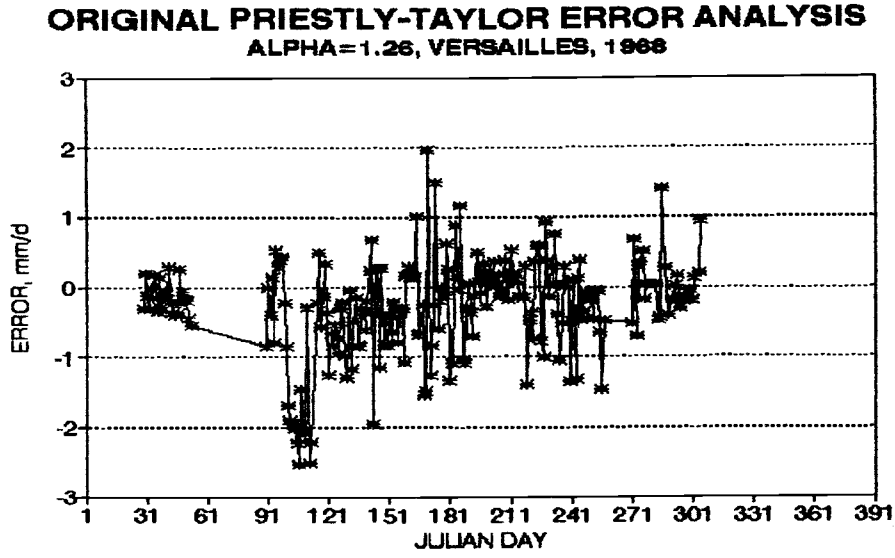

Figure 29. Plot of error versus Julian day for original Priestly-Taylor, Versailles, 1968.

The graphs presented displayed some typical seasonal trends. For Davis, 1965 the method underestimated ET_r from Julian day 31 to Julian day 151. The same applied to the months of September, October, and November (Julian days 244 to 334). In 1968, September and October have low ET_r values. In 1970, the same phenomena occurred. It was concluded the Priestly-Taylor underestimated reference evapotranspiration during the fall at Davis.

For Kimberly, the method tends to underestimate reference evapotranspiration for the growing season. This can be noted in Figure 28 since all the errors are positive in sign. For Versailles, the method tends to overpredict ET_r from Julian day 91 to 151 (April 1 to June 1) as shown in Figure 29.

As a final verification, cumulative ET_r plots were produced at the three sites. Figures 30, 31, and 32 present the cumulative results for Davis. Figure 33 displays the results for Kimberly and Figure 34 the results for Versailles.

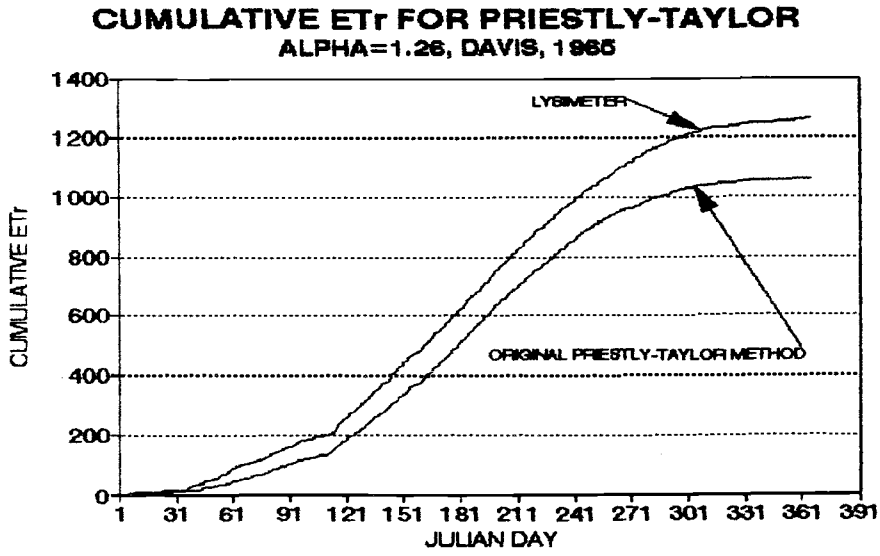

Figure 30. Cumulative ETr (mm) versus Julian day for original Priestly-Taylor, Davis, 1965.

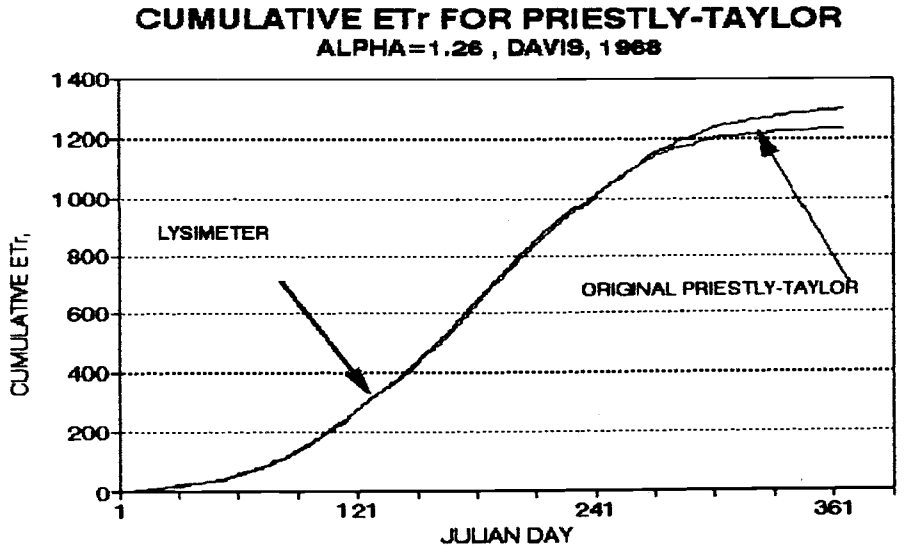

Figure 31. Cumulative ETr (mm) versus Julian day for original Priestly-Taylor, Davis, 1968.

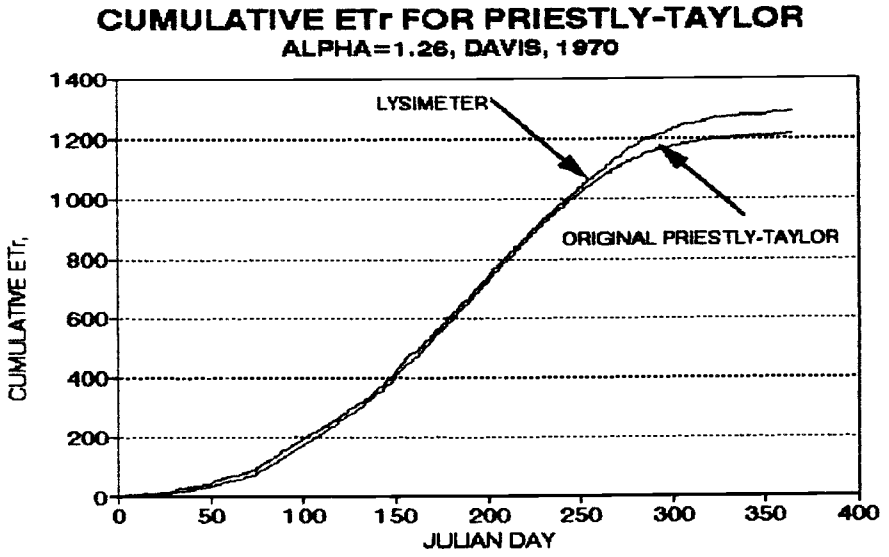

Figure 32. Cumulative ETr (mm) versus Julian day for original Priestly-Taylor, Davis, 1970.

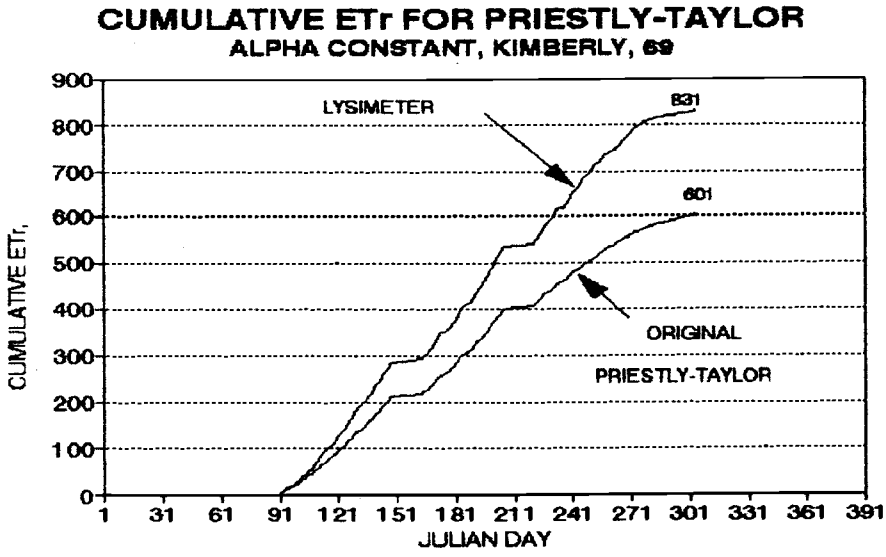

Figure 33. Cumulative ETr (mm) versus Julian day for original Priestly-Taylor, Kimberly, 1969.

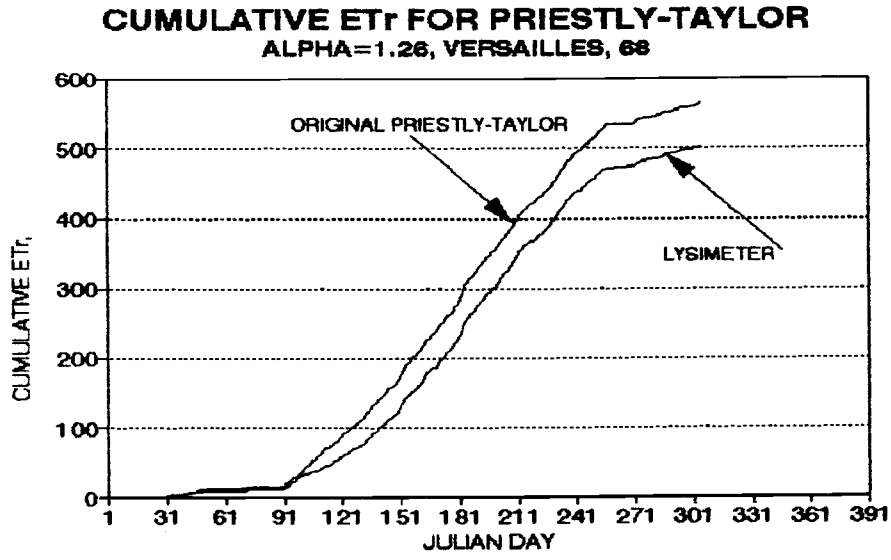

Figure 34. Cumulative ETr (mm) versus Julian day for original Priestly-Taylor, Versailles, 1968

For Davis, the slopes of the cumulative plots deviate at the end of the summer season. In addition, for 1965 and 1966 the Priestly-Taylor method tends to underestimate during winter.

Lysimeter evapotranspiration did not drop in proportion to net radiation during the fall season. Aerodynamic effects can enhance reference evapotranspiration during fall days. Nevertheless, the Priestly-Taylor method seems to correlate well with lysimeter data during spring-summer months at Davis. This can be noted by observing the slopes of the cumulative plots during the spring-summer periods.

For Kimberly, the slope of the cumulative plot for the original Priestly-Taylor was lower than the lysimeter throughout the growing season. This plot was typical for Kimberly indicating the method consistently underpredicted reference evapotranspiration. For Versailles, the slopes were equal for the spring-summer months. The drift from the cumulative lysimeter plot occurred during the month of April (Julian day 91 to Julian day 121).

4.3.2 Regression Analysis

Regression analysis was performed between the estimated reference evapotranspiration values and the lysimeter values. These results are presented in Table 21, 22, 23 for the three sites.

Table 21. Summary of regression analysis for original Priestly-Taylor, Davis.

Year	Coefficient of Determination (r^2)	SEER (mm d^{-1})	Slope of Regression	Constant of Regression	Z Statistic (95 %) (T/F)
1965	0.73	1.21	0.90	0.94	3.47 (F)
1966	0.75	1.11	0.84	0.91	6.08 (F)
1967	0.75	1.07	0.77	0.93	9.60 (F)
1968	0.80	1.07	0.87	0.69	4.94 (F)
1969	0.81	1.07	0.82	0.95	8.18 (F)
1970	0.81	1.02	0.90	0.57	4.08 (F)
1971	0.79	0.94	0.89	0.69	4.53 (F)

Table 22. Summary of regression analysis for original Priestly-Taylor, Kimberly.

Year	Coefficient of Determination (r^2)	SEER (mm d^{-1})	Slope of Regression	Constant of Regression	Z Statistic (95 %) (T/F)
1969	0.81	1.00	1.45	0.23	8.30 (F)
1970	0.72	1.12	1.30	0.26	4.40 (F)
1971	0.72	1.37	1.93	-3.20	9.11 (F)

Table 23. Summary of regression analysis for original Priestly-Taylor, Versailles.

Year	Coefficient of Determination (r^2)	SEER (mm d^{-1})	Slope of Regression	Constant of Regression	Z Statistic (95 %) (T/F)
1968	0.80	0.66	1.00	-0.25	0.00 (T)
1969	0.89	0.57	1.01	-0.11	0.60 (T)
1971	0.78	0.73	0.99	0.08	0.43 (T)
1972	0.76	0.58	0.83	0.25	5.12 (F)
1973	0.82	0.73	0.98	0.00	0.72 (T)
1974	0.85	0.63	0.89	0.21	3.83 (F)
1975	0.86	0.67	1.02	0.07	0.90 (T)
1976	0.84	0.88	1.28	-0.36	8.30 (F)

For Davis, the coefficient of determination indicated adequate and consistent correlation between computed ET_r and lysimeter measurements. The slope for each year was statistically different from unity. It can be concluded the Priestly-Taylor method underestimates reference evapotranspiration and a value of α greater than 1.26 should be applied, especially during the low radiation periods. This observation served as the basis for the modified Priestly-Taylor method.

For Kimberly, significant correlation was noted from year to year. The method correlated well with the lysimeter data for 1969. A weaker but consistent correlation was noted in 1970 and 1971. The regression slope was consistently different from unity indicating some adjustment is necessary.

For Versailles, the regression analysis indicated that three out of eight years the slope was statistically significant from unity. The correlation was high between measured and estimated reference evapotranspiration as indicated by the coefficient of determination for each year.

4.4 Modified Priestly-Taylor

As discussed in Section 4.3.1.1, the original Priestly-Taylor method underestimated ET_r for Davis and Kimberly. A method to increase α during those months was attempted and the value of α was obtained for each day as discussed in Section 3.5.2. In this modification, α was assumed to be dependent on the vapor pressure deficit.

The variation of computed α using equation [60] with Julian day is displayed in Figures 35, 36, 37, 38, 39, 40, and 41 for Davis, Kimberly, and Versailles. The modified Priestly-Taylor was not very accurate in Versailles since minimum daily relative humidity were not available and long term monthly values were used.

underestimated ET_r for Davis and Kimberly. A method to increase α during those months was attempted and the value of α was obtained for each day as discussed in Section 3.5.2. In this modification, α was assumed to be dependent on the vapor pressure deficit.

The variation of computed α using equation [60] with Julian day is displayed in Figures 35, 36, 37, 38, 39, 40, and 41 for Davis, Kimberly, and Versailles. The modified Priestly-Taylor was not very accurate in Versailles since minimum daily relative humidity were not available and long term monthly values were used.

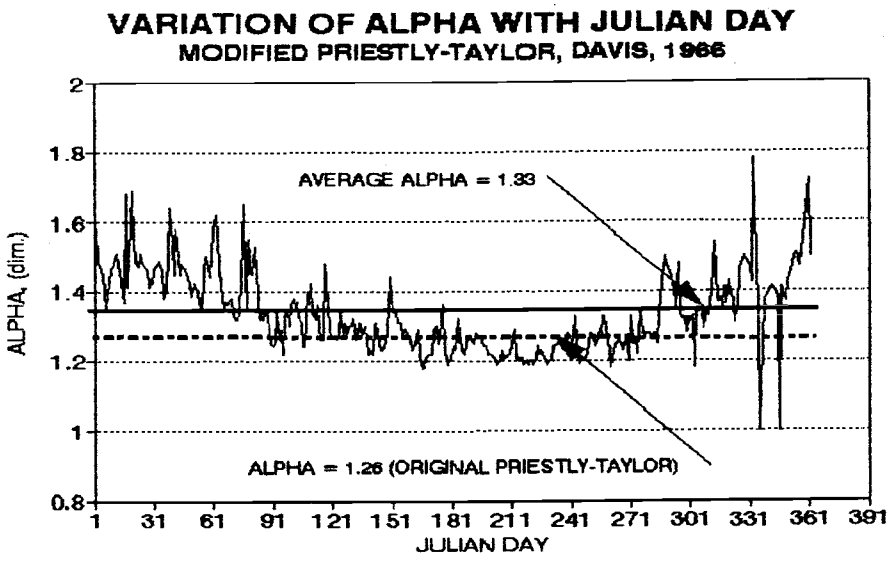

Figure 35. Variation of α versus Julian day, Davis, 1966.

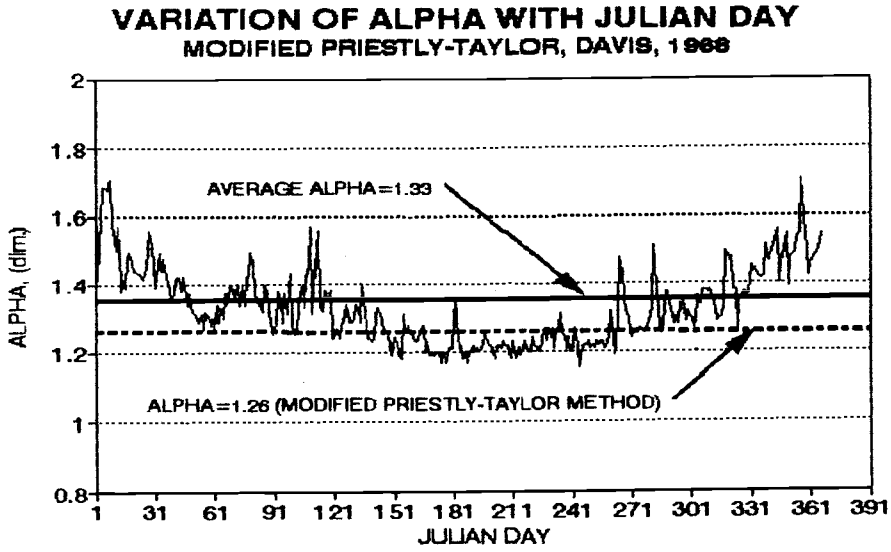

Figure 36. Variation of α versus Julian day, Davis, 1968.

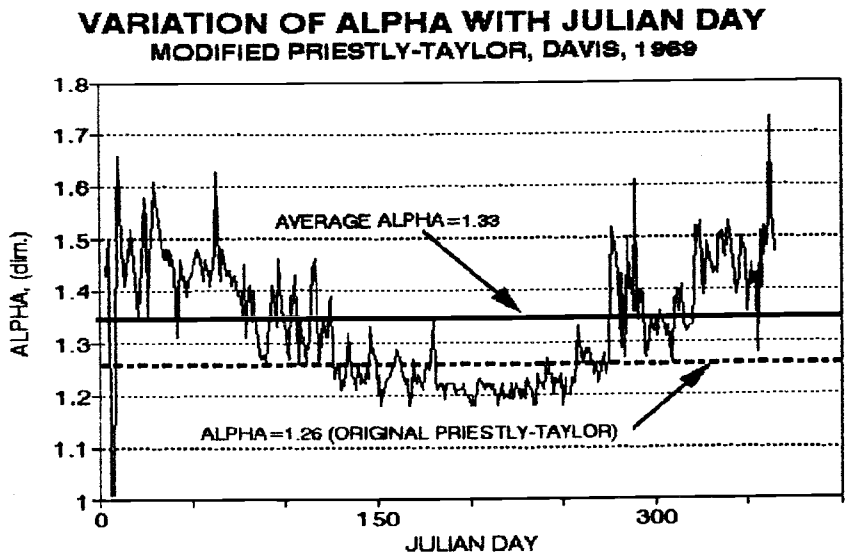

Figure 37. Variation of α versus Julian day, Davis, 1969.

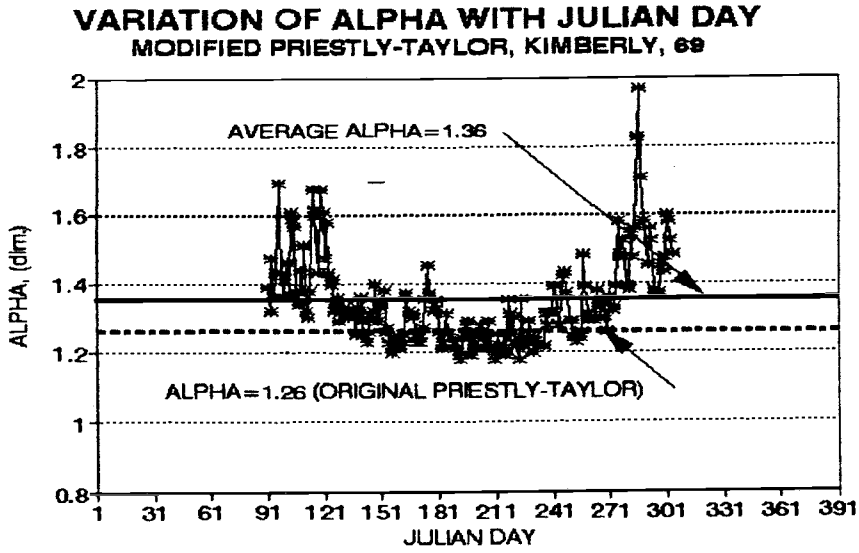

Figure 38. Variation of α versus Julian day, Kimberly, 1969.

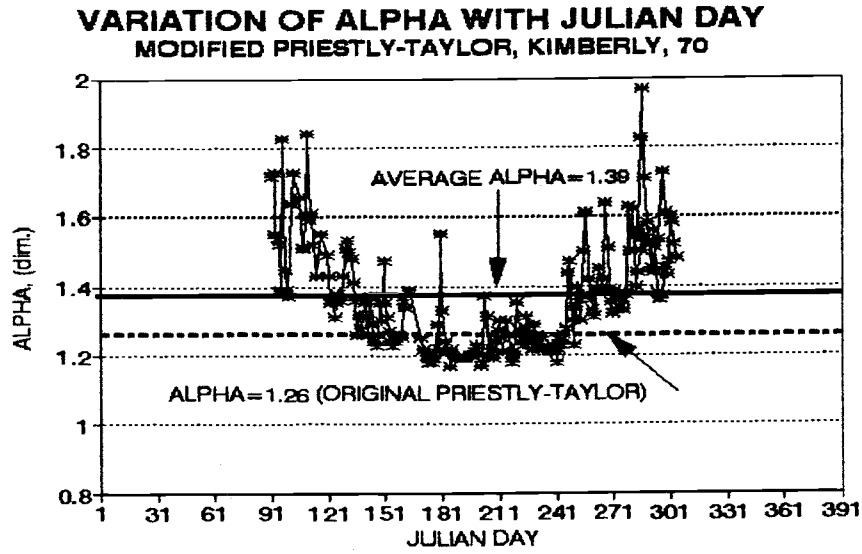

Figure 39. Variation of α versus Julian day, Kimberly, 1970.

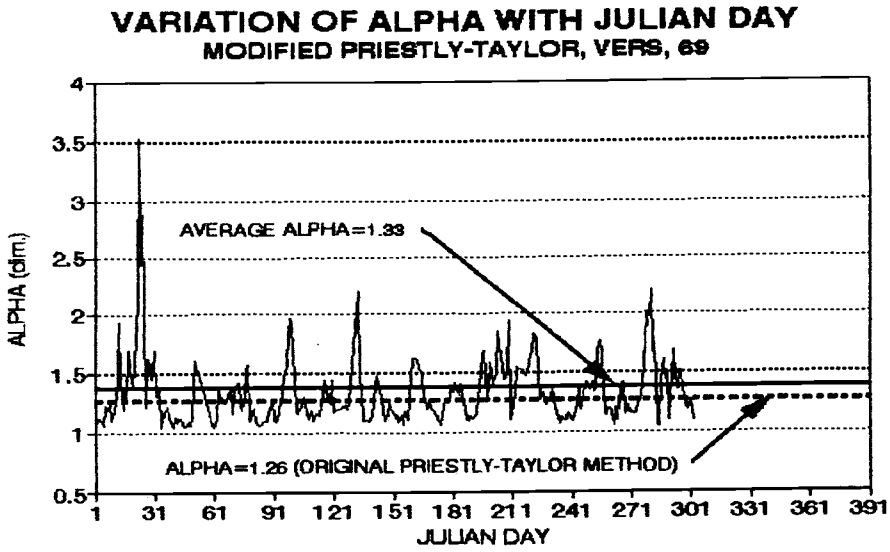

Figure 40. Variation of α versus Julian day, Versailles, 1968.

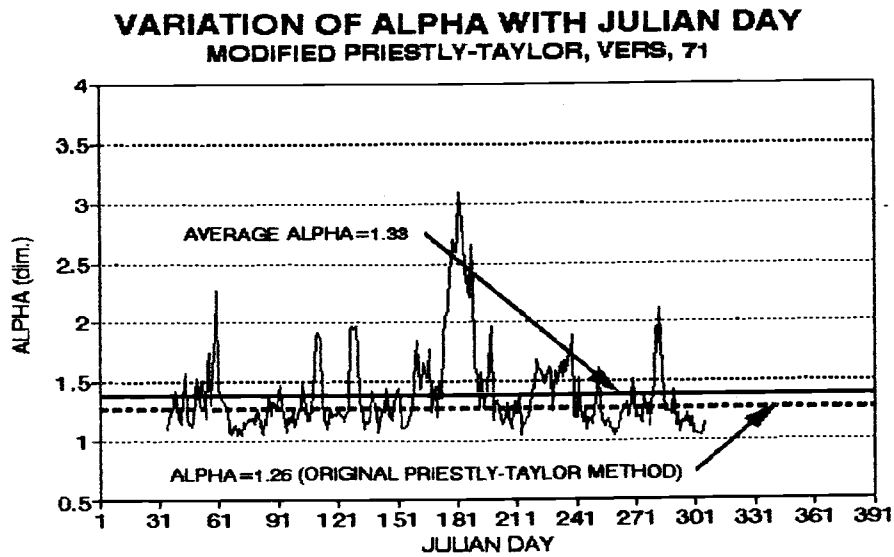

Figure 41. Variation of α versus Julian day, Versailles, 1971.

It is noted that the computed α was consistently higher than 1.26 for the fall and winter months for Davis and Kimberly. The value of α

decreased in the spring and summer months for Davis and Kimberly. The average annual value of α obtained fluctuated between 1.32 and 1.34 for Davis. Allen (1986) recommended a constant value of 1.34 for α at Davis.

Regression analysis between P1, the energy component of the Penman equation, and measured lysimeter ET_r for the combined data set from 1965 to 1971 (2379 days used in the regression) forced through the origin indicated a value for α of 1.28 for Davis. Priestly and Taylor (1972) reported a value for α of 1.28 when the days of cold and warm advection were rejected from their analysis.

For Kimberly, the average value of α fluctuated between 1.38 and 1.40. This value was higher by about 10% than the original value recommended by Priestly and Taylor (1972). Regression analysis between P1 and the lysimeter data for Kimberly indicated a value of 1.71 for α. This value is 26% higher than the value recommended by Priestly and Taylor.

4.4.1 Error Analysis

The error analysis was performed in accordance with the procedure discussed in Section 3.6. The error was computed by subtracting estimated ETr from measured ET_r. The Z test was employed to check whether the average annual reference evapotranspiration computed using the original Priestly-Taylor was significantly different from the lysimeter. The results are summarized in Tables 24, 25, and 26.

Table 24. Summary of Z statistics for modified Priestly-Taylor method, Davis.

Year	Mean Estimated ETr (mm d^{-1})	Standard Deviation (mm d^{-1})	Coefficient Of Variation (%)	SEE (mm d^{-1})	Z Statistic (T/F)
1965	3.20	2.21	66.58	1.35	3.45 (F)
1966	3.72	2.24	60.31	1.19	1.61 (T)
1967	3.47	2.23	64.56	1.24	0.73 (T)
1968	3.59	2.35	65.32	1.11	1.04 (T)
1969	3.57	2.37	66.65	1.14	1.63 (T)
1970	3.68	2.31	62.63	1.08	0.51 (T)
1971	3.54	2.19	61.98	1.11	1.31 (T)

Table 25. Summary of Z statistic for modified Priestly-Taylor, Kimberly.

Year	Mean Estimated ETr (mm d^{-1})	Standard Deviation (mm d^{-1})	Coefficient Of Variation (%)	SEE (mm d^{-1})	Z Statistic (T/F)
1969	2.58	1.53	59.87	1.77	11.13 (F)
1970	2.58	1.49	57.74	1.78	10.82 (F)
1971	4.16	1.03	24.78	1.94	1.27 (T)

Table 26. Summary of Z statistic for modified Priestly-Taylor method, Versailles.

Year	Mean Estimated ETr (mm d^{-1})	Standard Deviation (mm d^{-1})	Coefficient Of Variation	SEE (mm d^{-1})	Z Statistic (T/F)
1968	2.62	1.53	58.57	0.86	0.86 (T)
1969	2.46	1.90	77.46	0.74	0.74 (T)
1971	2.93	1.69	57.74	0.81	0.81 (T)
1972	2.40	1.26	52.31	0.65	0.65 (T)
1973	3.03	2.02	66.67	1.02	1.02 (T)
1974	2.72	1.85	68.05	0.78	0.78 (T)
1975	2.64	1.96	74.28	0.87	0.87 (T)
1976	3.25	2.47	76.30	1.04	1.04 (T)

The null hypothesis was true for six years in Davis, and the method can be used for estimating average annual reference evapotranspiration without significant loss in accuracy. The null hypothesis was false two

out of three years in Kimberly. This created a high degree of uncertainty whether the method can be used for estimating average annual reference evapotranspiration without significant loss of accuracy. The null hypothesis was consistently true for each year in Versailles, and the method can be used for estimating average annual reference evapotranspiration without significant loss in accuracy.

The error distribution was computed for each site. Sample plots are presented in Figures 42, 43, 44 for Davis, Figures 45 and 46 for Kimberly and Versailles, respectively.

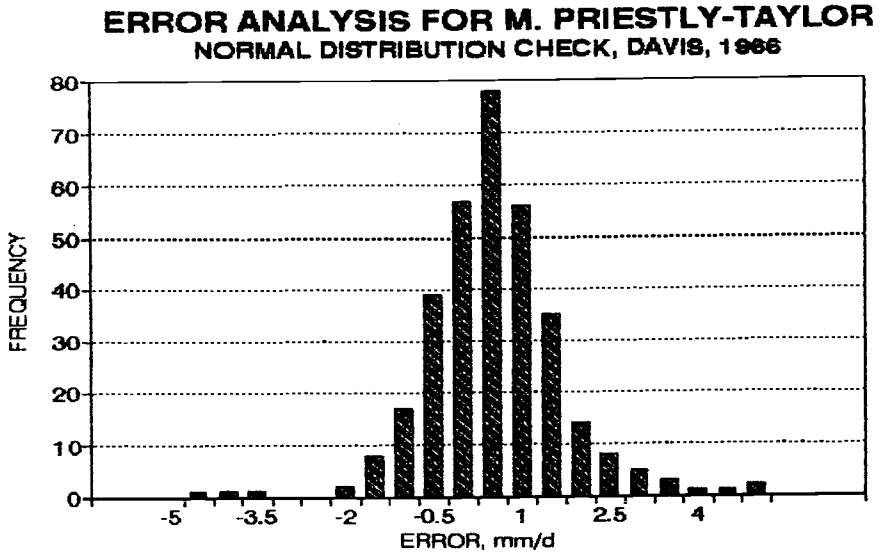

Figure 42. Plot of the error distribution versus frequency of occurrence for modified Priestly-Taylor, Davis, 1966.

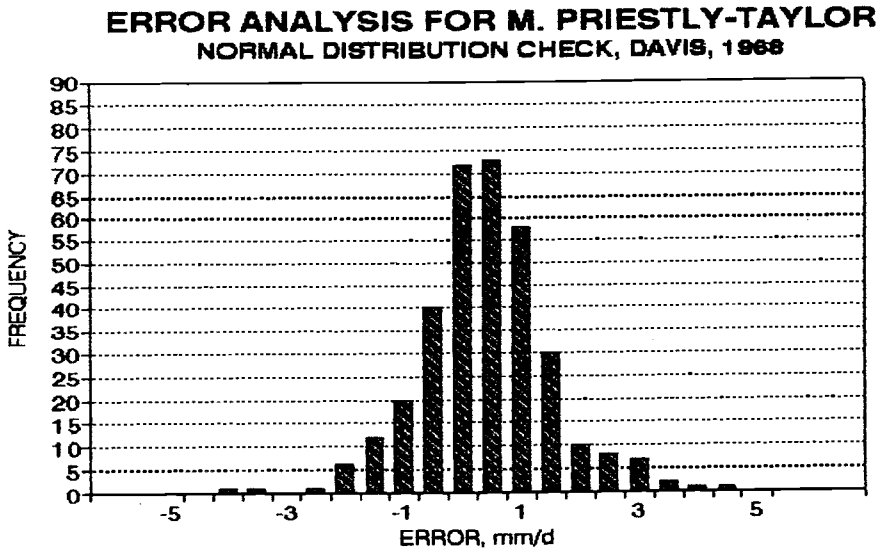

Figure 43. Plot of the error distribution versus frequency of occurrence for modified Priestly-Taylor, Davis, 1968.

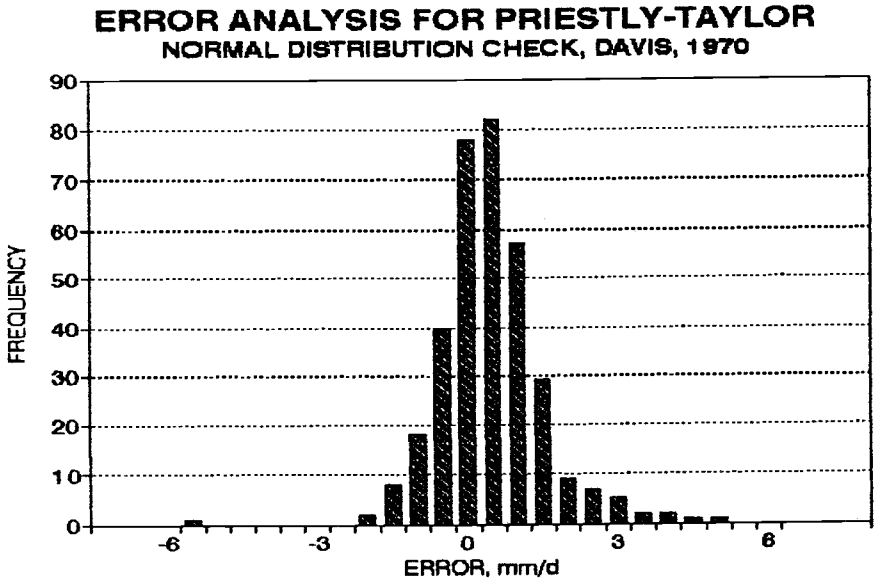

Figure 44. Plot of the error distribution versus frequency of occurrence for modified Priestly-Taylor, Davis, 1970.

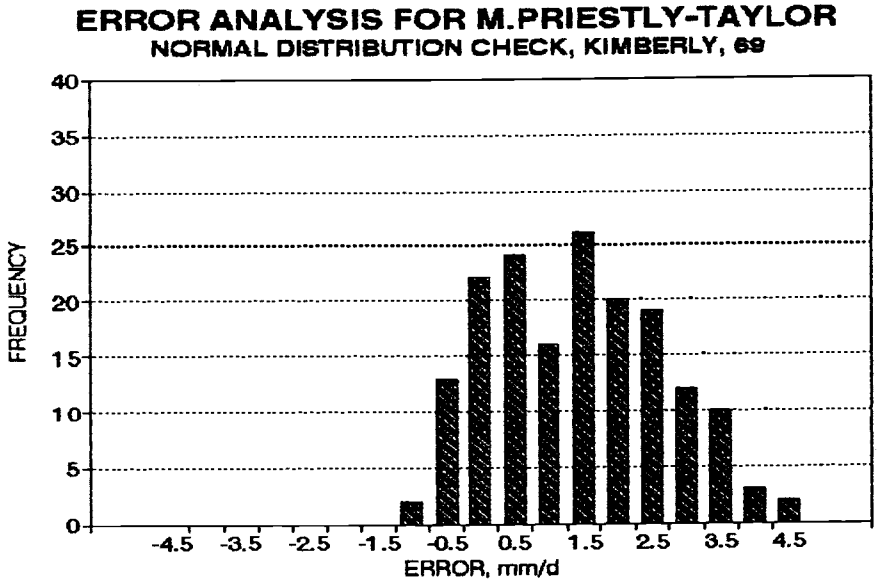

Figure 45. Plot of the error distribution versus frequency of occurrence for modified Priestly-Taylor, Kimberly, 1969.

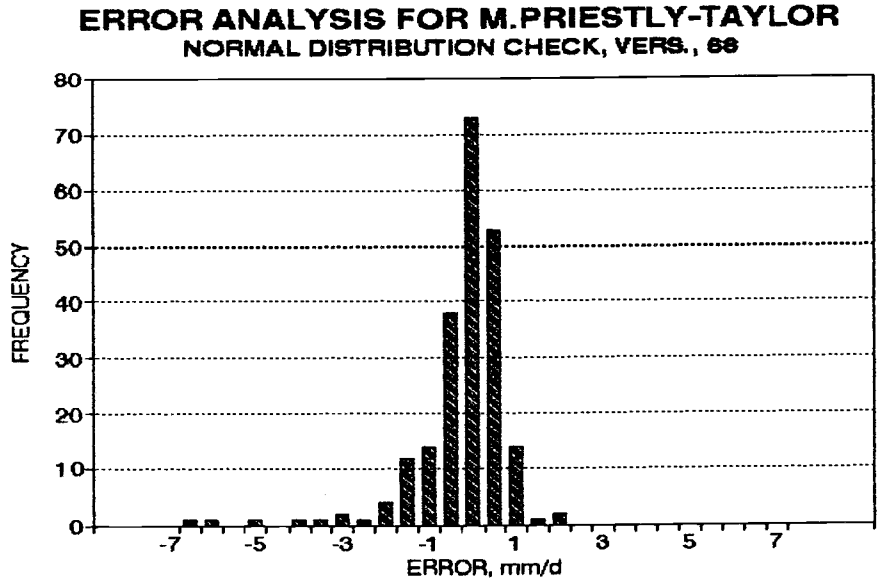

Figure 46. Plot of the error distribution versus frequency of occurrence for modified Priestly-Taylor, Versailles, 1968

It was noted the error distribution seems to be normal in Davis and Versailles with the highest frequencies occurring at zero. This was not the case in Kimberly where the distribution did not appear normal, and more frequencies on the positive error side were noted. To check seasonal trends, the error versus Julian day was plotted for Davis, Kimberly, and Versailles. Figures 47, 48, 49, and 50 present sample plots for Davis, Kimberly, and Versailles.

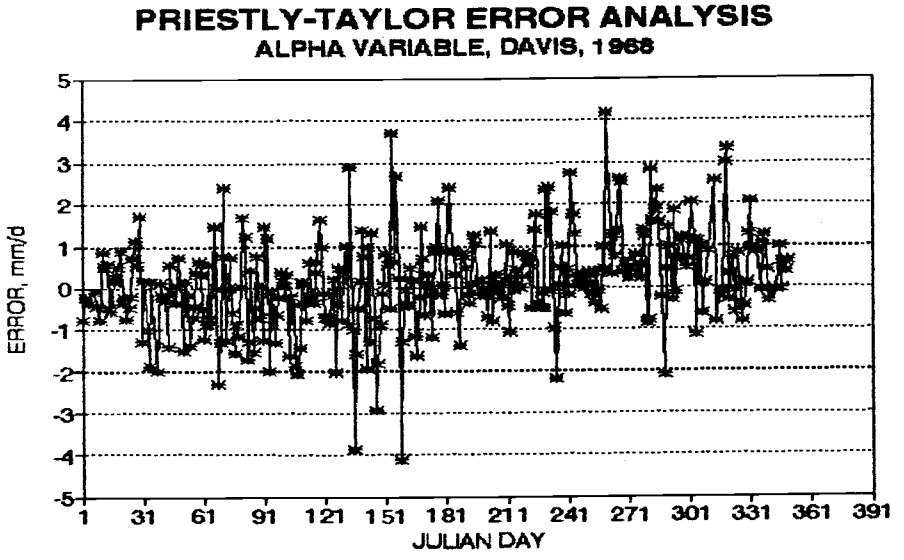

Figure 47. Plot of error versus Julian day for modified Priestly-Taylor, Davis, 1968.

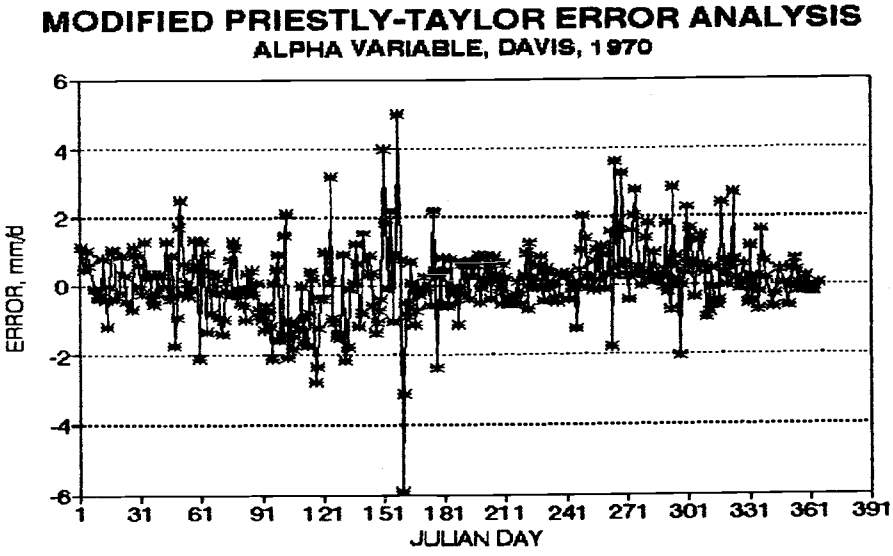

Figure 48. Plot of error versus Julian day for modified Priestly-Taylor, Davis, 1970.

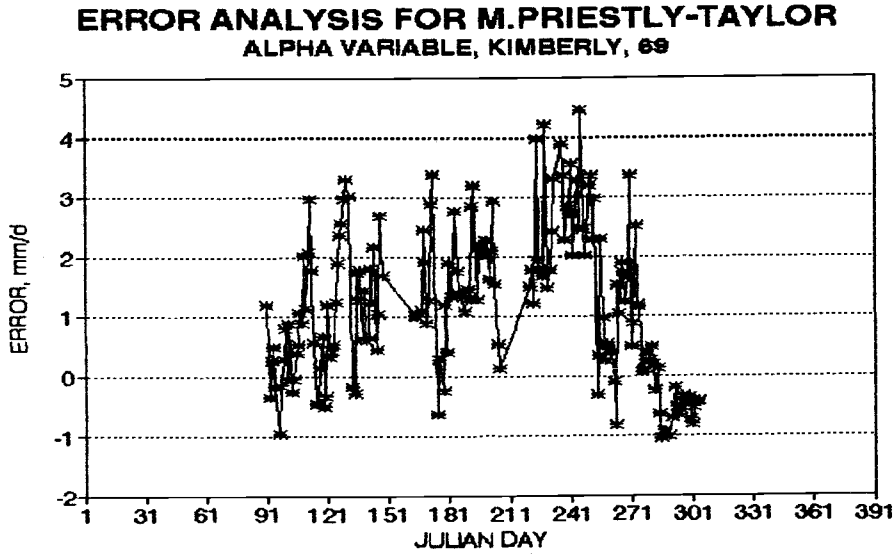

Figure 49. Plot of error versus Julian day for modified Priestly-Taylor, Kimberly, 1969.

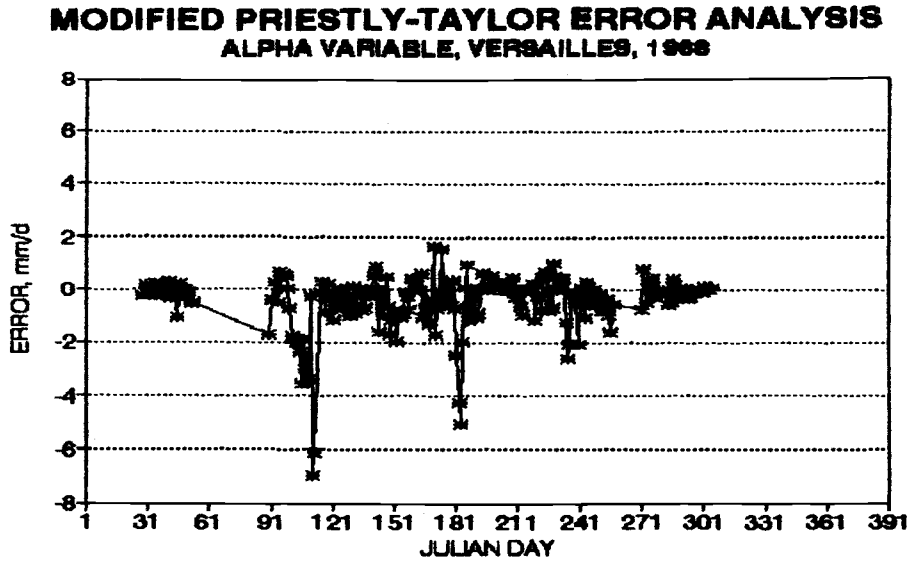

Figure 50. Plot of error versus Julian day for modified Priestly-Taylor, Versailles, 1968

For Davis, the method seems to underpredict reference evapotranspiration from Julian day 271 till the end of the year. For Kimberly, the method consistently underpredicted reference evapotranspiration. A typical variation is displayed in Figure 49. For Versailles, the method overpredicted reference evapotranspiration from Julian day 121 to Julian day 243 (May 1 to September 1). This variation was typical for each year in Versailles.

To validate the error analysis, sample cumulative plots are presented in Figures 51, 52, and 53.

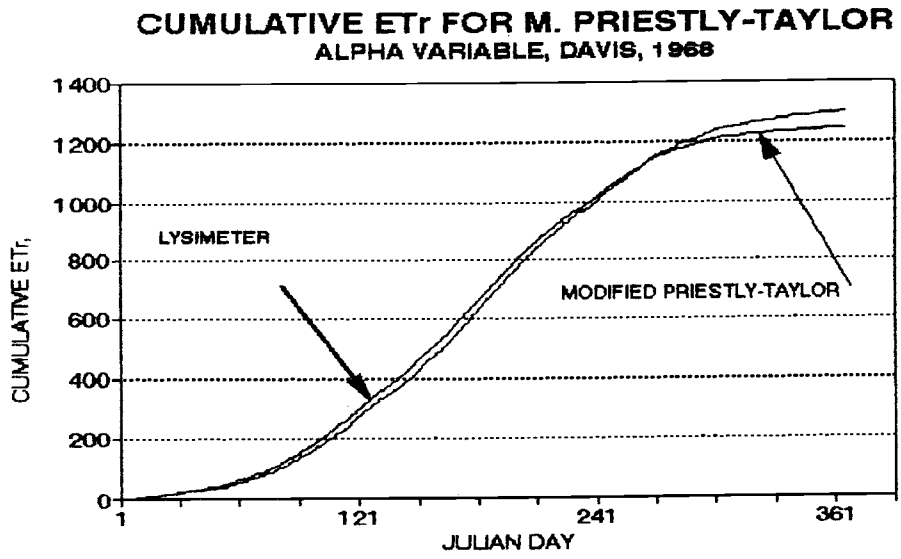

Figure 51. Cumulative ETr (mm) versus Julian day for modified Priestly-Taylor, Davis, 1968.

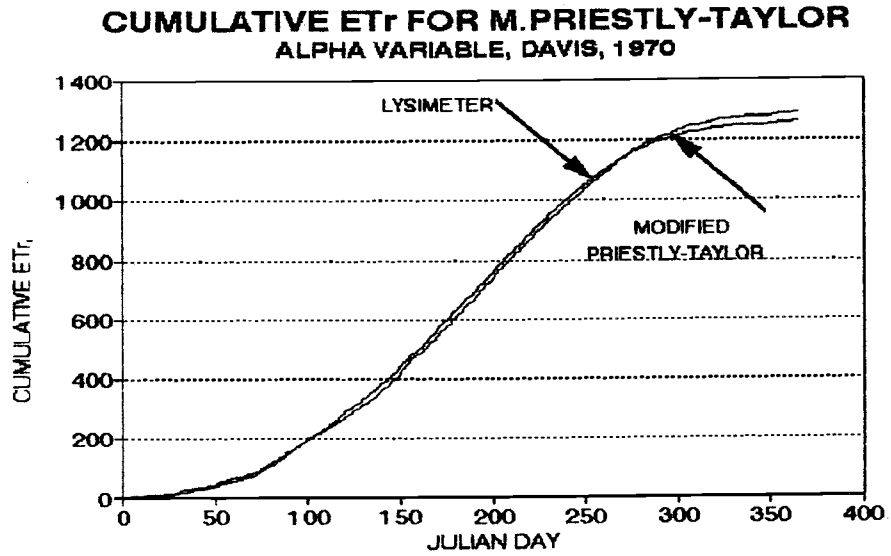

Figure 52. Cumulative ETr (mm) versus Julian day for modified Priestly-Taylor, Davis, 1970.

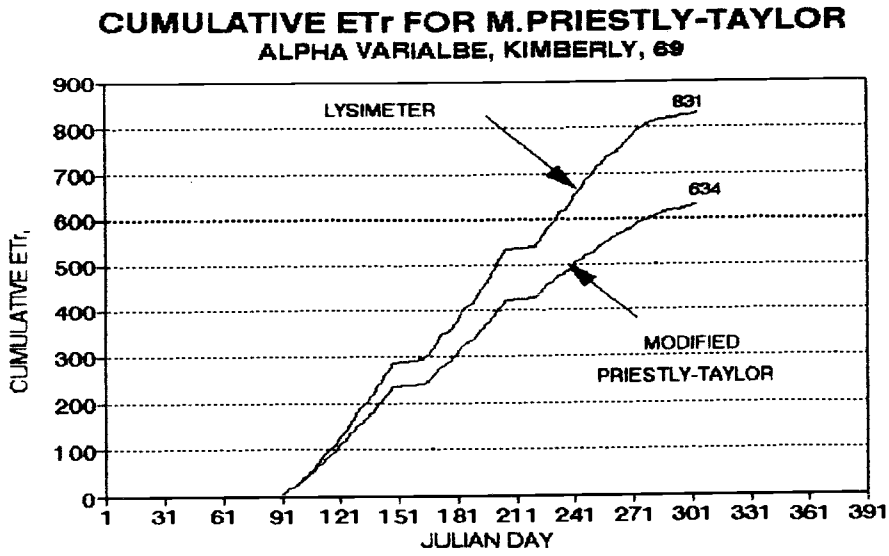

Figure 53. Cumulative ETr (mm) versus Julian day for modified Priestly-Taylor, Kimberly, 1968.

For Davis, the slopes of the cumulative lysimeter plot and the modified Priestly-Taylor indicate an improvement over the original Priestly-Taylor. For the spring-summer season, α was low, and for the low radiation fall-winter seasons, α was high. For Kimberly, the result was very similar to the original Priestly-Taylor and no improvements were noted.

For Versailles, the cumulative plots were very similar to the one presented for the original Priestly-Taylor. It should be noted that the SEE values for the original Priestly-Taylor were lower than the SEE for the modified Priestly-Taylor. Therefore, there was no advantage of varying α with Julian day at Versailles.

4.4.2 Regression Analysis

The Z test was applied to check whether the slope of the regression line was statistically different from unity for each year. The results of this analysis is presented in Tables 27, 28, and 29 for Davis, Kimberly, and Versailles.

Table 27. Summary of regression analysis for modified Priestly-Taylor, Davis.

Year	Coefficient of Determination (r^2)	SEER (mm d^{-1})	Slope of Regression	Constant of Regression	Z Statistic (95 %) (T/F)
1965	0.73	1.20	0.93	0.83	2.30 (F)
1966	0.75	1.11	0.86	0.79	4.95 (F)
1967	0.70	1.10	0.79	0.86	7.76 (F)
1968	0.80	1.09	0.91	0.56	3.58 (F)
1969	0.80	1.03	0.85	0.84	6.55 (F)
1970	0.80	1.05	0.91	0.42	3.64 (F)
1971	0.78	1.08	0.92	0.52	3.13 (F)

Table 28. Summary of regression analysis for modified Priestly-Taylor, Kimberly.

Year	Coefficient of Determination (r^2)	SEER (mm d^{-1})	Slope of Regression	Constant of Regression	Z Statistic (95 %) (T/F)
1969	0.78	1.02	1.51	-0.76	8.46 (F)
1970	0.60	1.33	1.32	-0.11	3.58 (F)
1971	0.71	1.40	2.10	-4.26	9.67 (F)

For Davis, correlation between the lysimeter and the modified Priestly-Taylor results were not higher than the correlation between the original Priestly-Taylor and the lysimeter. The method did not improve the ET_r estimations on a daily basis. The SEE and the SEER were of the same order as the original Priestly-Taylor results for daily estimates

Table 29. Regression analysis for modified Priestly-Taylor for Versailles.

Year	Coefficient of Determination (r^2)	SEER (mm d^{-1})	Slope of Regression	Constant of Regression	Z Statistic (95 %) (T/F)
1968	0.65	0.90	0.69	0.40	9.09 (F)
1969	0.87	0.59	0.82	0.14	9.08 (F)
1971	0.79	0.67	0.89	0.32	3.03 (F)
1972	0.74	0.61	0.81	0.42	5.51 (F)
1973	0.78	0.81	0.75	0.44	8.70 (F)
1974	0.78	0.69	0.74	0.73	8.30 (F)
1975	0.83	0.74	0.82	0.30	7.51 (F)
1976	0.83	0.92	0.81	0.55	8.51 (F)

each year. However, improvements shown in the cumulative plots indicate over a longer averaging period, the modified Priestly-Taylor might perform better than the original Priestly-Taylor for Davis. This point is discussed when all the estimating methods are compared for Davis.

For Kimberly, the coefficients of determination were low for the modified Priestly-Taylor and no evident improvements can be concluded by varying α with time. For Versailles, the regression results indicate no gain was observed by varying α with the Julian day. It is difficult to confirm this observation since α was computed using long term monthly minimum relative humidity instead of minimum daily relative humidity as in Davis and Kimberly. All sites had a slope statistically different from unity as indicated by the Z test.

4.5 Original Penman Method

The original Penman method was applied to all sites. Daily estimates of reference evapotranspiration were performed as outlined in Section

3.5.3 and the formulation developed in Chapter 2. This section presents the results of the analysis performed for original Penman method for Davis, Kimberly, and Versailles. The analysis includes two parts. The first part presents the error analysis, and the second presents the regression analysis.

4.5.1 Error Analysis

The error analysis was performed in accordance with the procedure discussed in Section 3.6. The error was calculated by subtracting estimated ETr from measured ETr. The Z test was employed to check whether the average annual reference evapotranspiration computed using the original Penman method was significantly different from the lysimeter data. The results are summarized in Tables 30, 31, and 32 for Davis, Kimberly, and Versailles.

Table 30. Summary of Z statistics for original Penman method, Davis.

Year	Mean Estimated ETr (mm d^{-1})	Standard Deviation (mm d^{-1})	Coefficient Of Variation (%)	SEE (mm d^{-1})	Z Statistic (T/F)
1965	3.53	2.09	59.13	0.97	1.58 (T)
1966	4.33	2.37	54.75	0.95	1.79 (T)
1967	3.99	2.19	55.04	0.98	2.44 (F)
1968	4.20	2.55	60.48	0.94	2.20 (F)
1969	4.17	2.47	59.22	0.91	2.20 (F)
1970	4.39	2.61	59.52	1.13	3.26 (F)
1971	4.20	2.29	54.62	0.98	2.60 (F)

Table 31. Summary of Z statistics for original Penman method, Kimberly.

Year	Mean Estimated ETr (mm d^{-1})	Standard Deviation (mm d^{-1})	Coefficient Of Variation (%)	SEE (mm d^{-1})	Z Statistic (T/F)
1969	4.86	1.57	32.05	1.04	0.28 (T)
1970	4.75	1.40	29.63	1.09	0.64 (T)
1971	4.64	1.59	34.20	1.45	0.74 (T)

Table 32. Summary of Z Statistics for original Penman method, Versailles.

Year	Mean Estimated ETr (mm d^{-1})	Standard Deviation (mm d^{-1})	Coefficient Of Variation (%)	SEE (mm d^{-1})	Z Statistic (T/F)
1968	3.15	1.19	47.72	1.50	6.09 (F)
1969	2.82	0.86	56.48	1.59	4.60 (F)
1971	3.22	0.77	43.40	1.40	3.44 (F)
1972	2.82	0.75	41.92	1.18	3.81 (F)
1973	3.21	0.81	51.28	1.65	2.96 (F)
1974	3.01	0.72	50.73	1.53	2.34 (F)
1975	2.88	0.84	55.42	1.59	2.86 (F)
1976	3.30	0.87	50.80	1.67	0.78 (T)

The null hypothesis was false for four out of seven years in Davis, and the method cannot be used for estimating average annual reference evapotranspiration without significant loss of accuracy. The null hypothesis was false one out of three years at Kimberly, and the method might be used for estimating average annual reference evapotranspiration without significant loss of accuracy. The null hypothesis was false seven out of the eight years in Versailles, and the method cannot be used for estimating average annual reference evapotranspiration without significant loss in accuracy. The error distribution was plotted for Davis, Kimberly, and Versailles as shown in Figures 54, 55, 56, 57, 58, and 59.

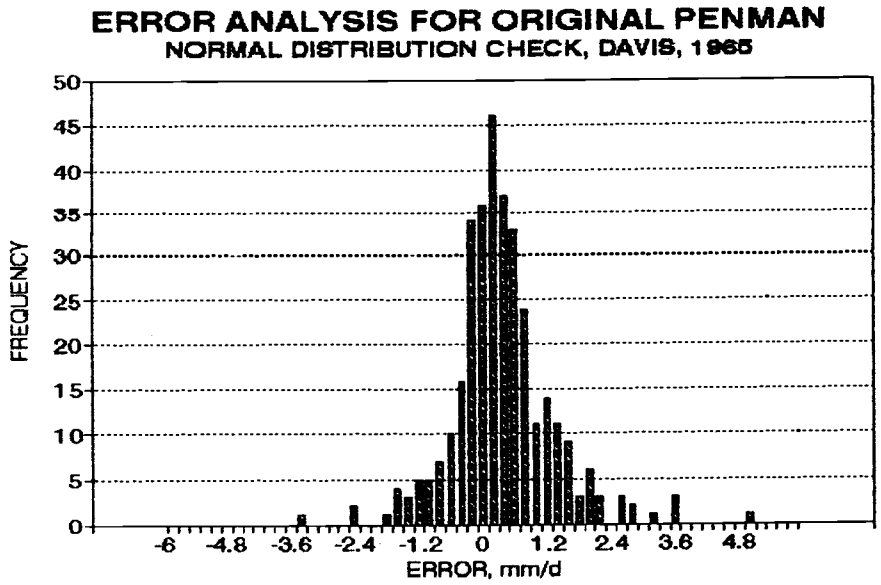

Figure 54. Plot of the error distribution versus frequency of occurrence for original Penman method, Davis, 1965.

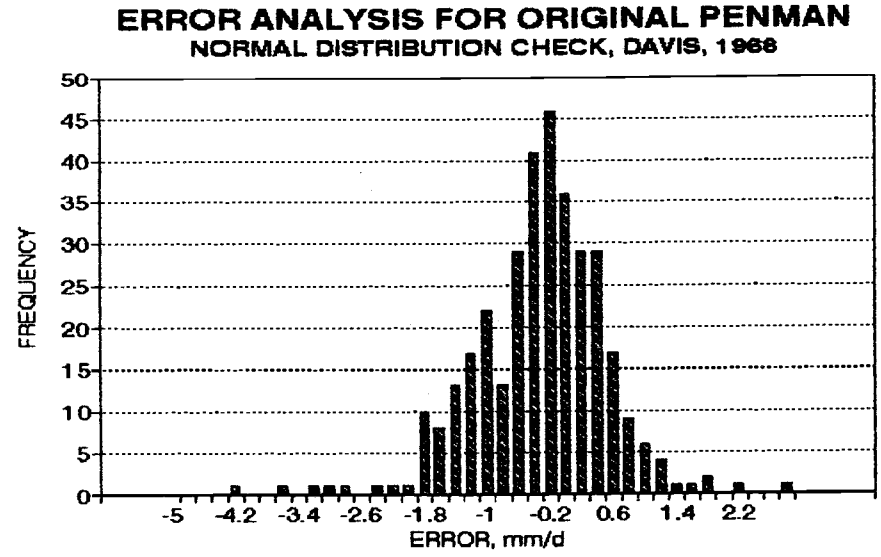

Figure 55. Plot of the error distribution versus frequency of occurrence for original Penman method, Davis, 1968.

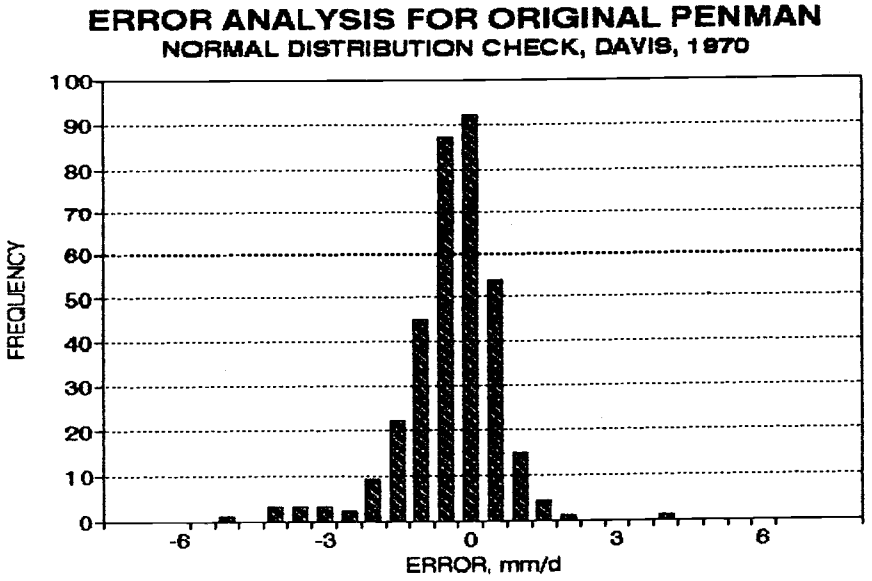

Figure 56. Plot of the error distribution versus frequency of occurrence for original Penman method, Davis, 1970

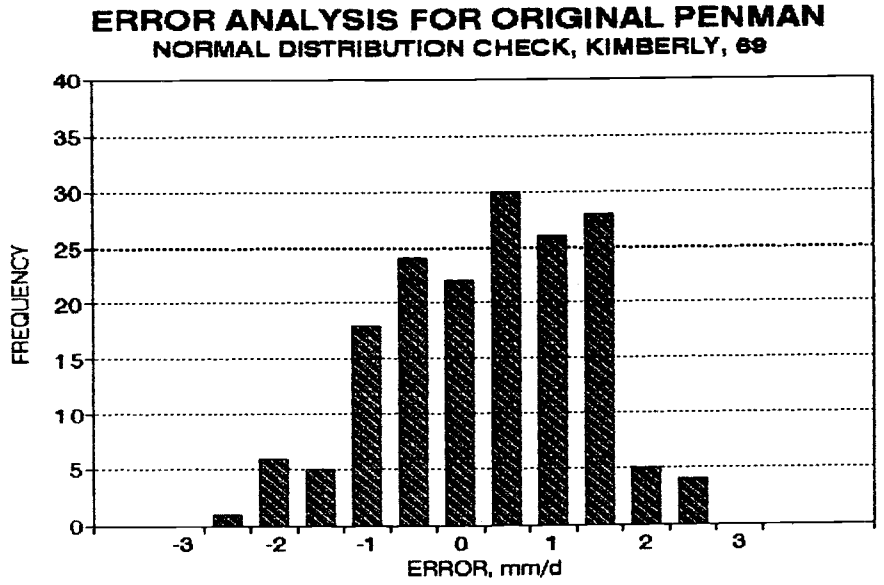

Figure 57. Plot of the error distribution versus frequency of occurrence for original Penman method, Kimberly, 1969.

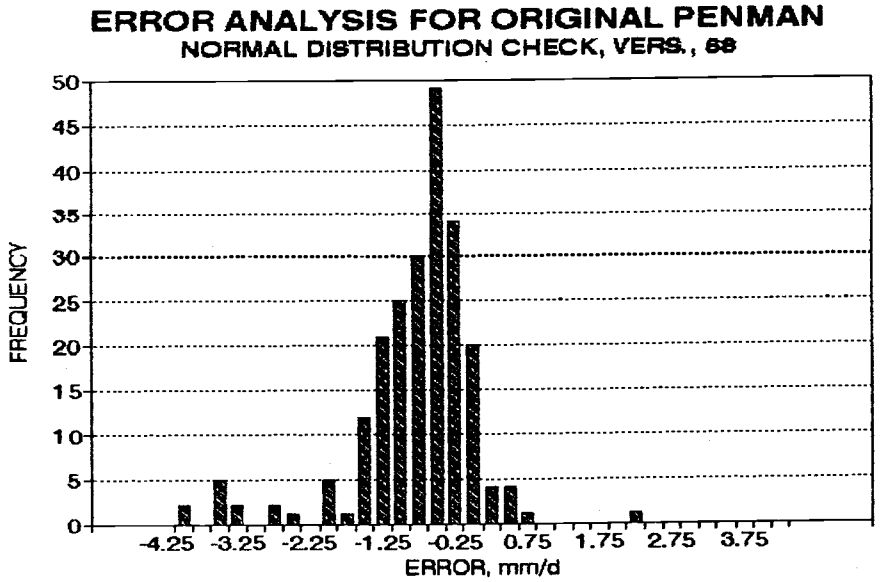

Figure 58. Plot of the error distribution versus frequency of occurrence for original Penman method, Versailles, 1968.

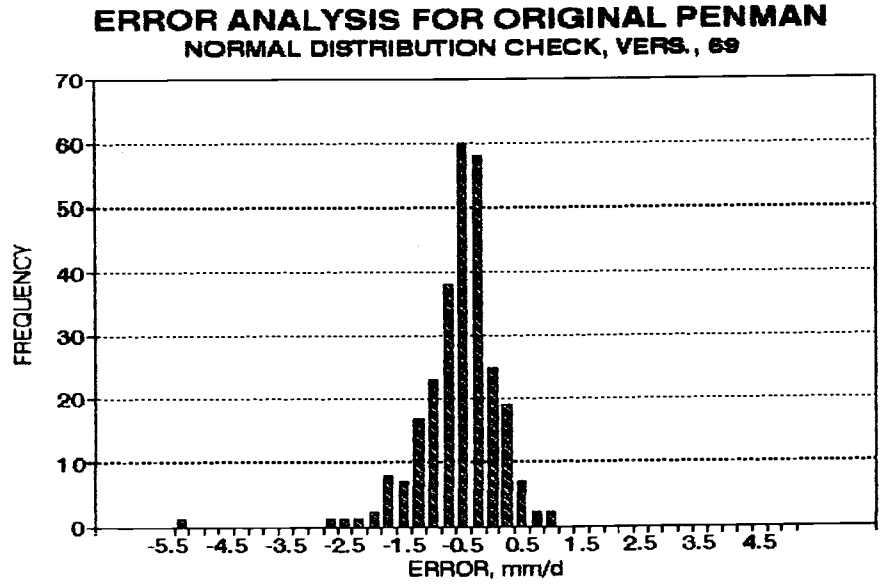

Figure 59. Plot of the error distribution versus frequency of occurrence for original Penman method, Versailles, 1969.

For Davis, the error distribution did appeared normal for each year but the maximum frequency did not occur at zero. This was also the case in Kimberly and Versailles. The distribution plots confirmed the results of the Z test. To check seasonal trends, the error versus Julian day was plotted for each year at each site. Sample plots are presented in Figures 60, 61, and 62 for Davis, Figure 63 for Kimberly, and Figures 64 and 65 for Versailles.

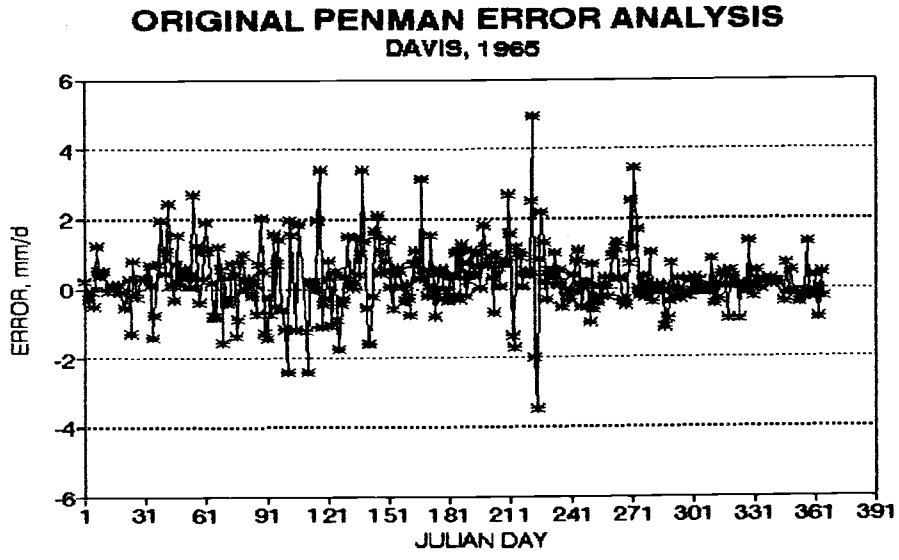

Figure 60. Plot of error versus Julian day for original Penman method, Davis, 1965

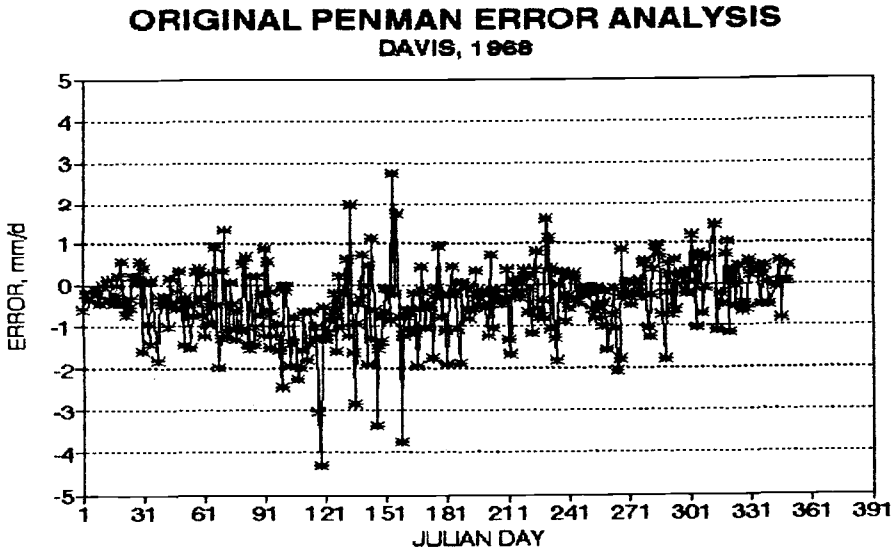

Figure 61. Plot of error versus Julian day for original Penman method, Davis, 1968

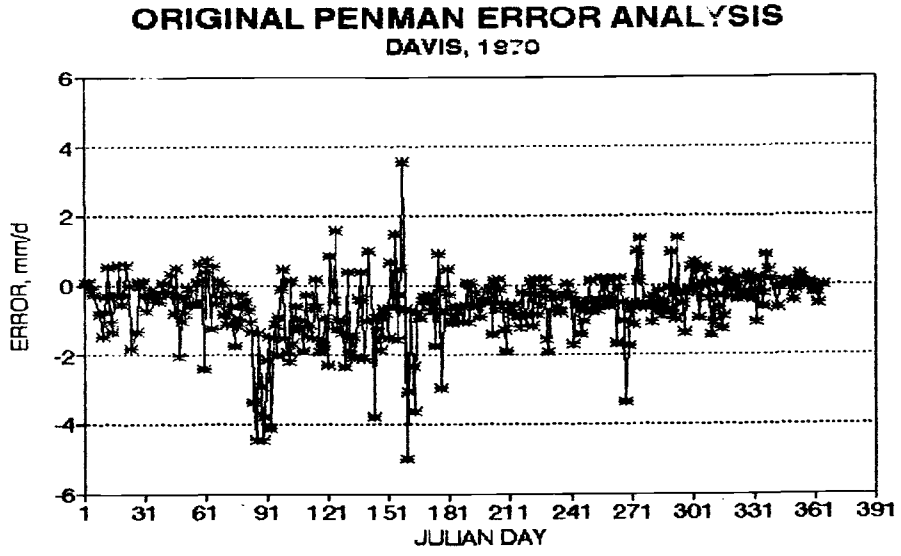

Figure 62. Plot of error versus Julian day for original Penman method, Davis, 1970

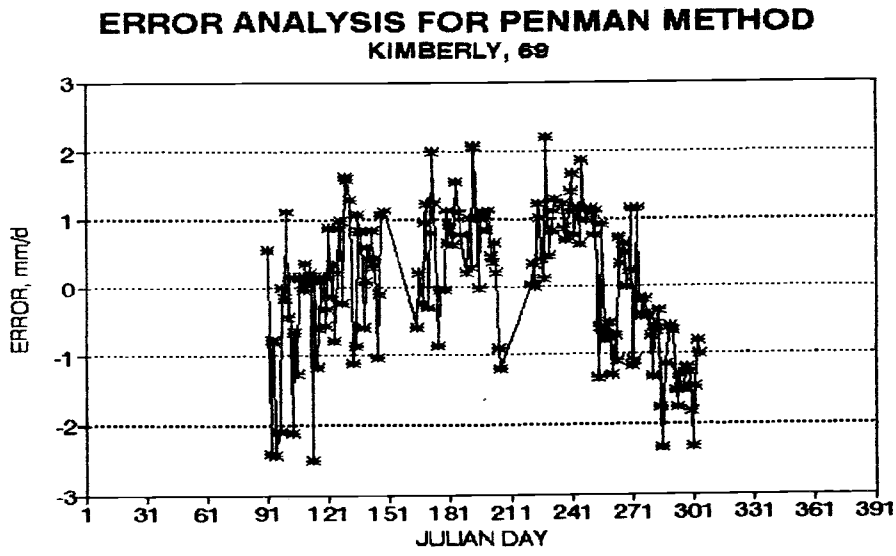

Figure 63. Plot of error versus Julian day for original Penman method, Kimberly, 1969.

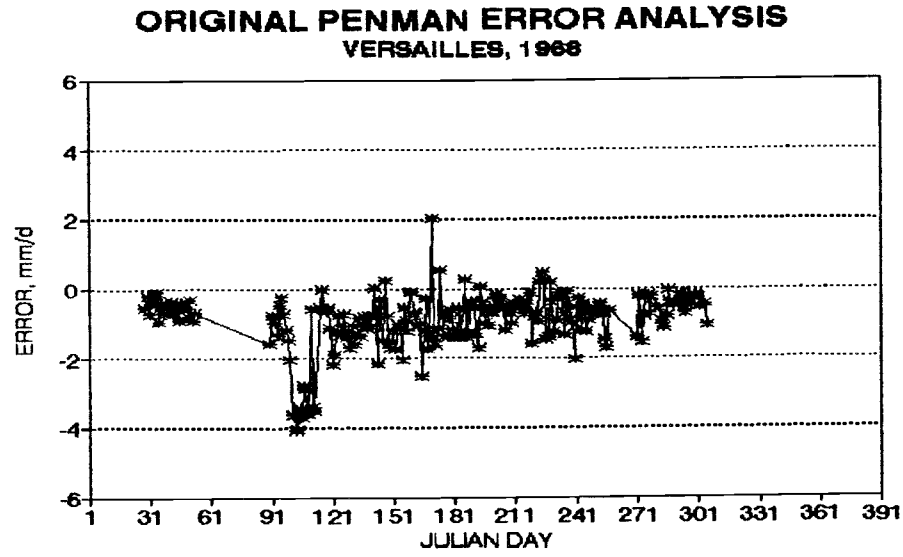

Figure 64. Plot of error versus Julian day for original Penman method, Versailles, 1968.

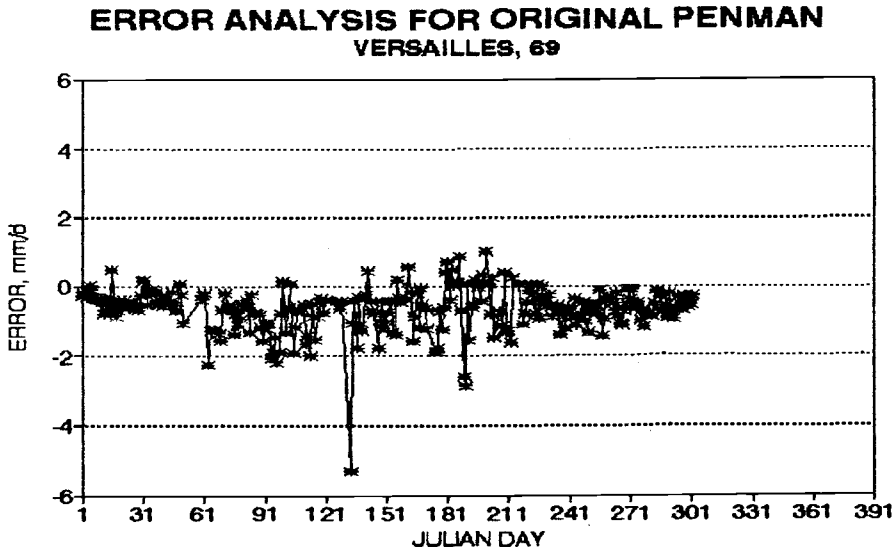

Figure 65. Plot of error versus Julian day for original Penman method, Versailles, 1969.

For Davis, the 1965 plot indicated no seasonal trend, and confirmed the Z test result. For all other years, the method overpredicted ET_r from Julian day 1 to Julian Day 271. This can be noted from Figures 60, and 61. For Kimberly, the method underestimates reference evapotranspiration for the summer months June, July, and August. Similar variation of error plots were noted for 1970 and 1971 at Kimberly. For Versailles, the method constantly overpredicted reference evapotranspiration through out the year and for each year.

Cumulative plots were employed to verify the observations of the error plots. Sample plots are presented in Figures 66, 67, 68, and 69.

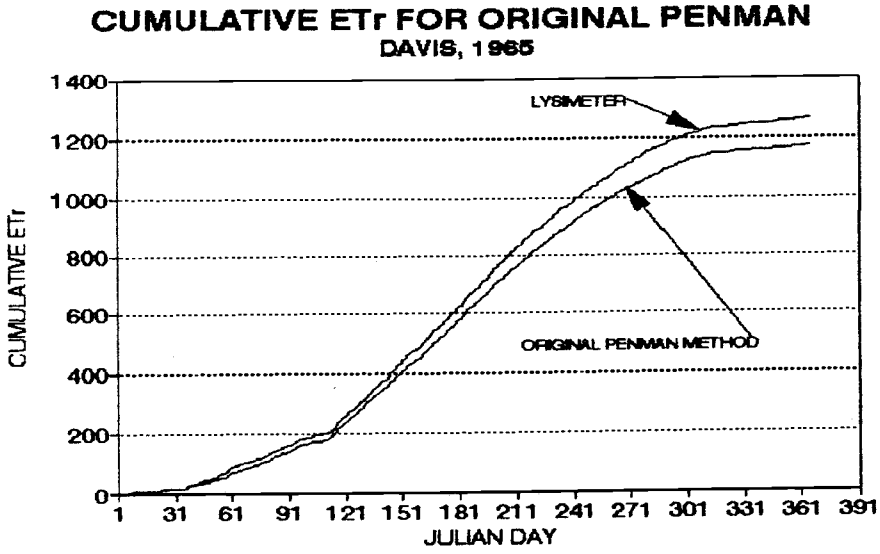

Figure 66. Cumulative ETr (mm) versus Julian day for original Penman method, Davis, 1965.

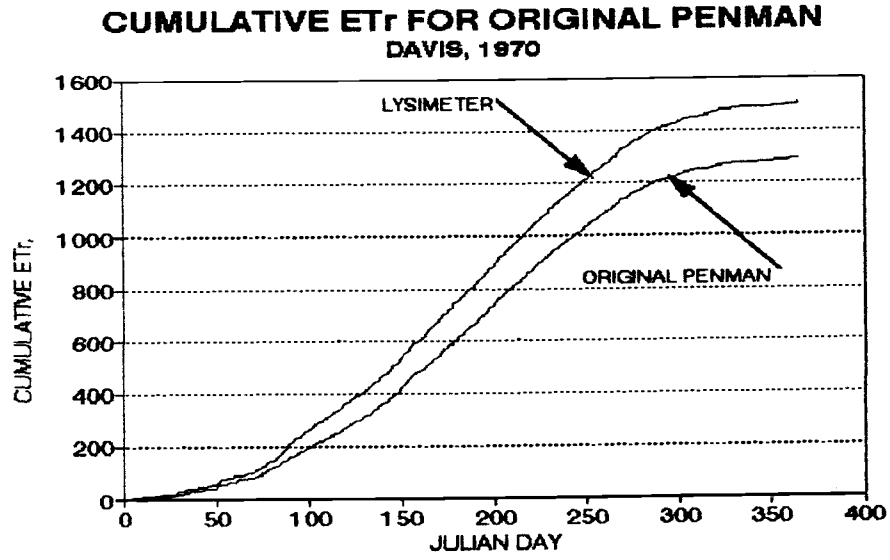

Figure 67. Cumulative ETr (mm) versus Julian day for original Penman method, Davis, 1970.

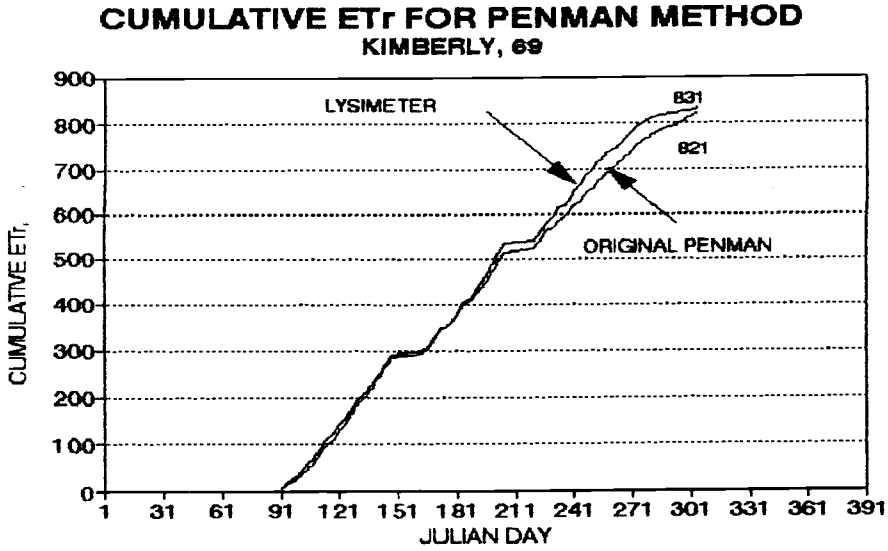

Figure 68. Cumulative ETr (mm) versus Julian day for original Penman method, Kimberly, 1969.

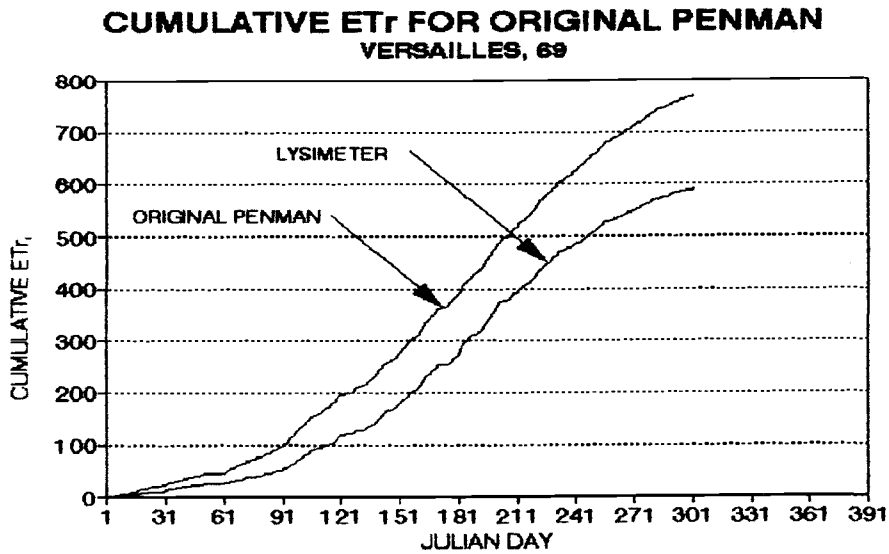

Figure 69. Cumulative ETr (mm) versus Julian day for original Penman method, Versailles, 1969.

The original Penman equation consistently underpredicted ET_r at Davis. The slopes of the cumulative curves drift from each other and

are equal by fall they become parallel to the horizontal. For Kimberly, the slopes start drifting after Julian Day 181. For Versailles, the method consistently overpredicts ET_r as can be noted from the sample plot presented in Figure 69.

4.5.2 Regression Analysis

Regression analysis was performed to check the consistency of the correlation and performance between lysimeter ET_r and computed ET_r from year to year. In addition, the Z test was applied to check whether the slope was different from unity, and whether the drift from unity was local. Results are summarized in the following tables.

Table 33. Summary of regression analysis for original Penman method, Davis.

Year	Coefficient of Determination (r^2)	SEER (mm d^{-1})	Slope of Regression	Constant of Regression	Z Statistic (95 %) (T/F)
1965	0.84	0.94	1.02	0.22	0.60 (T)
1966	0.75	1.11	0.84	0.91	6.42 (F)
1967	0.75	1.07	0.77	0.93	6.33 (F)
1968	0.80	1.07	0.87	0.69	7.05 (F)
1969	0.81	1.01	0.82	0.95	8.12 (F)
1970	0.81	1.02	0.90	0.57	9.24 (F)
1971	0.79	1.05	0.90	0.70	3.95 (F)

Table 34. Summary of regression analysis for original Penman method, Kimberly.

Year	Coefficient of Determination (r^2)	SEER (mm d^{-1})	Slope of Regression	Constant of Regression	Z Statistic (95 %) (T/F)
1969	0.86	0.86	1.37	-1.73	8.65 (F)
1970	0.79	0.97	1.32	-1.39	5.66 (F)
1971	0.75	1.25	-2.04	-1.40	5.90 (F)

Table 35. Summary of regression analysis for original Penman method, Versailles.

Year	Coefficient of Determination (r^2)	SEER (mm d^{-1})	Slope of Regression	Constant of Regression	Z Statistic (95 %) (T/F)
1968	0.74	0.76	0.85	-0.41	4.30 (F)
1969	0.89	0.57	0.99	-0.65	0.24 (T)
1971	0.83	0.63	1.00	-0.43	0.00 (T)
1972	0.76	0.57	0.87	-0.11	3.54 (F)
1973	0.87	0.63	0.97	-0.41	1.17 (T)
1974	0.86	0.60	0.99	-0.35	0.45 (T)
1975	0.83	0.72	1.01	-0.46	0.32 (T)
1976	0.88	0.77	1.23	-0.88	8.06 (F)

The coefficient of determination was consistent from year to year in Davis indicating consistent correlation between computed and measured reference evapotranspiration. The slope of the regression line was significantly different from unity except for 1965 indicating the method overestimated ET_r. However, the Penman equation is well correlated with lysimeter data indicating the potential of applying adjustment coefficients to reduce the overprediction in Davis.

In Kimberly, the regression analysis indicated high correlation consistently from year to year. In Versailles, the coefficient of determination was consistently greater than 0.8 except for 1968 and 1972. The slope of the regression line was statistically different from

unity in four years. Since the correlation coefficient was greater than 0.8, the method can predict reference evapotranspiration if a reduction factor is applied. This observation will be discussed later in the chapter. It was concluded that the original Penman equation correlates well with the lysimeter data for all climates. However, the method tends to overpredict or underpredict depending upon the climate.

4.6 Penman-Monteith Method

The Penman-Monteith method was applied only to Davis and Kimberly due to data availability. Daily estimates of reference evapotranspiration were performed as outlined in Section 3.5.4 and the formulation developed in Chapter 2 was employed. The values obtained for Kimberly were converted to equivalent grass as discussed in Section 3.3.2.

The Z statistic, standard error of the estimate, and linear regression analysis analogous to the Penman method were performed to evaluate the performance of the method over the growing season.

4.6.1 Error Analysis

The Z statistics test was performed in accordance with the procedure outlined in Section 3.6.1. The error was calculated by subtracting estimated ET_r from measured ET_r. The results of the test for Davis and Kimberly are presented in Tables 36 and 37.

Table 36. Summary of Z statistic for Penman-Monteith method, Davis.

Year	Mean Estimated ETr (mm d^{-1})	Standard Deviation (mm d^{-1})	Coefficient Of Variation (%)	SEE (mm d^{-1})	Z Statistic (T/F)
1965	3.56	1.79	50.32	1.05	1.49 (T)
1966	3.97	2.02	50.82	0.88	0.23 (T)
1967	3.67	1.99	54.12	0.73	0.56 (T)
1968	3.84	2.12	55.08	0.79	0.30 (T)
1969	3.83	2.03	52.98	0.72	0.18 (T)
1970	3.86	2.07	53.52	0.90	0.54 (T)
1971	3.70	1.95	52.61	0.80	0.37 (T)

Table 37. Summary of Z statistic for Penman-Monteith method, Kimberly.

Year	Mean Estimated ETr (mm d^{-1})	Standard Deviation (mm d^{-1})	Coefficient Of Variation (%)	SEE (mm d^{-1})	Z Statistic (T/F)
1969	5.12	1.61	31.40	1.10	0.90 (T)
1970	4.89	1.54	31.52	1.08	0.08 (T)
1971	4.86	1.65	33.87	1.50	1.50 (T)

For Davis, the null hypothesis was consistently true every year, and the method can be used with confidence for estimating average annual reference evapotranspiration without significant loss in accuracy. For Kimberly, the method was consistently true for the three years indicating that the method can be used for estimating reference evapotranspiration for the growing season. Normal probability plots were performed in Davis and Kimberly to research nature of the error distribution. Sample plots are presented in Figures 70, 71, and 72.

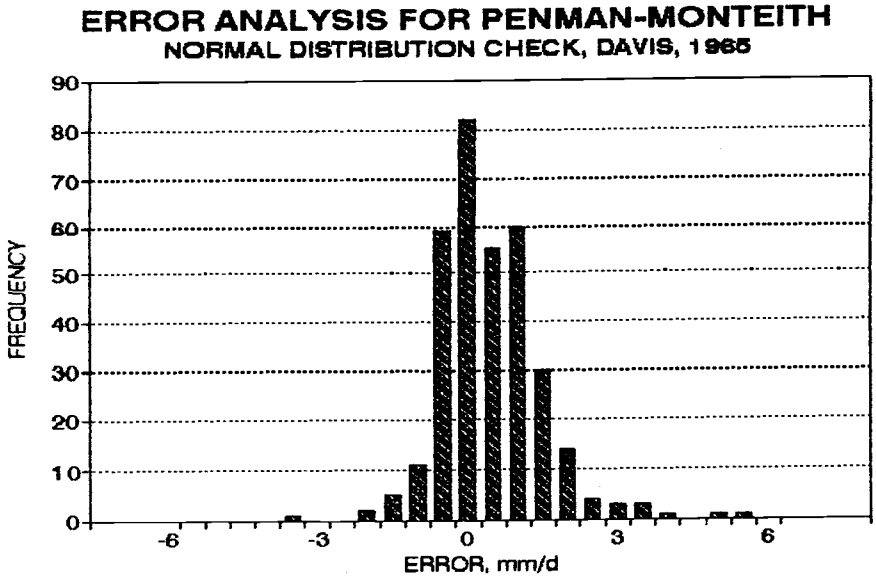

Figure 70. Plot of the error distribution versus frequency of occurrence for Penman-Monteith method, Davis, 1965.

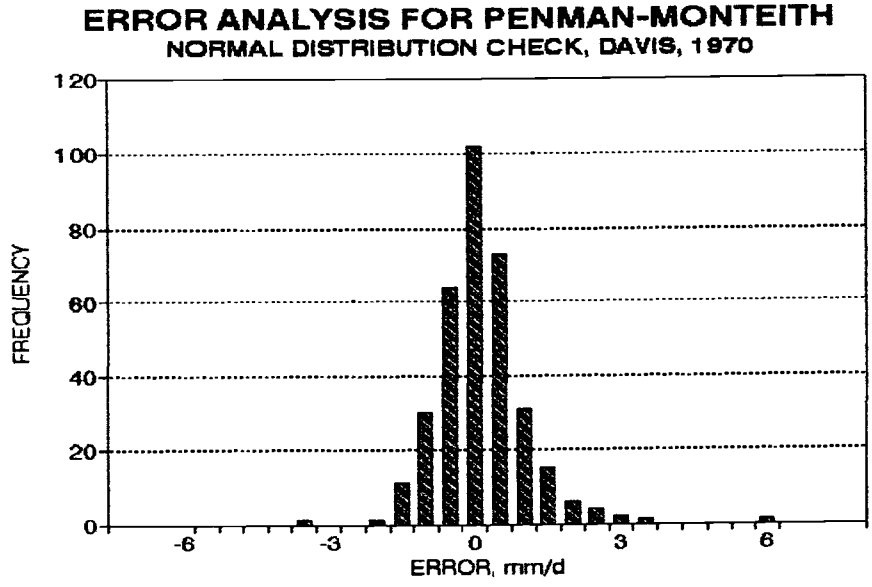

Figure 71. Plot of the error distribution versus frequency of occurrence for Penman-Monteith, Davis, 1970

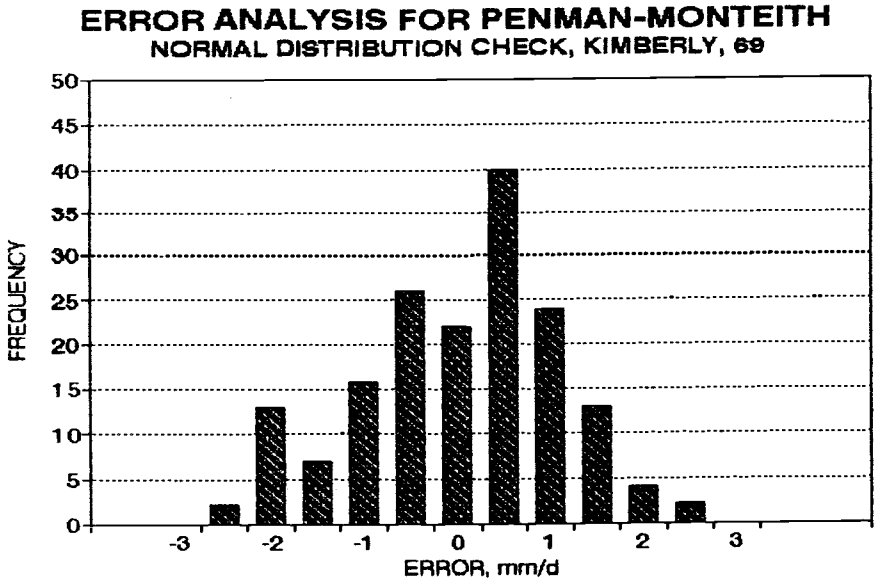

Figure 72. Plot of the error distribution versus frequency of occurrence for Penman-Monteith, Kimberly, 1969.

It appears the errors were normally distributed in Davis and Kimberly from the bell-shaped plot. To check for Seasonal trends, the error was plotted versus Julian day for each year at each site. Sample plots are presented in Figures 73, 74, and 75.

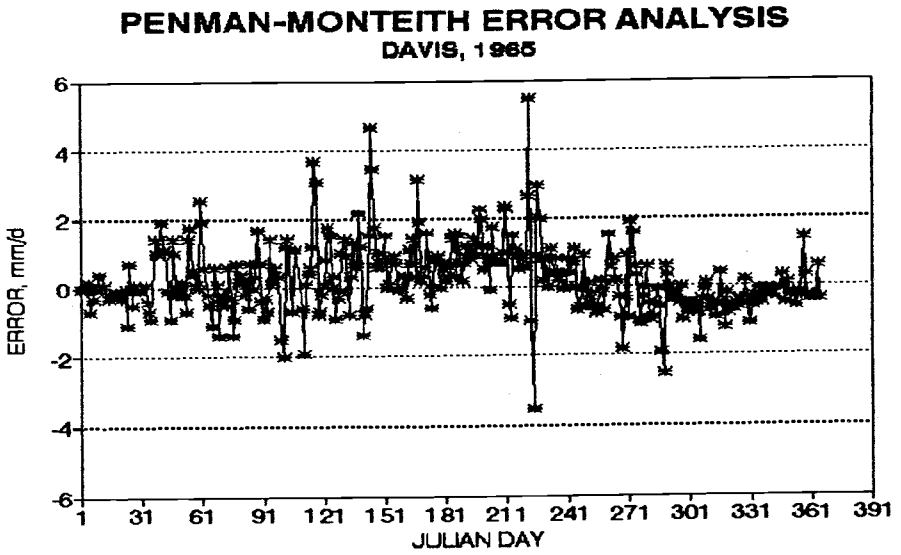

Figure 73. Plot of error versus Julian day for Penman-Monteith, Davis, 1965.

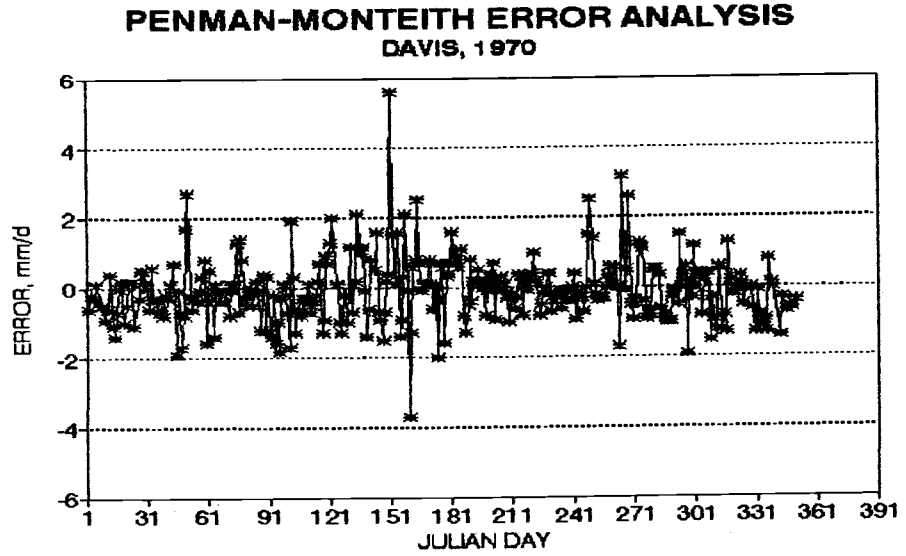

Figure 74. Plot of error versus Julian day for Penman-Monteith, Davis, 1970.

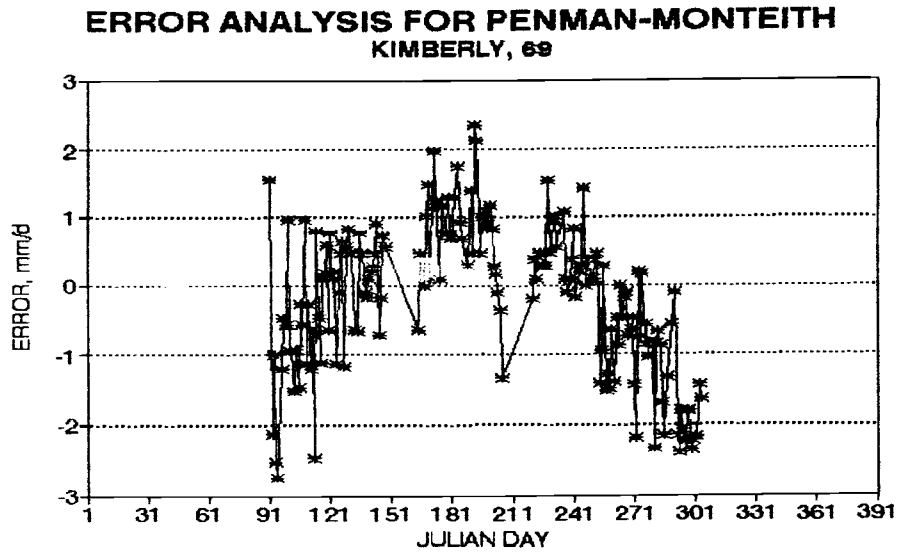

Figure 75. Plot of error versus Julian day for Penman-Monteith, Kimberly, 1969.

In Davis, it was noted in 1965 the method underestimated ET_r from Julian day 151 to Julian day 241. This range starts at the beginning of June and ends at the beginning of September. In addition, for 1965, the method overestimated ET_r from Julian day 271 till Julian day 365. This range starts at October and ends in December. For all other years no seasonal trend was noted.

In Kimberly, the method tends to underestimate from Julian Day 151 to Julian day 241. The method overestimates reference evapotranspiration for all other months. This was a typical plot for Kimberly.

The cumulative plots were employed to verify the conclusions derived from the error plots. Sample plots were presented in Figures 76, 77, and 78.

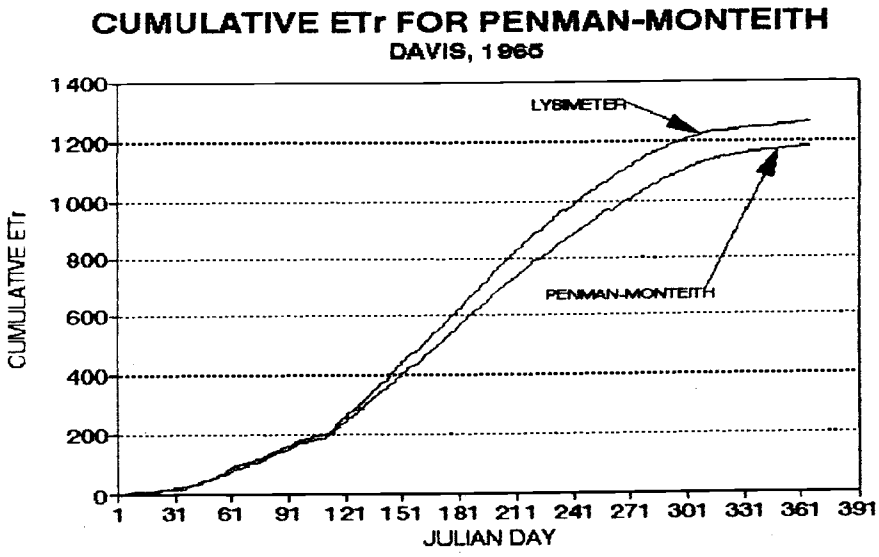

Figure 76. Cumulative ETr (mm) versus Julian day for Penman-Monteith, Davis, 1965.

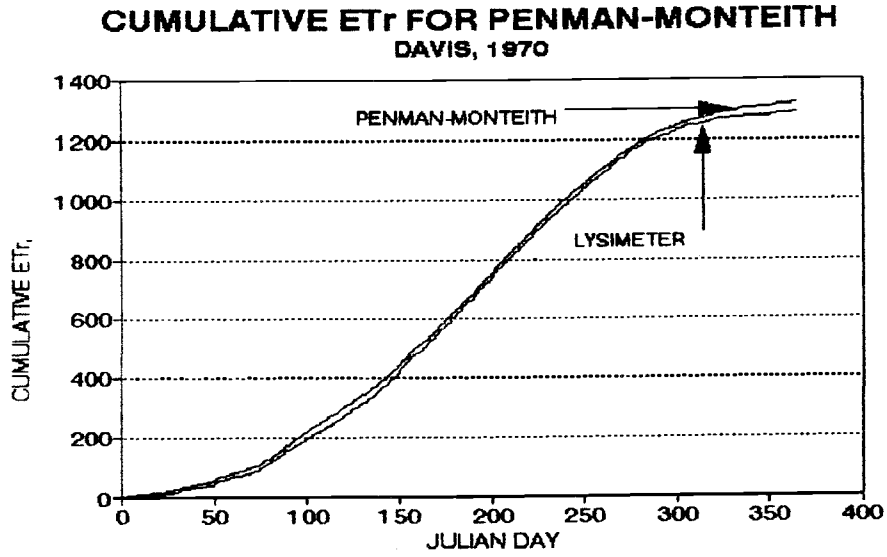

Figure 77. Cumulative ETr (mm) versus Julian day for Penman-Monteith, Davis, 1970.

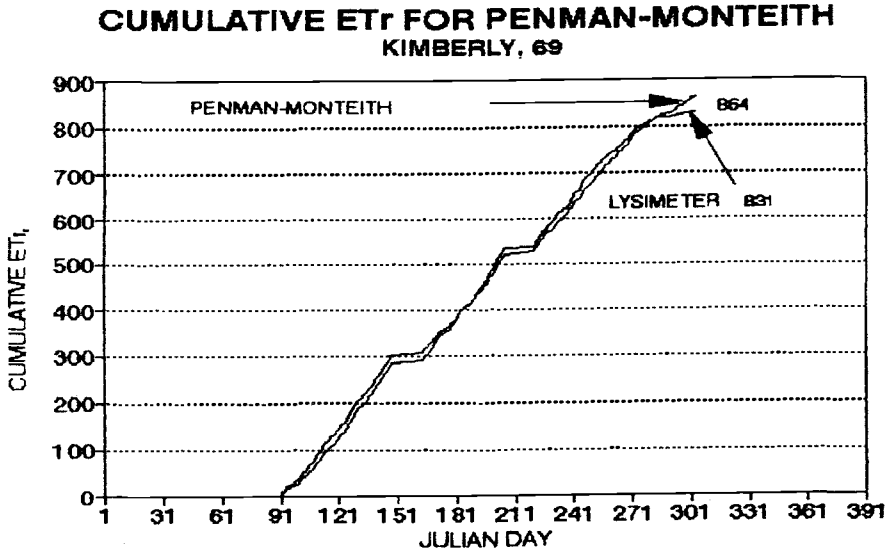

Figure 78. Cumulative ETr (mm) versus Julian day for Penman-Monteith, Kimberly, 1969.

For Davis, the cumulative plots indicated the deficiency of the method in 1965. Note the slope drift occurs at the same periods in which the errors indicate some bias. However, good agreement between the lysimeter and the Penman-Monteith was revealed for all other years. In Kimberly, the two cumulative curves trace each other. This indicates the method can perform better over a longer averaging period.

4.6.2 Regression Analysis

The regression analysis was performed to check the consistency of the correlation between the Penman-Monteith and the lysimeter. The results of this analysis are presented in Tables 38 and 39.

Table 38. Summary of regression analysis of Penman-Monteith method, Davis.

Year	Coefficient of Determination (r^2)	SEER (mm d^{-1})	Slope of Regression	Constant of Regression	Z Statistic (95 %) (T/F)
1965	0.82	0.98	1.17	-0.37	5.75 (F)
1966	0.85	0.87	1.02	-0.04	0.86 (T)
1967	0.88	0.73	0.98	-0.02	0.91 (T)
1968	0.89	0.77	1.07	-0.32	3.49 (F)
1969	0.90	0.71	1.05	-0.19	3.03 (F)
1970	0.86	0.89	1.05	-0.29	2.23 (F)
1971	0.89	0.77	1.10	-0.32	4.92 (F)

Table 39. Summary of regression analysis of Penman-Monteith Method, Kimberly.

Year	Coefficient of Determination (r^2)	SEER (mm d^{-1})	Slope of Regression	Constant of Regression	Z Statistic (95 %) (T/F)
1969	0.83	1.00	1.30	-1.73	6.50 (F)
1970	0.79	0.97	1.21	-1.02	4.01 (F)
1971	0.65	1.25	1.13	-0.58	1.67 (T)

For Davis, strong correlation was noted from the regression analysis. The correlation was consistent and varied form 0.82 in 1965 (when the method did show some bias) to 0.90 in 1969. The slopes were significantly different from unity five years out of seven indicating that a unit change in estimated reference evapotranspiration does not correspond to a unit change in measured lysimeter data. Good agreement between the cumulative plots indicate the potential for applying the method over a longer time period. For Kimberly, the coefficients of determination were high for 1969 and 1970. The slope of the regression was significantly different from unity two years out of three at Kimberly.

4.7 Comparisons of Methods

This section compares all the methods employed at one site to check which method performed best under given climatic conditions. In addition, the results of this section were utilized to derive climatic calibration coefficients for the original Penman method and the original Priestly-Taylor method.

4.7.1 Davis

The regression equations developed for estimated and measured reference evapotranspiration for Davis are shown in Table 40. The Z test for the slope using the two regression models is also given. A total of 2379 days were used in the regression analysis at Davis. In each case, the second row of values in Table 40 correspond to forcing the regression through the origin, i.e. setting the constant to zero. The slope obtained by forcing the regression through zero can be interpreted as the ratio of measured to estimated reference evapotranspiration. Figure 79 displays a sample graph of the two regression models for the original Priestly-Taylor for Davis, 1965-1971. The two lines presented indicate graphically the difference between forcing the fit through the origin and not forcing the fit through the origin.

It can be noted that the difference between forcing the regression through the origin and computing the actual intercept did not affect the SEER and the r^2 for the Penman-Monteith, the original Penman, and the pan evaporation. It should be noted that the SEER indicates the standard error of estimate if the regression equation was used to estimate ET_r while SEE indicates the standard error of estimate of the

estimating method and is not related to the regression equation. The fit forced through the origin was used for evaluating and comparing the methods.

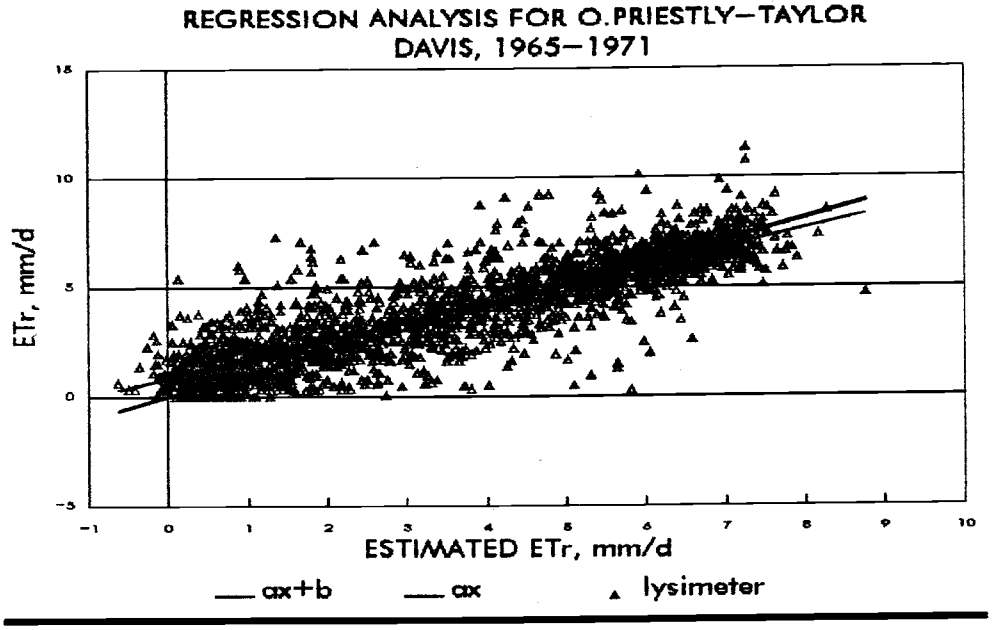

Figure 79. Comparisons between forcing the two regression models for the original Priestly-Taylor, Davis, 1965-1971.

For the Priestly-Taylor and the modified Priestly-Taylor, the difference in SEER with and without forcing the fit through the origin was about eight percent. The constant in the regression model not forced through the origin was large, and integrating the effect of this large constant into the slope introduced additional error. The large intercept from the regression model not forced through the origin was due to the fact that the Priestly-Taylor method underestimates reference evapotranspiration for the fall and winter months. Nevertheless, the regression model forced through the origin was used to evaluate the Priestly-Taylor methods.

Table 40. Summary of regression analysis for estimating methods, Davis (1965-1971).

Method	SEE mm d^{-1}	r^2	SEER mm d^{-1}	Constant	Slope	Z (T/F)
Pan	0.76	0.89	0.75	0.32	0.94	6.0 (F)
		0.89	0.76	0.00	1.00	0.0 (T)
Original Priestly-Taylor	1.17	0.77	1.08	0.81	0.85	15.0 (F)
		0.74	1.17	0.00	1.01	2.54 (F)
Modified Priestly-Taylor	1.17	0.76	1.11	0.69	0.88	12.2 (F)
		0.74	1.17	0.00	1.01	2.47 (F)
Original Penman	0.98	0.85	0.88	0.17	0.88	16.5 (F)
		0.85	0.88	0.00	0.91	23.5 (F)
Penman-Monteith	0.84	0.85	0.83	-0.19	1.05	5.17 (F)
		0.87	0.84	0.00	1.01	3.12 (F)

From the above statistics, the pan evaporation method proved to be the best when compared to other methods at Davis. The pan method shows the least SEE and the highest coefficient of determination. It should be noted that the slope of the pan evaporation method was not statistically different from unity when the regression was forced through the origin. No additional calibration seemed necessary to apply the constant pan evaporation method for the semiarid climate of Davis.

The original Priestly-Taylor regression slope was significantly different from unity. Therefore, the increase from unity as predicted by the slope is appreciable and should be adjusted for. It is recommended to increase the calculated daily values for the original Priestly-Taylor method by 1% for Davis. This increase can be incorporated into α by using a value of 1.28 for α in lieu of the 1.26 for Davis. Similarly, the modified Priestly-Taylor can be increased by 1% for better daily estimations. Pruitt and Doorenbos (1977) noted a value of α for Davis of 1.33. This value was computed for the period from January to May.

Allen (1986) concluded the original Priestly-Taylor should be multiplied by a factor of 1.11 for Davis. Allen (1986) used different formulations for computing net radiation, soil heat flux, and the slope of saturation vapor pressure temperature curve. In addition, Allen (1986) used only three years (1967-1969) for computing reference evapotranspiration.

The original Penman method forced through the origin had a slope of 0.91 which was significantly different from unity. Therefore, it is recommended to reduce the computed ETr by 9% for Davis. Allen (1986) noted the Penman method overestimated reference evapotranspiration for 1967-1969 by 10%.

The Penman-Monteith values may be increased by 1.01 since the slope obtained was significantly different from unity. Although the increase is small in magnitude, the Z test for the slope indicated it is significantly different from unity. Allen (1986) estimated the slope of the regression line forced through the origin for 1967-1969 using the Penman-Monteith as 0.98.

Figure 80 presents the SEE bar graph indicating the relative magnitude of the SEE for each method at Davis.

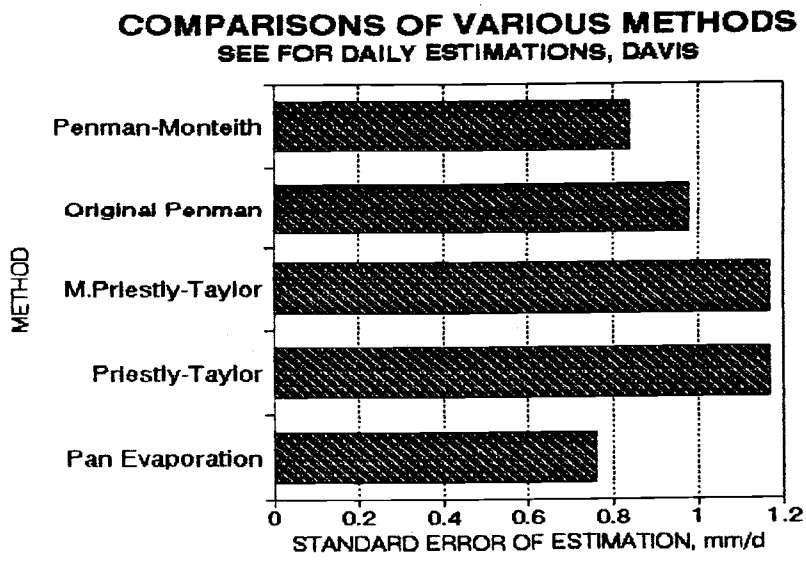

Figure 80. Standard error of estimate for various methods, Davis.

4.7.2 Kimberly

Analogous to Davis, regression equations were developed for each method. The results are presented in Table 41. Two rows of values are presented for each method. The first row presents the regression results without forcing the regression through the origin. The second row forces the line through the origin. For the following discussion, the regression results forced through the origin are used. The slopes obtained by forcing the regression through the origin can be interpreted as an average ratio of measured to estimated reference evapotranspiration.

Table 41. Summary of regression analysis for estimating methods, Kimberly (1969-1971).

Method	SEE mm d^{-1}	r^2	SEER mm d^{-1}	Slope	Constant	Z (T/F)
Pan	1.25	0.74 0.73	1.20 1.21	1.20 1.06	-0.75 0.00	6.02 (F) 4.86 (F)
Original Priestly-Taylor	1.78	0.70 0.69	1.29 1.30	1.46 1.31	-0.60 0.00	10.13 (F) 20.14 (F)
Modified Priestly-Taylor	1.76	0.65 0.63	1.38 1.42	1.53 1.25	-1.16 0.00	10.05 (F) 15.56 (F)
Original Penman	1.18	0.80 0.75	1.04 1.16	1.37 1.04	-1.76 0.00	11.7 (F) 3.41 (F)
Penman-Monteith	1.23	0.76 0.72	1.14 1.23	1.26 0.99	-1.46 0.00	7.81 (F) 0.79 (T)

The pan evaporation method proved to well correlated when compared to the Priestly-Taylor methods. The second least SEE and the second highest coefficient of determination were found for the pan evaporation method at Kimberly. The slope of the regression forced through the origin was statistically different from unity. It is recommended to reduce the pan evaporation results by 6% for Kimberly. As indicated by r^2, the variation of the pan evaporation method only accounts for 73% of the variation of lysimeter measured ET_r.

The Priestly-Taylor method underpredicted reference evapotranspiration by 25 percent. The value of α recommended for Kimberly is 1.65 if the net radiation, psychrometeric constant, and the slope of the saturation vapor pressure versus temperature curve are computed as for the original Penman method. The value of α can be obtained by multiplying the computed regression slope from Table 41 by 1.26. To validate this ratio, a regression analysis between P1, the energy component of the Penman equation, and the lysimeter data was performed. The regression was forced through the origin to integrate all errors into the slope. The value of the regression slope was 1.66.

Pruitt and Doorenbos (1977) indicated some values of α for certain arid sites. They noted a value of 1.6 for α for Phoenix, and 2 for Tal-Amara, Lebanon during summer.

Allen (1986) concluded that the Priestly-Taylor method must be increased by 1.58 for an alfalfa reference crop. If Allen's factor was converted to an average equivalent grass value, the recommended factor would be 1.37. Allen's value would differ from the computed value in Table 41 by 5%. His calculation of net radiation for the Priestly-Taylor method was based on the equation developed by Wright (1982). In addition, Allen (1986) included the soil heat flux in his computations of reference evapotranspiration using an equation developed by Wright (1982) for Kimberly. The original Penman equation underestimated reference evapotranspiration by 4%. The slope of the Penman-Monteith was not statistically different from unity in Kimberly indicating the method does not require any adjustment.

Figure 81 indicates the relative magnitude of SEE for each method at Kimberly.

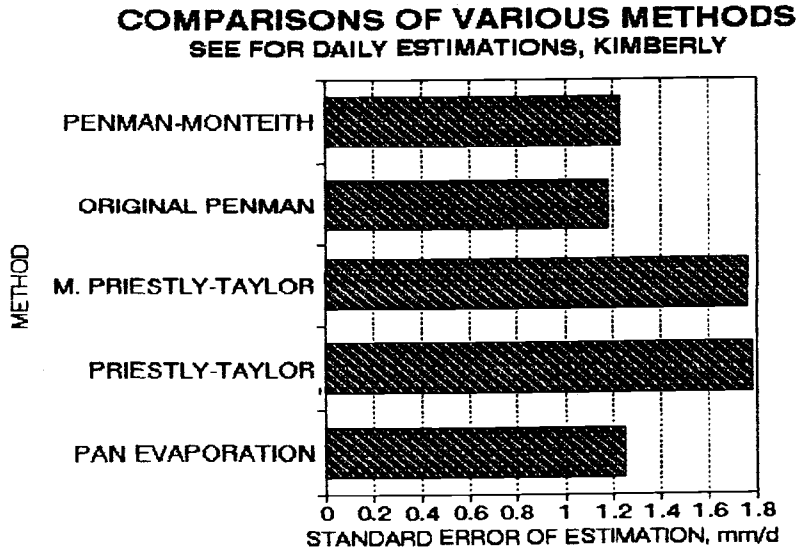

Figure 81. Standard error of estimate for various methods, Kimberly.

4.7.3 Versailles

The regression equations obtained for Versailles with the Z test for the slope using the two regression models are presented in Table 42. A total of 1706 days were used in the regression analysis at Versailles.

From the above statistical calculations, the original Priestly-Taylor proved to be the most suitable when compared with other methods. The original Priestly-Taylor showed the least SEE and the highest coefficient of determination. No calibration was necessary for Versailles, and the a value of α equal to 1.26 proved to be adequate. Allen (1986) performed a similar study for Coshocton, Ohio. He computed a slope of 1.08 when

Table 42. Summary of regression analysis for estimating methods, Versailles (1968-1976).

Method	SEE mm d^{-1}	r^2	SEER mm d^{-1}	Slope	Constant	Z (T/F)
Original Priestly-Taylor	0.77	0.80 0.80	0.77 0.77	1.02 1.00	0.10 0.00	1.77 (F) 0.00 (T)
Modified Priestly-Taylor	0.92	0.76 0.76	0.80 0.82	0.79 0.89	-0.50 0.00	20.8 (F) 19.0 (F)
Original Penman	0.89	0.81 0.80	0.75 0.78	1.01 0.88	-0.93 0.00	0.59 (T) 22.4 (F)

the regression was forced through the data of Coshocton for the growing season. The growing season at Coshocton was from March 16 to November 15. Pruitt and Doorenbos (1977) reported a value for α of 1.21 for Copenhagen (Denmark). The value of α 1.21 was the lowest value recorded by Pruitt and Doorenbos (1977).

The graph presented in Figure 82 indicates the relative magnitude of SEE for each method at Versailles.

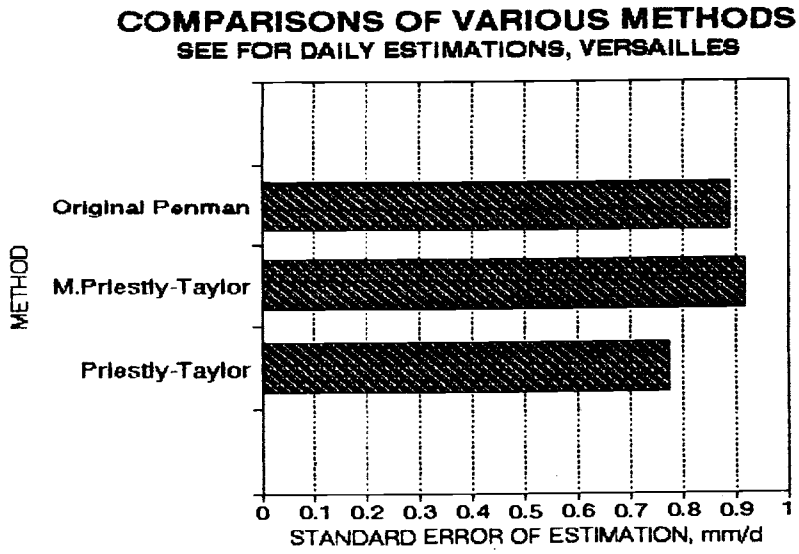

Figure 82. Standard error of estimate for various methods, Versailles.

4.8 Daily Climatic Calibration Coefficients

From the results of Section 4.7 it was noted that some of the estimating methods significantly overpredict or underpredict reference evapotranspiration when compared to lysimeter data. Since the procedure employed for estimating reference evapotranspiration was the same in each site and for each method, the difference in the coefficients from regression analysis performed in Section 4.7 was attributed to climate.

This section attempts to quantify the effect of climate for the original Penman method and the original Priestly-Taylor method. These were the only two methods for which adequate data existed at all three sites. The quantification includes a climatic factor, CF, that can improve

the estimating potentials of the method depending on the climate. The other estimating methods were not considered in this calibration since they could not be applied at all sites.

4.8.1 Derivation of the Climatic Calibration Coefficients

Evapotranspiration requires three physical processes. Energy should be available for evaporation, a vapor pressure gradient should be available for vapor movement, and a vapor removal mechanism. These three mechanisms influence evapotranspiration as demonstrated by the combination equation presented in Section 2.3.3.1. Since three sites were used with extremely different climates, the number of variables that can be used to quantify the climate is limited to three.

The three variables chosen to quantify climate were chosen to correct for the three processes responsible for evapotranspiration. Incoming shortwave radiation can serve as an indication of the available energy for evapotranspiration. Relative humidity can serve as an indication of vapor pressure deficit. Wind speed at 2 m height can serve as an indication of vapor transport. These same variables were also employed to adjust the FAO-Penman equation (Doorenbos and Pruitt, 1977; Cuenca and Jensen, 1988; Cuenca, 1989).

The climatic adjustment for the original Penman method and the original Priestly-Taylor method is made up of a linear combination of these three variables. Therefore, if incoming shortwave radiation, average air relative humidity, and wind speed were computed for the growing season of a certain climate, the necessary adjustment could be obtained for the particular method. The average relative humidity, average wind speed, and average incoming shortwave radiation for the growing season were computed at each site from the available data. The results are summarized in Table 43.

Table 43. Summary of the average climatic variables at each site.

Site	No. of Days Averaged	Relative Humidity RH (%)	Wind speed U ($m\ s^{-1}$)	Short Wave R_s ($MJ\ m^{-2}\ d^{-1}$)
Davis	2379	67.00	2.32	19.80
Kimberly	545	58.00	2.68	22.00
Versailles	1705	77.00	2.35	12.72

As noted from the regression analysis performed in Section 4.7, the suggested correction factors for the original Penman method and the original Priestly-Taylor were obtained. A summary of the coefficients are presented in Table 44. The coefficients presented in table 44 are attributed to the fact that the original Penman equation and the Priestly-Taylor method perform differently under different climatic regimes quantified by relative humidity, wind speed, and incoming shortwave radiation. For example, for the climate at Davis with a mean relative humidity of 67%, wind speed of 2.32 $m\ s^{-1}$, and an incoming shortwave radiation of 19.80 $MJ\ m^{-2}\ d^{-1}$, the original Penman ET_r needs to be adjusted by 0.92, on the average, to agree with the lysimeter.

Table 44. Summary of climatic calibration coefficients for each site.

Site	Original Priestly -Taylor	Original Penman
Davis	1.01	0.91
Kimberly	1.31	1.04
Versailles	1.00	0.88

To obtain the adjustment for other climates, the adjustment was assumed to be a linear combination of relative humidity, wind speed, and incoming shortwave radiation. A relative humidity coefficient, XRH, an incoming shortwave radiation coefficient, XSW, and a wind speed

coefficient XU were obtained for each method. These coefficients were solve for using a system of three equations with three unknowns as shown in the matrix equations for the original Penman and the original Priestly-Taylor:

$$\begin{bmatrix} 67.00 & 2.32 & 19.80 \\ 58.00 & 2.68 & 22.00 \\ 77.00 & 2.35 & 12.72 \end{bmatrix} \begin{bmatrix} XRH \\ XU \\ XSW \end{bmatrix} = \begin{bmatrix} 0.91 \\ 1.04 \\ 0.88 \end{bmatrix} \quad [70]$$

$$\begin{bmatrix} 67.00 & 2.32 & 19.80 \\ 58.00 & 2.68 & 22.00 \\ 77.00 & 2.35 & 12.72 \end{bmatrix} \begin{bmatrix} XRH \\ XU \\ XSW \end{bmatrix} = \begin{bmatrix} 1.014 \\ 1.31 \\ 1.00 \end{bmatrix} \quad [71]$$

Note the left matrix represents the climatic variables RH, U, and R_s for each site used in this study. The correction matrix on the righthand side of the two matrix equations represents the correction factors obtained for the corresponding site from linear regression analysis shown in Table 44).

The results of solving two matrix equations for XRH, XSW, and XU for the original Penman method and the original Priestly-Taylor method are presented in Table 45.

Table 45. Results of XRH, XSW, and XU for each method.

Coefficient	**Original Priestly -Taylor**	**Original Penman**
XRH	-0.00697	0.004788
XU	0.6730	0.1725
XSW	0.00408	0.009547

The results of Table 45 can be used to quantify the climatic correction factor to be utilized with the Penman equation or the Priestly-Taylor equation. To obtain the climatic correction factor for the original Penman equation or the original Priestly-Taylor for a certain site the following steps should be followed:

1. Compute the average incoming shortwave radiation, air relative humidity, and wind speed for the growing season.

2. Using the results of step 1, compute the climatic correction factor employing the formulation below for the Penman or Priestly-Taylor method where XRH, XU, and XSW are obtained from Table 45.

$$CF = (XRH)RH + (XU)U + (XSW)R_s \quad [72]$$

3. Adjust the daily estimates for the Penman or Priestly-Taylor using CF as shown:

$$ETr = CF \times ETr_{computed} \quad [73]$$

ETr= adjusted daily evapotranspiration, mm d^{-1}

CF= climatic correction factor

$ETr_{computed}$= computed reference evapotranspiration using the Penman or the Priestly-Taylor equation, mm d^{-1}

It should be emphasized that the coefficient CF is obtained based on the growing season and should not be varied on a daily basis. The growing season for Davis varies from January 1 to December 31, for Kimberly from April 1 to October 1, and for Versailles from January 1 to December 31. Therefore, for a specific climate characterized by R_s, RH, and U, there is a unique climatic factor CF for the Penman equation or the Priestly-Taylor equation.

4.8.2 Validation Studies

The Corvallis site data was not considered representative of the climate at Corvallis since all the available Bowen ratio data were collected in the fall. Moreover, the Bowen ratio latent heat flux estimates were considered low since a fungus disease affected the grass plot. Appendix C presents a comparison between the Bowen ratio data collected, the original Penman method, the Priestly-Taylor method, and the CIMIS model. The CIMIS (California Irrigation Management Information System) is a modified Penman combination model developed for hourly computations of reference evapotranspiration at Davis by Pruitt and Doorenbos (Schneider, 1987). The model has a wind function calibrated on an hourly basis which is a function of the net radiation sign. Since the Corvallis site data could not be used to validate the derived climatic factor, a random data set was chosen from each site by using a criteria that is discussed.

Validation was performed using a combined data set made up of 55 days chosen every 30th day from the eight year data set of Versailles, every 10 days from the three year Kimberly data set, and every 30 days from the seven year Davis data set. Two years, 1965 and 1970, were not used in the data selection from Davis. A general hypothetical climate was then formed by combining the above data sets. Evaluation was made of the performance of the Priestly-Taylor method and the original Penman method with and without the coefficients at each site and at the hypothetical site. Table 46 presents the correction factor CF1 for the original Penman method, and the correction factor CF2 for the original Priestly-Taylor obtained using the methodology outlined in Section 4.7.1

Three types of validation analysis were performed on the above four sites. The analysis includes regression analysis, error analysis, and standard error of estimation reduction analysis. The purpose of

Table 46. Summary of calculated calibration coefficients at each site for the validation study.

Site	No. of Days Averaged	Relative Humidity RH (%)	Wind speed U (m s^{-1})	Short Wave R (MJ m^{-2} d_s^{-1})	CF1 (Penman)	CF2 P-T
Davis	64	65.06	2.36	20.67	0.92	1.05
Kimberly	54	55.40	2.66	21.80	0.93	1.32
Versailles	55	70.10	2.37	13.10	0.87	1.04
General	173	63.70	2.46	18.61	0.91	1.135

these analyses was to verify whether an improvement was noted by applying the methodology outlined in Section 4.7.2. These results are presented in Tables 47, 48, 49, and 50.

4.8.2.1 Standard Error of Estimation Analysis

The standard error of estimation (SEE) was computed according to the procedure outlined in Section 3.6.3. The original Penman method, the Penman method modified by CF1, the Priestly-Taylor method, and the Priestly-Taylor method modified by CF2 were compared to check whether a reduction in SEE was noted. The results are presented in Table 47.

It can be noted that the SEE for the adjusted data set was less than or equal to that for the unadjusted data set for each climate. The general hypothetical climate showed a reduction in SEE for both methods. Therefore, it was concluded the climatic calibration coefficient reduced the errors and provided an improvement over the original method.

Table 47. Results of standard error of estimate analysis.

Site	Modified By CF (Y/N)	Original Priestly-Taylor mm d^{-1}	Original Penman mm d^{-1}
Davis	N	1.87	1.288
	Y	1.05	1.284
Kimberly	N	1.84	1.50
	Y	1.63	1.44
Versailles	N	0.77	0.83
	Y	0.78	0.70
General	N	1.35	1.14
	Y	1.32	1.03

4.8.2.2 Regression Analysis

Regression analysis was performed to check whether the slope was statistically different from unity with and without the adjustment for the two methods. The slope was forced through the origin to integrate the errors into the regression slope. Tables 48 and 49 present the results for the original Priestly-Taylor and original Penman methods. The null hypothesis in this case states the slope is unity.

The climatic calibration factor CF2 obtained from Table 46 improved the regression by adjusting the slope to unity. Therefore, one unit of change in lysimeter evapotranspiration corresponds to 1 unit change of ET_r computed using the adjusted Priestly-Taylor. The same analysis was performed for the original Penman equation. The results are presented in Table 49.

Table 48. Summary of regression analysis for original Priestly-Taylor validation study.

Site	Modified CF2 (Y/N)	r^2	Slope	Standard Error of Slope	Z (T/F)
Davis	N	0.68	1.03	0.0370	0.83 (T)
	Y		0.98	0.0350	0.59 (T)
Kimberly	N	0.55	1.25	0.0512	4.90 (F)
	Y		0.97	0.0400	0.85 (T)
Versailles	N	0.82	0.98	0.0324	0.60 (T)
	Y		1.02	0.0306	1.94 (T)
General	N	0.66	1.09	0.0226	1.90 (T)
	Y		1.00	0.0257	0.00 (T)

Table 49. Summary of regression analysis for original Penman validation study.

Site	Modified By CF1 (Y/N)	r^2	Slope	Standard Error of Slope	Z (T/F)
Davis	N	0.86	0.88	0.021	5.55 (F)
	Y		0.97	0.023	1.56 (T)
Kimberly	N	0.58	0.93	0.036	2.06 (F)
	Y		0.99	0.039	0.22 (T)
Versailles	N	0.85	0.88	0.0260	4.58 (F)
	Y		1.03	0.0309	0.92 (T)
General	N	0.79	0.90	0.0165	6.07 (F)
	Y		1.00	0.0183	0.17 (T)

The climatic calibration factor CF1 adjusted the slope to unity at each site. Note that at each site the slope was statistically different from unity for the original Penman before adjustment.

4.8.2.3 Error Analysis

As a final verification and evaluation of the improvements gained by the climatic calibration, the error of estimate was compared to zero. This was done by comparing the average lysimeter data to the unadjusted and adjusted Priestly-Taylor (OPT) and Penman method (PEN). The Z test procedure described in Section 3.6 was utilized. The results are presented in Table 50.

Table 50. Summary of error analysis for validation study.

Site	Modify CF (Y/N)	Avg. Lys. mm d^{-1}	STD Lys. mm d^{-1}	PEN ETr mm d^{-1}	STD PEN mm d^{-1}	Z	OPT ETr mm d^{-1}	STD OPT mm d^{-1}	Z
Davis	N	3.98	2.333	4.40	2.51	T	3.63	2.21	T
	Y			4.03	2.30	T	3.82	2.33	T
Kimberly	N	4.66	2.201	5.10	1.56	T	3.73	1.44	F
	Y			4.73	1.45	T	4.85	1.86	T
Versailles	N	2.67	1.762	3.21	1.52	T	2.75	1.57	T
	Y			2.79	1.30	T	2.90	1.65	T
General	N	3.77	2.230	4.25	2.10	F	3.39	1.85	T
	Y			3.85	1.89	T	3.85	2.10	T

This analysis indicates slight improvements for both methods. In all the adjusted cases, the error was not statistically different from zero. This was not the case for the unadjusted case for the General hypothetical site with the original Penman method and at Kimberly for the original Priestly-Taylor method.

4.9 Moving Averages and Optimal Averaging Intervals

Moving averages were performed for a period of 1, 2, 3, 5, 7, 10, 15, 20, and 30 days to evaluate the reduction in the SEE and the increase in r^2 for the increase in number of days averaged. Moving average analysis tends to attenuate local peaks that may arise due to error in measurements or extreme cases. This type of analysis can be useful for determining an averaging interval for a given standard error criteria for a particular method at a specific site. The results are presented graphically for each site. Tabulation of the results are presented in Appendix B.

4.9.1 Davis

The decrease in the standard error with increase in the days averaged is presented graphically in Figure 83. The graph indicates the most rapid drop in SEE was with the two days averaging interval for all methods. This can be concluded by noting the slopes of the plots. After five days averaging interval, the slopes tend to approach the horizontal such that a large number of averaging days are required to obtain a small decrease in SEE.

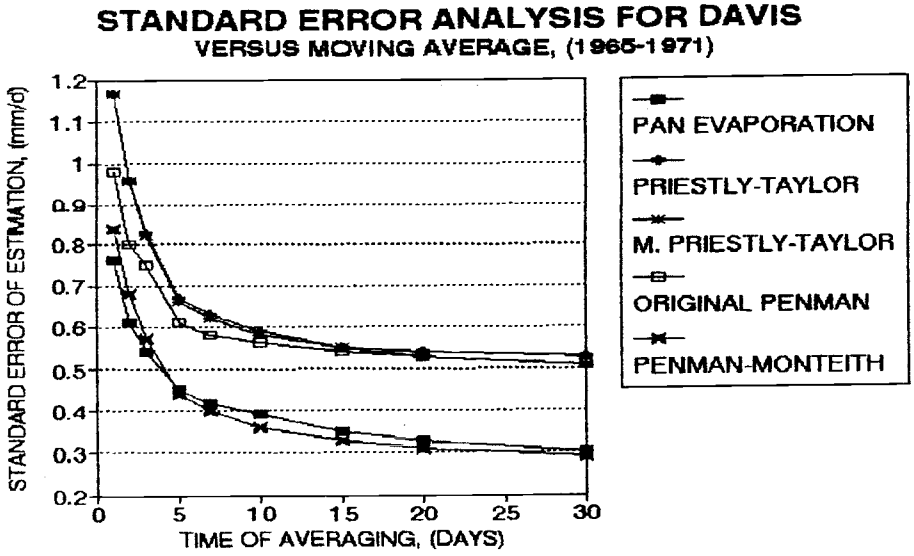

Figure 83. Standard error of estimate versus moving average, Davis.

The increase in the coefficient of determination computed forcing the regression through the origin is displayed in Figure 84. The slopes in this case display a rapid increase up to five days after which little change is noted by increasing the days averaged. All methods have a coefficient of determination higher than 0.90 after the five days moving average analysis.

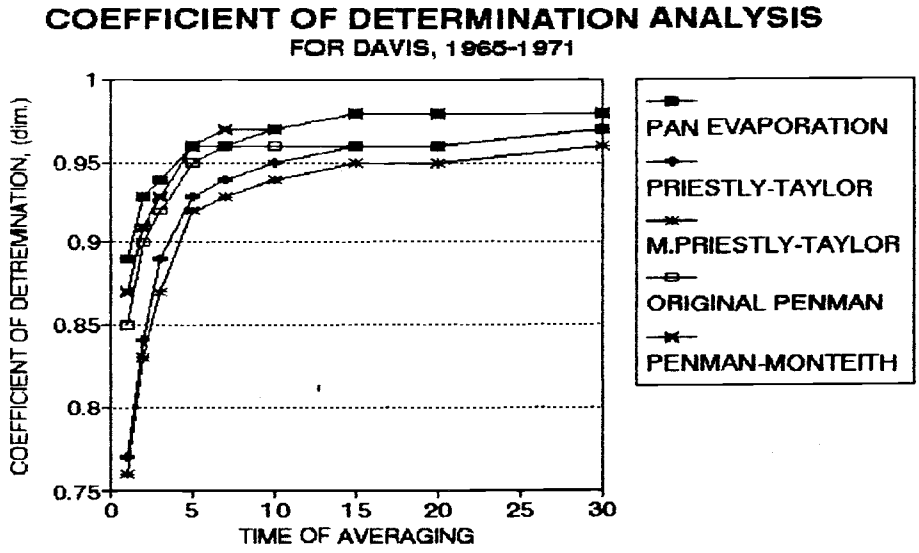

Figure 84. Coefficient of determination versus moving average, Davis.

4.9.2 Kimberly

Analogous to the analysis done for Davis, a moving average of reference evapotranspiration for various methods was computed for Kimberly. Figure 85 displays the relation between the days averaged and SEE. Note the slopes of the SEE versus the days averaged for Kimberly did not approach the horizontal. The other distinct feature is that the Penman method, the Penman-Monteith, and the pan traced each other with original Penman method having the minimum SEE. It was noted that after five days of averaging, the decrease in SEE was less pronounced when compared with the decrease noted before the five days

interval. Figures 85 and 86 display the relation between the number of days averaged, the standard error of estimate, and the coefficient of determination.

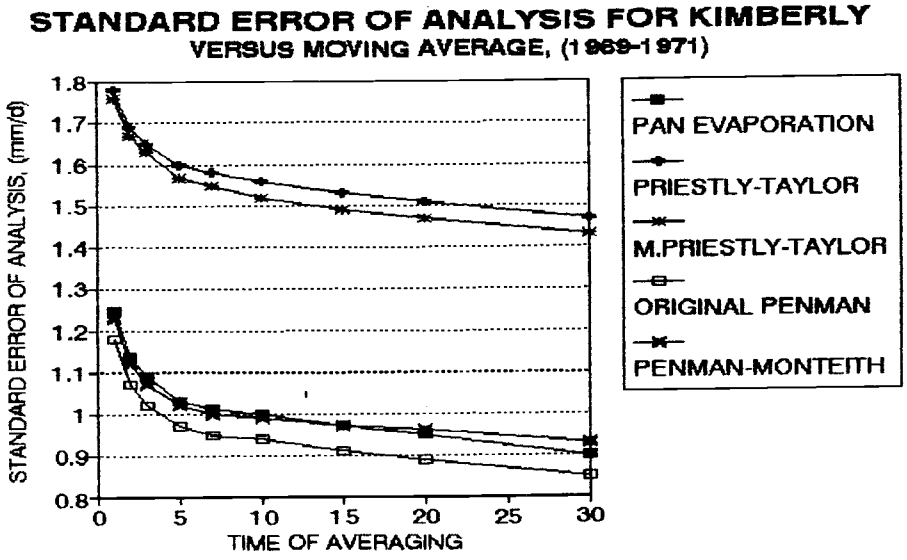

Figure 85. Standard error of estimate versus moving average, Kimberly.

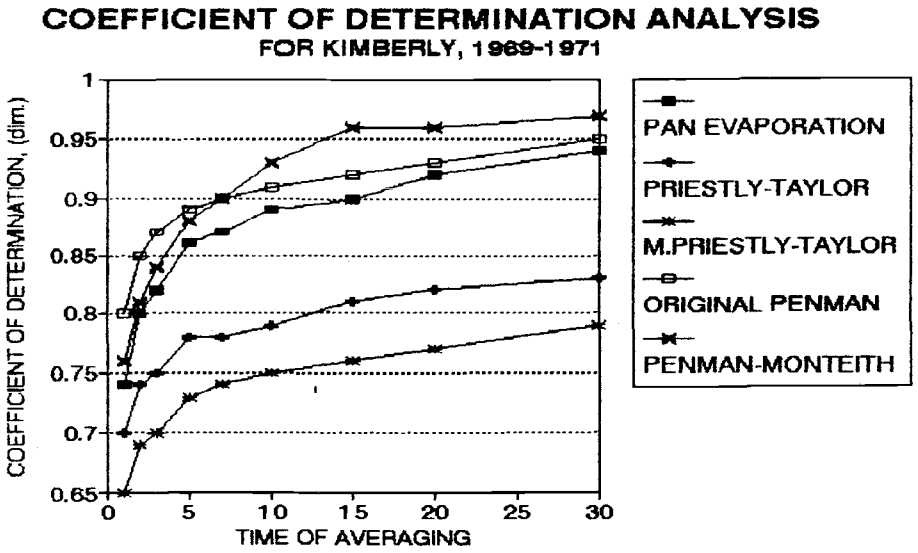

Figure 86. Coefficient of determination versus moving average, Kimberly.

After 10 days of averaging, the Penman-Monteith demonstrated the highest correlation with lysimeter data. After a five days averaging interval, the pan method, the Penman-Monteith, and the original Penman had a coefficient of determination higher than 0.8. This indicates that 80 % of the variation of the lysimeter can be explained by the above three estimating methods. A five days averaging interval seems to be adequate to use.

4.9.3 Versailles

Similar analysis was performed for Versailles. The results are presented in Figures 87 and 88.

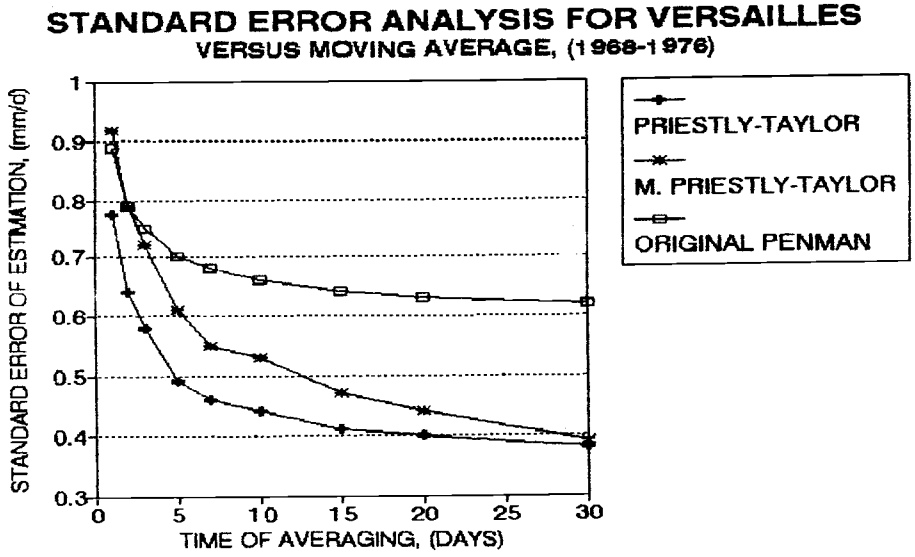

Figure 87. Standard error of estimate versus moving average, Versailles

Figure 87 displays the inverse relation between the SEE and the days averaged. The SEE for the original Penman method approached the horizontal slope asymptotically, and little decrease was noticed after 7 days of averaging.

The decrease in SEE for the Priestly-Taylor methods was largest for the first five days of averaging. After five days of averaging, a continuing decrease in SEE was observed.

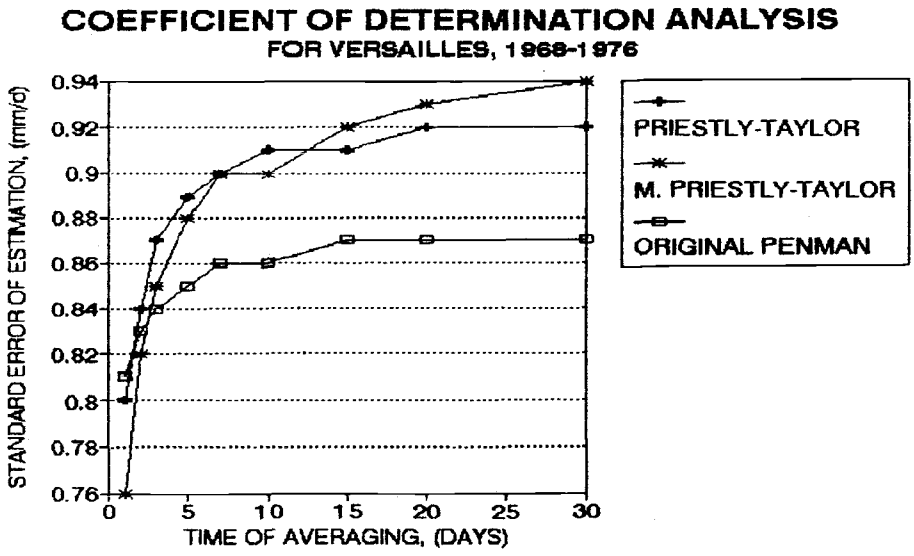

Figure 88. Coefficient of determination versus moving average, Versailles

Figure 88 displays the relation between the increase in averaging days and the coefficient of determination. The modified Priestly-Taylor for a 1 day averaging time had the lowest r^2. For a 30 days averaging period, the r^2 was the highest compared with other methods. This may be due to the procedure employed for computing α at Versailles. Long term monthly minimum relative humidity was used to estimate α at Versailles.

5 CONCLUSIONS AND RECOMMENDATIONS

5.1 Summary

This study focused on the performance of various reference evapotranspiration estimating methods under different climatic regimes. Estimates of the evaporative flux and crop water requirements based on meteorological data are important due to the difficulty of obtaining field measurements in many places around the world. Usually methods need to be applied under climatic conditions very different from those under which they were originally developed. This study focused on several reference evapotranspiration estimating methods with varying physical laws underlying their derivation. The methods presented include pan evaporation, the original Priestly-Taylor, the original Penman method, and the Penman-Monteith. These estimating methods cover the evaporation process from a free water surface, the conservation of energy, and the combination of energy and aerodynamic principles with and without biological adjustments.

The estimating methods were applied at three sites having distinct climates. These sites were chosen since daily evaporative flux was measured with very precise weighing lysimeters. The Davis site represents a semiarid climate. The Kimberly site represents an arid, windy climate. The Versailles site represents a humid climate with little advection. Reference evapotranspiration was computed using the above mentioned estimating methods at each site and the performance of each method was evaluated. Extensive statistics and regression analysis were employed in the evaluation. The methods were checked for seasonal trends and time dependent consistent bias for the period of available data. In addition, consistent correlation between estimated reference evapotranspiration and measured reference evapotranspiration was checked for each year at each site.

The comparisons between methods at each site was performed by computing the coefficient of determination and the standard error of estimate using all available days without regard to time of year. The coefficient of determination quantified the correlation between the estimating method and the lysimeter data for each climate. The standard error of estimate quantified the magnitude of the error for each method. These two quantities can be utilized to objectively compare the various estimating methods at each site and therefore for each climate.

Unfortunately, data availability limited the application of different methods at the sites selected for this study. Only two methods were considered at all sites, the Priestly-Taylor methods and the original Penman method. It was noted that these two methods performed differently for different climates, and the regression analysis performed at each site indicated significant adjustments could be applied. An attempt to quantify the climatic effect and to predict a climatic adjustment was made. Climate was quantified by average air relative humidity, average wind speed, and average incoming shortwave radiation for the period of interest. A linear combination between these three variables was obtained to quantify the reduction factor for the original Penman equation and the original Priestly-Taylor equation. These reduction factors were validated and significant improvements were obtained for daily reference evapotranspiration estimates.

Finally, moving averages for various number of days were employed to attenuate extreme days in the data sets at each site. The reduction of standard error of estimate and the increase in the coefficient of determination as a function of the number of days averaged was investigated. The optimum number of days to be averaged can be determined for a desired standard error of estimate or degree of correlation using graphical results presented.

5.2 Conclusions for Evaluated Methods

This Section presents some concluding remarks and recommendations of the application on each method for various climates.

5.2.1 Pan Evaporation Method

The pan evaporation method was analyzed for Davis and Kimberly. It was noted that the pan evaporation performed extremely well compared to other estimating methods at both sites. The correlation between the pan evaporation and lysimeter data was high for Davis and Kimberly. The coefficient of determination for Davis was 0.89 and for Kimberly 0.74. Therefore, 89 percent of the variation of measured reference evapotranspiration can be explained by the pan evaporation variation in Davis. Only 74 percent of measured reference evapotranspiration variation can be explained by the pan evaporation variation in Kimberly. Very high correlation were noted at both sites when a 30-day averaging interval was used. At both sites, the coefficient of determination for the 30-day average was above 0.85.

Pan evaporation can be used with confidence to estimate reference evapotranspiration for the growing season as demonstrated by the Z test performed year by year for Kimberly and Davis. Therefore, the pan can be a potential instrument for hydrologic balance studies and water management planning for arid and semiarid climates.

It should be noted that the conversion of reference evapotranspiration from alfalfa to grass induced errors in the lysimeter data set used to evaluate the pan method at Kimberly. This may explain partially the large magnitude of errors obtained at Kimberly for all estimating methods. Difficulty in quantifying the fetch distance and the

effect of errors in this variable on the estimated pan coefficient can be significant. An error of 10 m in the fetch distance can alter the pan coefficient by 0.02. Therefore, accurate fetch estimates are essential.

The pan coefficient was assumed constant throughout the growing season. An attempt to vary the pan coefficient on a daily basis was attempted. This attempt was very successful at Davis. No improvement in the standard error of estimation was noted in Kimberly when the pan coefficient was varied on a daily basis. Monthly variation of the pan coefficient to estimate daily reference evapotranspiration might improve the correlation. Further investigation is necessary.

5.2.2 Priestly-Taylor Method

The original Priestly-Taylor and the modified Priestly-Taylor were considered at all sites. The original Priestly-Taylor method underestimated reference evapotranspiration at Kimberly and Davis. The method gave the best results in the humid site of Versailles. It was concluded that the accuracy of the method is dependent on the climate under consideration. For a site with low advection the method can be applied with confidence. Where extreme advection conditions are expected, the method tends to underpredict reference evapotranspiration. At Davis, a fair correlation between measured reference evapotranspiration and the Priestly-Taylor estimates were noted. This study recommends increasing the Priestly-Taylor coefficient to 1.28 for Davis. It is not recommended to use the method for extreme arid-advective climates similar to Kimberly since the correlation between the energy component and evapotranspiration was not high.

An attempt to adjust the Priestly-Taylor method according to climate was performed. An empirical climatic factor involving wind speed, relative humidity, and incoming shortwave radiation improved the accuracy of the method on a daily basis for the arid climate and the semiarid climate.

Increasing the averaging period to 30 days reduced the standard error of estimation (SEE) by 55% at Davis, by 23% in Kimberly, and by 50% in Versailles. Corresponding to this reduction in SEE due to increasing the days averaged, an increase in the coefficient of determination between the original Priestly-Taylor method and the lysimeter data at all sites was noted. The increase in the coefficient of determination was 20% for a 30-day averaging period at Davis. A 28% increase was noted at Kimberly for the same over the 30-day period. A smaller 13% increase was noted in Versailles over the 30-day period. This small increase was due to the fact the method correlated well with the lysimeter data on a daily basis.

5.2.3 Modified Priestly-Taylor Method

A first-order modification in which the Priestly-Taylor α coefficient was varied by vapor pressure deficit was performed. No improvements in the coefficient of determination or the SEE were noted in Davis and Kimberly. The effect of advection should be integrated into the Priestly-Taylor to apply it successfully for various climates. This was performed by applying a climatic calibration incorporating wind, relative humidity, and incoming shortwave radiation for the original Priestly-Taylor. The modification of α by vapor pressure was not sufficient to improve the estimating potentials of the Priestly-Taylor method at all sites. It was noted in Versailles the method performed

better than the original Priestly-Taylor after a 20-day averaging interval. This might be due to using long term monthly relative humidity values to estimate the Priestly-Taylor coefficient.

5.2.4 Original Penman Method

The original Penman equation correlated well in Davis, Kimberly, and Versailles with measured reference evapotranspiration on a daily basis. The coefficient of determination for daily estimates was above 0.80 for the semiarid, arid and the humid sites. The Penman equation performed better than the pan method at Kimberly as can be noted from the coefficient of determination and the standard error of estimate for daily data. The method tends to overpredict reference evapotranspiration by 9 percent for Davis and by 12% for Versailles and underestimated by 5% for Kimberly. A climatic adjustment, analogous to that for the original Priestly-Taylor was derived. The adjustment improved daily estimated reference evapotranspiration. The validation studies for the climatic reduction factor was significant and has reduced the SEE at all sites.

Increasing the average period improves the estimating potentials of the method. Penman recommended that his equation should not be used for periods less than ten days. For that period, the SEE at Davis was less than 0.4 mm d^{-1}, at Kimberly the SEE was less than 1.00 mm d^{-1}, and at Versailles the SEE was less than 0.45 mm d^{-1}. The coefficients of determinations at all sites exceeded 0.90 for the 10-day averaging period. A five-day averaging period proved to be adequate.

5.2.5 Penman-Monteith Method

The Penman-Monteith provided good estimates at Davis and Kimberly. It should be noted that the Penman-Monteith requires several input variables that are difficult to measure. These variables were estimated using empirical equations which may cause some inaccuracy.

The Penman-Monteith assumed a constant zero plane displacement height at both sites. This assumption might not affect the results at Davis since grass does not require as frequent cutting as alfalfa. Alfalfa may require harvesting every four to six weeks to maintain the required length for reference conditions. In addition, the roughness terms can vary drastically for a rough crop like alfalfa. Just after harvesting, the bulk stomatal resistance can vary significantly when compared to the value just before harvesting. All those factors increased the errors for the Penman-Monteith method at Kimberly.

It was noted that the SEE was reduced by 13% when a 30-day moving average was employed at Davis. The decrease in SEE was more pronounced in Kimberly and amounted to 24%. This indicated better results can be obtained at Kimberly if a long averaging period is used. For Davis, the coefficient of determination increased by 11% for a 30-day averaging period. For Kimberly, the increase in the coefficient of determination was 22%. Shorter time periods of 5 days can be used with reasonable accuracy for both sites.

5.3 Recommendations For Further Research

Several recommendations for future research evolved from the results of this investigation.

1. The climatic coefficients derived for the original Penman method and the original Priestly-Taylor method need to be verified for a maritime climate which is between the arid Kimberly site and the humid Versailles site. Such a climate is available at the Corvallis site. More long term evaporative flux data are required at this site.

2. The performance of the pan evaporation method and the Penman-Monteith method at a humid site with a climate similar to Versailles should be investigated. Data limitations precluded such an analysis in this study.

3. Alternatives for integrating point estimations using one of the estimating methods into an area average evapotranspiration that can be included in a general circulation model (GCM) can be the topic of future projects.

4. Climatic calibration factors for the Penman-Monteith and the pan evaporation methods should be derived. Pan evaporation data are available in several places around the world and a convenient methodology to utilize this data base for estimating reference evapotranspiration can be useful for general circulation model (GCMs). Another possibility is to investigate conversions between different pans. Therefore, countries that utilize pans different than class A pan can convert the evaporation measurements into an equivalent class A pan data. Once all pan data are converted to an equivalent pan type, reference evapotranspiration estimations at several points around the world could be made. This data could then be incorporated into a GCM as a lower boundary condition.

5. Alternatives to vary the leaf area index and the resistance coefficients with time of year should be considered for improving the Penman-Monteith.

6. The possibility of varying the Priestly-Taylor coefficient depending on the types of crops for different climates is recommended for future studies. This can be performed by utilizing measured net

radiation and soil heat flux to estimate P1. Actual crop evapotranspiration can be estimated using hydrological balance methods in conjunction with the neutron probe soil moisture measuring device. A plot of P1 versus estimated crop evapotranspiration from the hydrologic balance estimations can be employed to estimate the Priestly-Taylor coefficient for the desired crop. Once the Priestly-Taylor coefficient is obtained for a desired crop, satellite information can produce net radiation data for a certain region. This information in conjunction with the information about the Priestly-Taylor crop coefficient can be used to estimate actual evapotranspiration for the crop.

This procedure can also be used to integrate evaporative flux over a large area comparable to a GCM grid (minimum 100 km x 100 km). Remote sensing data can be used to indicate the distribution of vegetation over the grid. A map with the different types of vegetation for the grid could be produced. Simple area calculations can indicate the percentages of each crop type for the GCM grid. Estimated net radiation from multispectral data can provide an average P1 for the grid. From the vegetation map produced, an area-averaged Priestly-Taylor coefficient can be obtained depending upon the area percentages of each crop. From the average P1 obtained from multispectral data and the area-weighted Priestly-Taylor coefficient from the vegetation map, an integrated evaporative flux could be computed for that GCM grid. Such an investigation could only be performed on regional experiment similar to the HAPEX-MOBILHY large-scale experiment.

7. The correlation between the Priestly-Taylor coefficient and the advection processes responsible for evapotranspiration could be a future research topic. This could be done by studying the correlation between the latent heat flux and P1 on a short time interval e.g. 20 minutes. A possible correlation between the Priestly-Taylor coefficient and the Bowen ratio could result. Such a study can be performed using the

Corvallis Bowen ratio system and the automated weather station available. Validation of this study should be performed in regions with a climate distinctly different from that of Corvallis.

6 BIBLIOGRAPHY

Aboukhaled, A., A. Alfaro, M. Smith. (1982). "Lysimeters". FAO Irrigation and Drainage Paper 39, U.N. Food and Agr. Org., 1-68.

Allen, R. G. (1986). "Penman for all seasons." *J. Irrig. and Drain. Div., ASCE*, 112(4), 348-368.

Allen R. G. (1989). Personal communications concerning Fritchen net radiometer calibration.

André, J. C., J. P. Goutorbe, A. Perrier, and others. (1988). "Evaporation over land-surfaces: First results from HAPEX-MOBILHY special observation period", *Annales Geophysicae*, Vol.6(5), 447-492.

André, J. C., J. P. Goutorbe, and A. Perrier (1986). "HAPEX-MOBILHY: A Hydrologic Atmospheric Experiment for the Study of Water Budget and Evaporative Flux at the Climate Scale". *Bulletin American Meteorological Society.* Vol.67(2), 138-144.

Blaney, H. F. and W. D. Criddle. (1950). "Determining water requirements in irrigated areas from climatological and irrigation data." U.S. Dept. of Agriculture, Soil Conservation Service, Technical Report No. 96

Bowen, I. S. (1926). "The ratio of heat losses by conduction and by evaporation from any water surface.", *Phys. Rev.*, 27, 779-787.

Brutsaert, W. H. (1982). "*Evaporation into the Atmosphere. Theory, History, and Applications*". Boston, D. Reidel publishing co.

Burman, R. D., R. H. Cuenca, and A. Weiss. (1983). "Techniques for estimating irrigation water requirements." *Advances in irrigation, vol.2*, ed. D. Hillel. New York: Acadamic Press, 336-394

Carrijo, O. A. (1988). "Analysis of a hydrologic balance model and Penman-Monteith evapotranspiration estimating methods", Ph.D. Thesis, Oregon State University.

Cuenca, R. H., and Nicholson, M.T.(1982). "Application of Penman equation wind function.", *J.Irrig. and Drain. Div., ASCE*, 108(1), 13-23.

Cuenca, R. H., J. Noilhan.(1990). "Use of soil moisture measurements in hydrologic balance studies." To appear in *Proceedings of Workshop on Land Surface Processes, Banyuls, France* (in press).

Cuenca, R. H. (1985). Evapotranspiration-Penman Equation. AE 511 - Irrigation Science - Oregon State University. (Class Notes).

Cuenca, R. H. (1989). "*Irrigation system design: An engineering approach.*", Englewood Cliffs, New Jersey: Prentice Hall.

Cuenca R. H., and K. Y. Amegee. (1987). "Analysis of evapotranspiration as a regionalized variable", *Advances in irrigation*, vol.4, Academic Press Inc., 181-218.

Dalton, J. (1801). "New theory of the constitution of mixed aeriform fluids, and particularly of the atmosphere.", J. Nat. Philos., Chemistry and the Arts (W. Nicholson). 241-244. (cited by Brutsaert, 1982).

de Pescara, C., M. Painine, and C. Garrigues. 1988. "Theory and operation of French energy balance, Bowen ratio, and micro-meteorology instrumentation", in *Proceedings of the ASCE Conference on Planning Now for Irrigation and Drainage in the 21st Century*, Lincoln, Nebraska, 617-624.

Devore, J. and R. Peck. (1986). "*Statistics, the exploration and analysis of data*". St. Paul, Minnesota: West Publishing Co.

Dickinson, R. E. (1984). "Modeling evapotranspiration for three-dimensional global models", Climate processes and climate sensitivity, J.E. Hansen, and T.Takahashi (eds.), *Geophysical Monograph No. 29, American Geophysical Union*, Washington D.C, 58-72.

Doorenbos, J., and Pruitt, W. O.(1977). "*Guidelines for Predicting crop water requirements.*" FAO Irrigation and Drainage Paper 24, U.N. Food and Agr. Org.

Eagleson P. S. (1986). "The emergence of global-scale hydrology", *Water Resour. Res.*, Vol.22(9), 65-145.

Hillel, D. (1982). "*Introduction to soil physics*". London : Academic Press Inc.

Howell T. A., R. L. McCormick, and C. J. Phene. (1985). "Design and installation of large weighing lysimeters.", *Trans. ASAE*, 106-117.

Jackson, R. D., J. L. Hatfield, P. J. Pinter, Jr., R. J. Reginato, (1985). "Net radiation calculated from remote multispectral and ground station meteorological data", *Agric. Meteorol.*, 35, 1324-1354.

Jensen, M. E., Ed. (1974). "Consumptive use of water and irrigation water requirements." Rep. by the Tech. Comm. Irrig. Water Req., *Irrig. and Drain. Div., ASCE.*

Kanemasu, E. T., M. L. Wesely, B. B. Hicks, and J. L. Heilman. (1979). "*Techniques for calculating energy and mass fluxes*", Modification of the Aerial Environment of Plants, B. J. Barfield, and J. F. Gerber (eds), ASAE, Saint Joseph, Michigan, 156-182.

Laval, K., C. Ottlé, A. Perrier, and Y. Serafini. (1984). "*Effect of parameterization of evapotranspiration on climate simulated by a GCM*". New Perspectives in Climate Modelling. Elsevier, Amsterdam, 223-247.

Linsely, R. K., Jr., M. A. Kohler, and J.L.H. Paulhus. (1982). "*Hydrology for engineers.*", New York, McGraw-Hill.

Martinéz-Cob, A. (1990). "Multivariate geostatistical analysis of evapotranspiration and elevation for various climatic regimes in Oregon", Ph.D Thesis, Oregon State University.

Monteith, J. L. (1965). "Evaporation and environment." *Symp. Soc. Exp. Biol.*, 19, 205-234.

Muller, M. J. (1982). "*Selected climatic data for a global set of standard stations for vegetation science.*", The Hague, the Netherlands: DR W. Junk Publishers.

Murray, F. W. (1967). "On the computation of saturation vapor pressure.", *J. Appl. Meteorol.*, Vol.6, 203-204.

Neter, J., W. Wasserman, and M.H. Kutner. (1983). "*Applied linear regression.*", Homewood, Illinois: IRWIN Inc.

Nichols, W. E. (1989). "Land surface energy balance and surface soil moisture variation in HAPEX-MOBILHY", M.S. Thesis, Oregon State University.

Nuss, J. L. (1989). "Analysis of evapotranspiration for various climatic regimes using geostatistics", M.S. Thesis, Oregon State University.

Penman, H. L. (1948). "Natural evaporation from open water, bare soil and grass.", *Proc. Roy. Soc. London*, A193, 120-146.

Priestly, C. H. B., and Taylor, R. J. (1972). "On the assessment of surface heat flux and evaporation using large scale parameters.", *Mon. Weath. Rev.*, 100, 81-92.

Pruitt, W. O., E. Fereres, K. Kaita, and R. L. Snyder. (1987). "Reference evapotranspiration (ET_o) for California.", Agricultural Experimental Station, University of California, Davis, Division of Agriculture and Natural Resources, Bulletin.

Pruitt W. O., and A. Angus. (1960). "Large weighing lysimeter for measuring evapotranspiration.", Trans. ASAE 3, 13-18.

Reed S. C., and T. D. Buzzell. 1973. "Land treatment of wastewaters for rural communities", *Rural Environmental Engineering Conference*, Corps of Engineers, U.S. Army, Warren, Vt, 2-15.

Ritchie J. T., and E. Burnett. (1968). "A precision weighing lysimeter for row crop water use studies.", *Agron. J.* 60, 545-549.

Robertson, J. A., and Crowe, C. T. (1980). "*Engineering fluid mechanics.*", 2nd ed. Houghton, Boston, Massachusetts.

Saeed M. (1986). "The estimation of evapotranspiration by some equations under hot and arid conditions.", Trans. ASAE, 434-438.

Salgado, E. A. (1985). "Calibration of a theoretically derived relationship between pan evaporation and evapotranspiration", Ph.D. Thesis, Oregon State University.

Schneider, S. H. (1989). "The changing climate.", *Scientific America*, 70-79.

Sharma M. L. (1985). "Estimating evapotranspiration.", *Advances in irrigation*, vol.3, Academic Press inc., 213-281.

Snyder R. (1987). Personal communications concerning the CIMIS model developed at University of California, Davis for computing reference evapotranspiration with hourly data.

Snyder R. L., R. H. Shaw, and K.T. Paw. (1987). "Humidity conversion program", *Applied Agricultural Research*, Vol.2 (3), 183-192.

Tanner, B. D. (1988). "Use requirements for Bowen ratio and Eddy correlation determination of evapotranspiration". *National Conference on Irrigation and Drainage Engineering, ASCE,* Lincoln, Nebraska, 605-616.

Tanner, C. B., and Pelton, W. L. (1960). "Potential evapotranspiration estimates by the approximate energy balance method of Penman." *J. Geophys. Res.*, 65, 3391-3413.

Wright, J. L., and Jensen, M. E. (1972). "Peak water requirements of crops in southern Idaho." *J. Irrig. and Drain. Div.*, ASCE, 96(IR1), 193-201.

Wright, J. L. (1982). "New evapotranspiration crop coefficients." *J. Irrig. and Drain. Div., ASCE*, 108(IR2), 57-74.

Young, A. A. (1947). "Some recent evaporation investigations", *Trans. Am. Geophys. Union*, vol28, 279-284.

APPENDICES

Appendix A List of Symbols

This appendix lists the symbols used throughout the study. Because there are so many more concepts than are English and suitable Greek letters, certain conflicts are unavoidable. However, where the same letter has been used for different concepts, the topics are so far apart from each other that no confusion should result. Any deviation from this list is clearly indicated. An attempt to adhere to the general accepted symbols has been made.

β = Bowen ratio or ratio of sensible to latent heat flux
ρ = density of the air at constant pressure
α_s = albedo or ratio of reflected to incident shortwave radiation
α_l = lapse ratio or drop in barometric pressure per unit increase in elevation
γ^* = modified psychrometeric constant with resistance terms
Δ = slope of saturation vapor pressure-temperature curve
ϵ = mass ratio of water vapor to dry air
σ = Stephan-Boltzman constant
α = Priestly-Taylor coefficient
θ = soil moisture content on a volume basis
γ = psychrometric constant
BD= bulk density of a soil
C_p= specific heat
CW= specific heat of water
d= fetch distance for a cropped surface
D= amount of water in deep percolation
dW= change in storage water for a control volume
E= water evaporation
e_a= actual vapor pressure in the air
Ea= aerodynamic vapor transport term
e_d= vapor pressure at mean dewpoint temperature
EL= elevation of a site
e_{os}= saturation vapor pressure at the evaporating surface
E_{pan}= pan evaporation
e_s= saturation vapor pressure
ET= actual evapotranspiration
ET_r= reference evapotranspiration
ET_{tp}= potential evapotranspiration

$f(u)$= wind function relating windspeed to advection of vapor
FC= field capacity
g= gravitational acceleration constant
G= soil heat flux
G_{plate}= soil heat flux as measured by a plate at 8 cm
h_c= mean canopy height
h_i= ith depth layer
H= sensible heat flux
I= irrigation water
Jday= Julian day
K_c= crop coefficient
K_p= class A pan coefficient
K_v= eddy diffusivity of vapor
L= latent heat of vaporization
L_e= latent heat flux
L_i= incident longwave radiation
L_r= reflected longwave radiation
M= Month
n= actual sunshine hours for a certain location
N= maximum possible sunshine hours at a certain location
P= atmospheric or barometric pressure
P1= first part of the Penman equation (energy component)
P2= second part of the Penman equation (aerodynamic part)
P_o= atmospheric pressure at mean sea level
P_r= precipitation
q= vapor density
R= gas constant of air
r^2= coefficient of determination
r_{av}= aerodynamic resistance to water vapor
r_c= bulk canopy stomatal resistance
RH_{avg}= average air relative humidity
R_n= net radiation
R_o= amount of water in surface runoff
R_r= reflected shortwave radiation
R_s= incoming shortwave radiation
R_{so}= clear sky incident shortwave radiation
T= average air temperature
t_1= initial time period
t_2= final time period
T_{3pd}= mean air temperature for prior three days
T_d= dewpoint temperature
T_o= temperature at the evaporating surface
T_r= transpiration from a cropped surface
T_{wet}= wet bulb temperature
u_{2m}= equivalent wind speed at 2 m height
u_z= wind speed at height z
z= height of measurement
Z_{om}= surface roughness length for momentum transport
Z_{ov}= surface roughness length for vapor transport

Z_r= root zone depth

Appendix B Moving Average Versus SEE and r^2 at Each Site

This appendix presents the results obtained for the standard error of estimate (SEE) and the coefficient of determination r^2 at each site for various estimating methods. The methods were abbreviated as follows:

PAN= pan evaporation method with constant pan coefficient
OPT= original Priestly-Taylor with α = 1.26
MPT= modified Priestly-Taylor with variable α
PEN= original Penman method
MON= Penman-Monteith method

Davis Site (1965–1971)

Method	Days	1	2	3	5	7	10	15	20	30
PAN	SEE	0.76	0.61	0.54	0.45	0.42	0.39	0.35	0.33	0.30
	r^2	0.89	0.93	0.94	0.96	0.96	0.97	0.98	0.98	0.98
OPT	SEE	1.17	0.96	0.83	0.67	0.63	0.59	0.55	0.54	0.53
	r^2	0.77	0.83	0.89	0.93	0.94	0.95	0.96	0.96	0.97
MPT	SEE	1.17	0.96	0.82	0.66	0.62	0.58	0.55	0.53	0.51
	r^2	0.76	0.83	0.87	0.92	0.93	0.94	0.95	0.95	0.96
PEN	SEE	0.98	0.80	0.75	0.61	0.58	0.56	0.54	0.53	0.51
	r^2	0.85	0.90	0.92	0.95	0.96	0.96	0.96	0.96	0.97
MON	SEE	0.84	0.68	0.57	0.44	0.40	0.36	0.33	0.31	0.29
	r^2	0.87	0.91	0.93	0.96	0.97	0.97	0.98	0.98	0.98

Versailles Site (1968–1976)

Method	Days	1	2	3	5	7	10	15	20	30
OPT	SEE	0.77	0.64	0.58	0.49	0.46	0.44	0.41	0.40	0.38
	r^2	0.80	0.84	0.87	0.89	0.90	0.91	0.91	0.92	0.92
MPT	SEE	0.92	0.79	0.72	0.72	0.61	0.55	0.47	0.44	0.39
	r^2	0.76	0.82	0.85	0.85	0.88	0.90	0.92	0.93	0.94
PEN	SEE	0.89	0.79	0.75	0.70	0.68	0.66	0.64	0.63	0.62
	r^2	0.81	0.83	0.84	0.85	0.86	0.86	0.87	0.87	0.87

Kimberly Site (1969–1971)

Method	Days	1	2	3	5	7	10	15	20	30
PAN	SEE	1.25	1.14	1.09	1.03	1.01	1.00	0.97	0.95	0.90
	r^2	0.74	0.80	0.82	0.86	0.87	0.89	0.90	0.92	0.94
OPT	SEE	1.78	1.69	1.65	1.60	1.58	1.56	1.53	1.51	1.47
	r^2	0.70	0.74	0.78	0.78	0.78	0.79	0.81	0.82	0.83
MPT	SEE	1.76	1.67	1.63	1.57	1.55	1.52	1.49	1.47	1.43
	r^2	0.65	0.69	0.70	0.73	0.74	0.75	0.76	0.77	0.79
PEN	SEE	1.18	1.07	1.02	0.97	0.95	0.94	0.91	0.89	0.85
	r^2	0.80	0.85	0.87	0.89	0.90	0.91	0.92	0.93	0.95
MON	SEE	1.23	1.12	1.07	1.02	1.00	0.99	0.97	0.96	0.93
	r^2	0.76	0.81	0.84	0.88	0.90	0.93	0.96	0.96	0.97

Appendix C Corvallis Bowen Ratio Data

This appendix presents the results obtained for the Corvallis Bowen ratio station during the fall of 1989. The data set was compared with the Original Penman Method, the Original Priestly-Taylor method, and the CIMIS model developed in California for hourly computations of reference evapotranspiration.

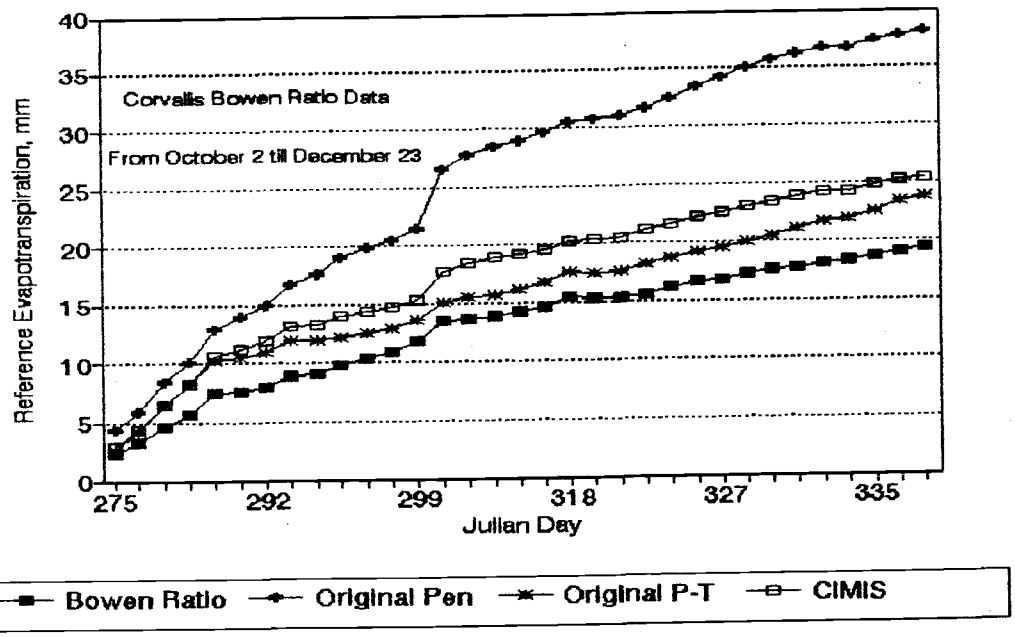

The cumulative plot presented clearly indicates the Bowen ratio data underestimated reference evapotranspiration due to the fungus disease affecting grass on the research plot. Difficulty in maintaining high soil moisture levels could be another factor.